Measurements of π^0-jet correlation $\sqrt{s}$ = 7 TeV pp collisions and in $\sqrt{s_{NN}}$ = 2.76 TeV central Pb-Pb collisions at ALICE experiment

2015/12/28

Daisuke Watanabe

outline

- Introduction
- Analysis procedure
- Correction
- Systematic uncertainties
- Results
- To do list
- summary

Introduction

Quark-gluon plasma (QGP)

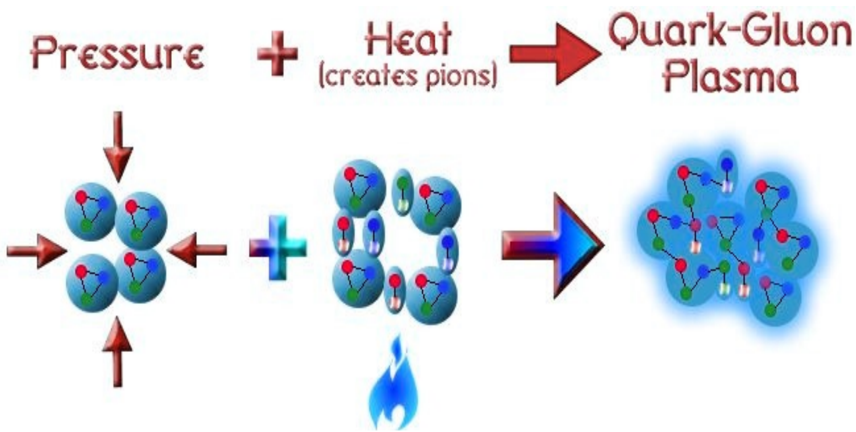

Quarks and gluons

- are confined in a hadron
- move freely beyond the boundary of hadrons at high temperature and energy density

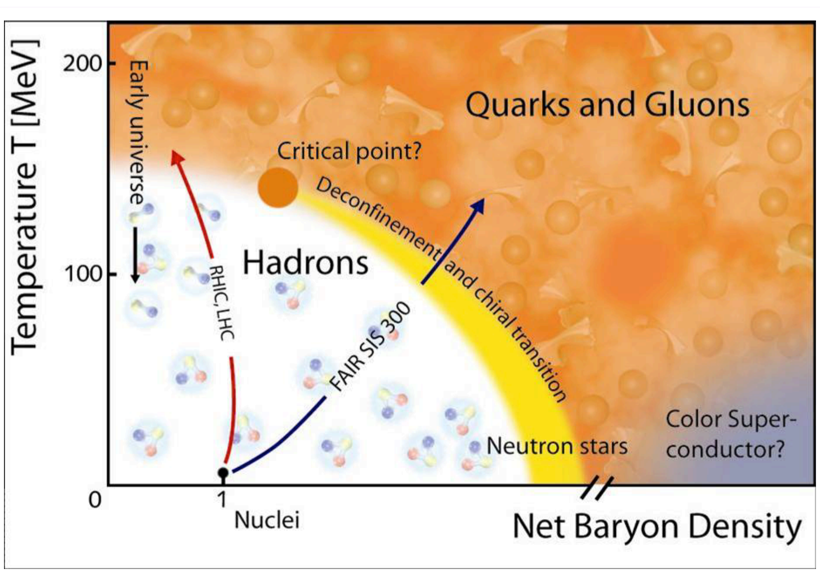

Quark-gluon plasma (QGP)

- created up to a few milliseconds after Big Bang
- T_c ~ 175 MeV, ε_c ~ 1 GeV/fm^3

Ultra relativistic heavy ion collision (RHIC, LHC)

Jet

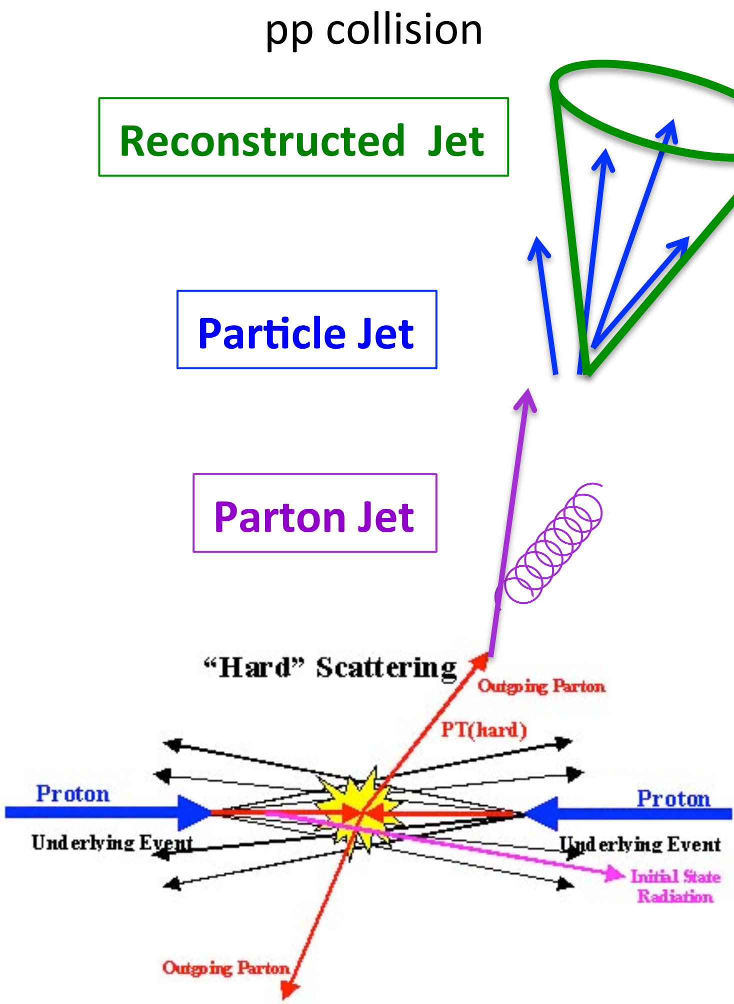

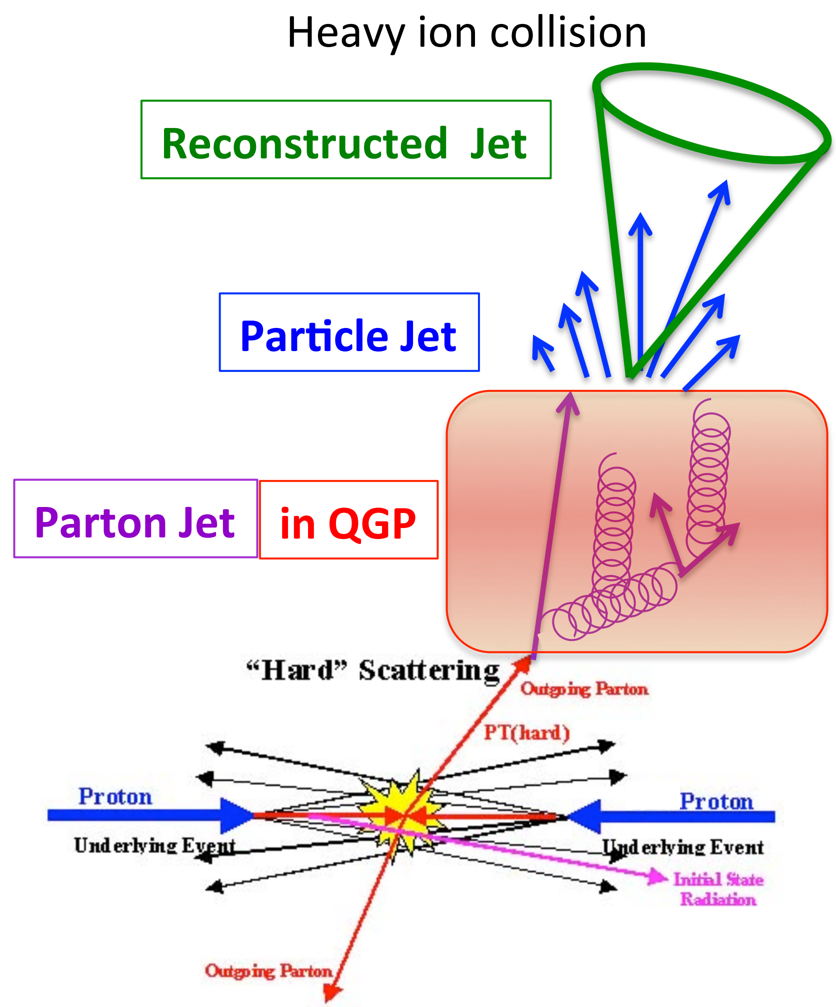

- Jets in heavy ion collisions lose their energy by collisional and radiative energy loss

Energy density and initial temperature

Energy density : ε = 15 GeV/fm³

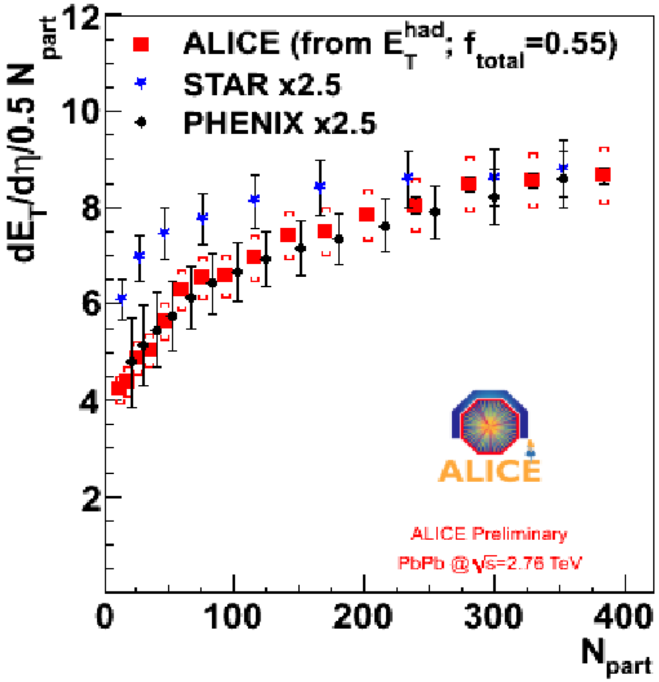

$$\varepsilon_{Bj} = \frac{1}{A_{\perp}\tau}\frac{dE_T}{dy}$$

Initial temperature : T= 304 MeV

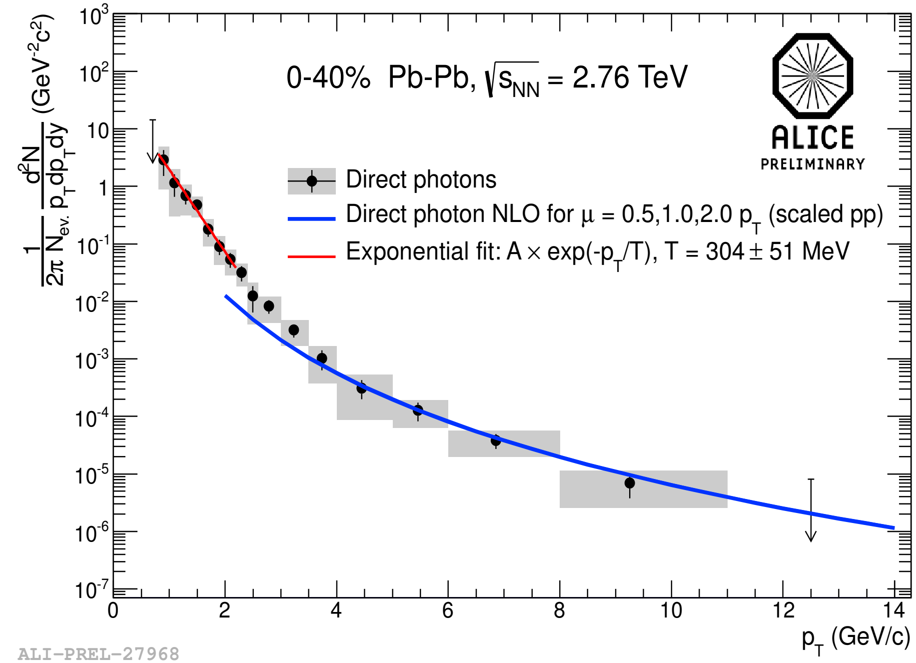

Exponential fit in the p_T range 0.8-2.2 GeV/c

- Energy density (3 times) and initial temperature (40 %) at the LHC increase compared with the RHIC due to collision energy

Azimuthal anisotropies

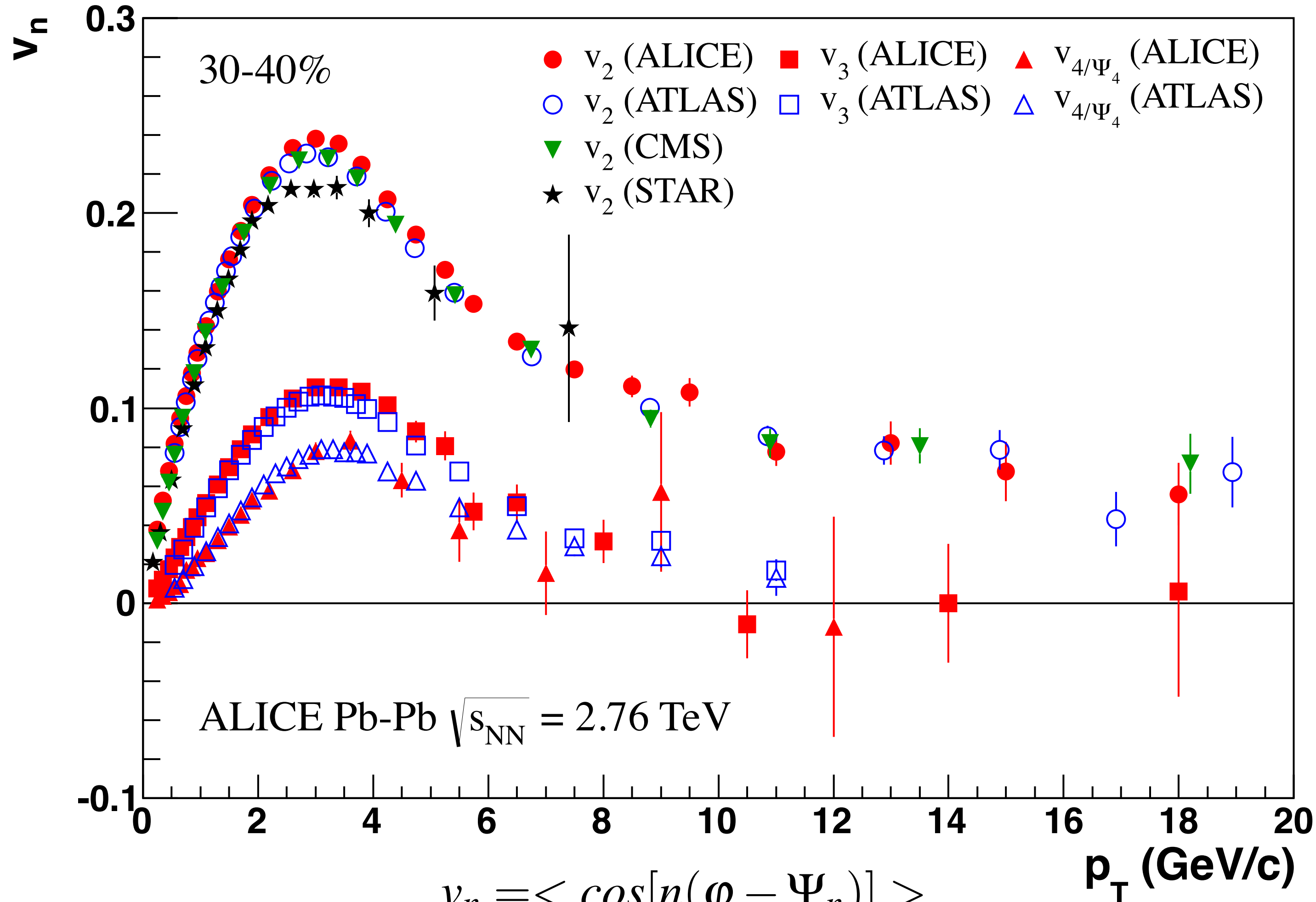

$$v_n = < cos[n(\varphi - \Psi_n)] >$$

The results of the LHC are good agreement with the RHIC in all p_T regions

High p_T physics of heavy ion collisions at the RHIC

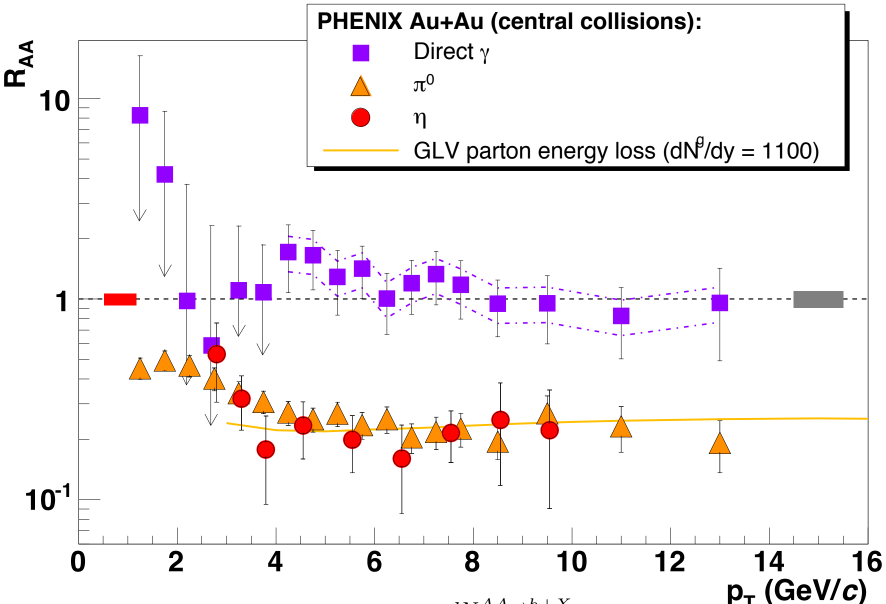

$$R^h_{AA}(p_T, b) \equiv \frac{\frac{dN^{AA\to h+X}}{d^2p_T}}{N_{bin}(b)\frac{dN^{pp\to h+X}}{d^2p_T}}$$

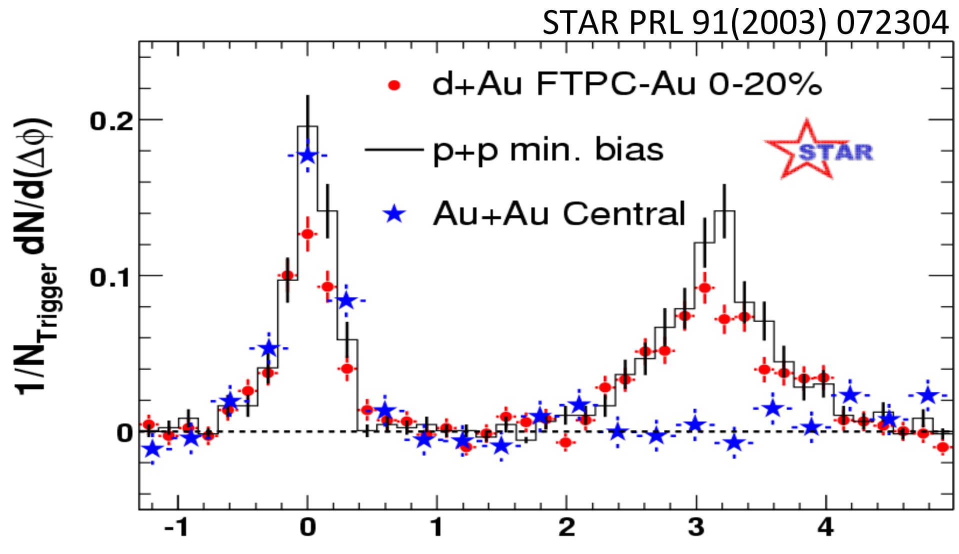

$4<p_T^{trig}<6$GeV/c, $2<p_T^{asso}<p_T^{trig}$

- Suppression of particle production in high p_T region were measured with experiments at the RHIC
- Nuclear modification factor R_{AA}
  - Suppression of π^0 of Au+Au compared with pp collisions scaled by # of collisions
- Two particle correlation
  - Suppression of away side peak of Au+Au compared with pp collisions

High p_T physics of heavy ion collisions at the LHC

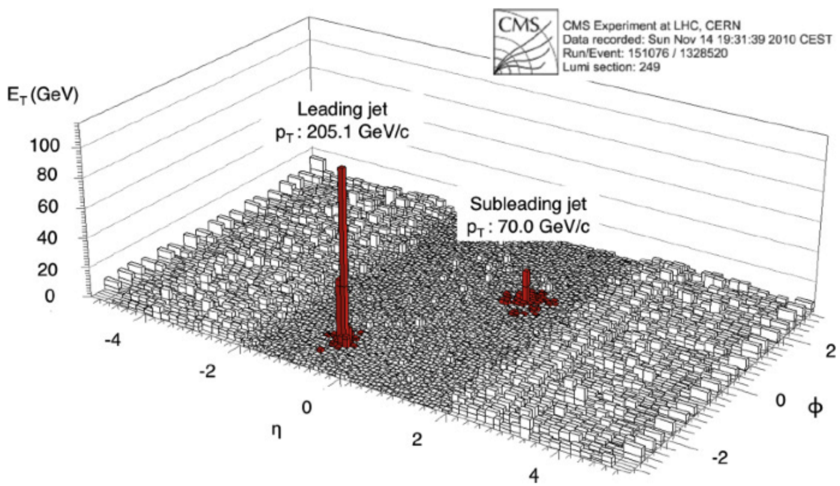

$A_j = (E^{lead} - E^{sublead})/(E^{lead} + E^{sublead})$

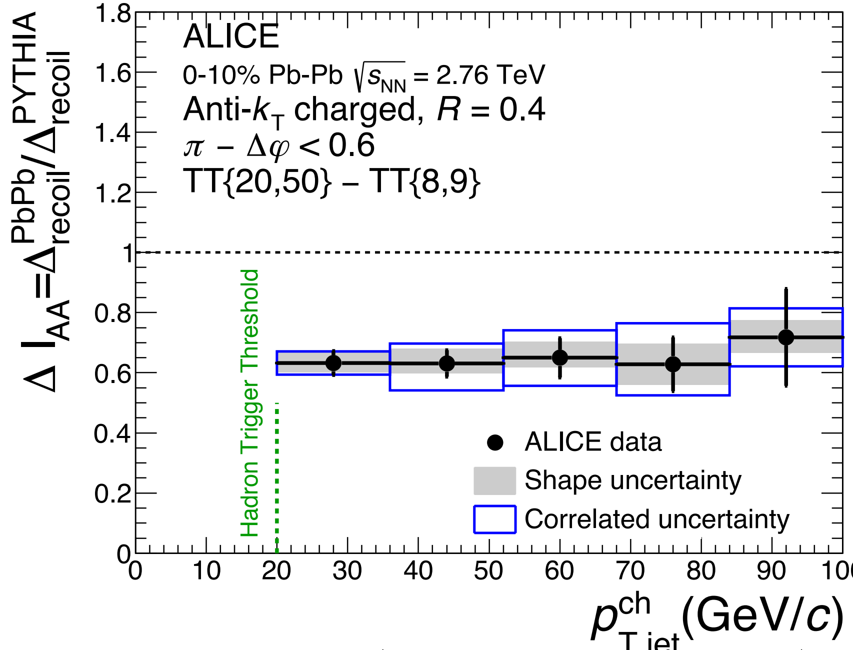

$$\Delta_{recoil} = \frac{1}{N_{trig}^{AA}} \frac{d^2 N_{jet}^{AA}}{dp_{T,jet}^{ch} d\eta_{jet}}\bigg|_{p_{T,trig} \in TT_{Sig}} - c_{ref} \cdot \frac{1}{N_{trig}^{AA}} \frac{d^2 N_{jet}^{AA}}{dp_{T,jet}^{ch} d\eta_{jet}}\bigg|_{p_{T,trig} \in TT_{Ref}}$$

- The experiments at LHC started direct measurements for jet and jet modification
- Di-jet energy un-balance measurement
  - can see sharp peak with huge transverse energy as leading jet and small peak compared with leading jet energy at opposite side
- Charged hadron-jet correlation measurement
  - Suppression of away side jet yields are observed with triggering high p_T charged hadrons

π^0-jet correlation

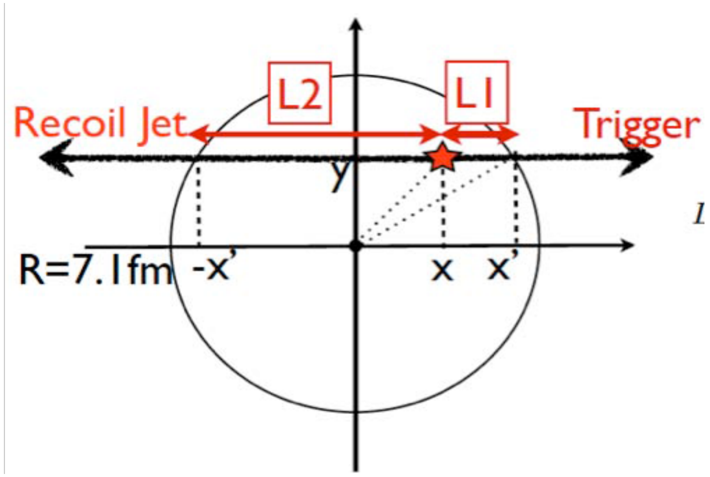

pi0 Et > 5GeV pi0 Et > 20GeV

Qhat=50 GeV2/fm

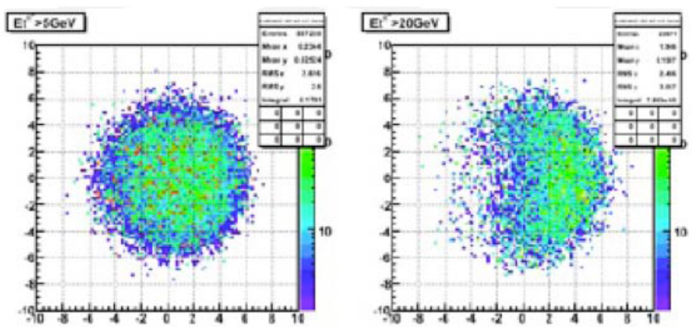

(CERN-LHCC-2010-011, ALICE-TDR-014-ADD-1)

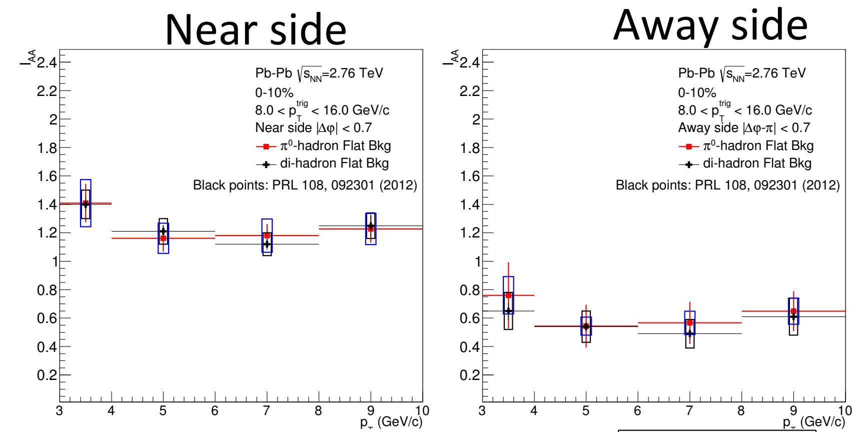

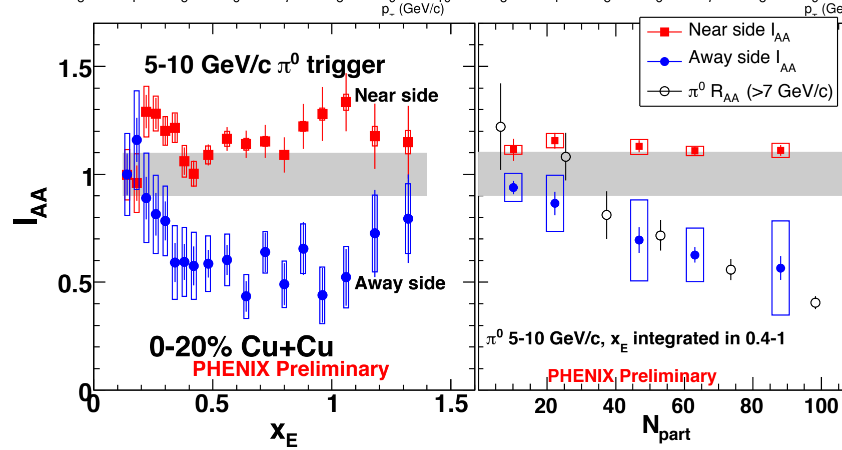

- Can control path length by tagging a recoil jet with triggered π^0 and changing p_T for π^0
- High p_T of π^0 -> longer path length of recoiling jets
- Direct measurement of path length dependence of “jet” quenching, not by hadron
- Observed enhancement of near side and suppression of away side from π^0- charged hadron

Physics motivation

- Signatures of QGP properties are observed by using several probes from the RHIC and LHC
- At the RHIC
  - Suppression of high momentum particles from nuclear modification factor R_{AA}
  - Suppression of away side peaks in two particle correlation
- At the LHC
  - Di-jet energy momentum unblance
  - Suppression of away side jet yields by triggering high momentum charged hadron

- Why jet analysis at the LHC
  - increase jet production cross section with increasing collision energy
  - can see a clear signal of jet modification compared with particle analysis
- Why π^0 – charged jet analysis
  - can observed behavior of jet production without effects of auto−correlation
  - can use a clear probe by using π^0 as trigger particles
- Physics motivation
  - check behavior of near side jet production with selecting high momentum hadron
  - select jets of different path-length in a medium at near and away sides

My activity

- Talk and poster
  - JPS 67th : Neutral pion and jet measurements in Pb-Pb collision at sqrt(sNN) = 2.76 TeV in ALICE (talk)
  - APW in Frascati : Hadron-jet and pi0-jet correlations in p+p and Pb+Pb (talk by D.sakata)
  - QM2012 : Jet-Hadron Azimuthal Correlation Measurements in pp Collisions at sqrt{s} = 2.76 TeV and 7 TeV with ALICE (poster)
  - JPS 68th : Neutral pion and jet measurements in Pb+Pb collisions at sqrt(sNN) = 2.76 TeV in ALICE (talk)
  - APW in Padova : pi0-jet correlations measurement for p+p and Pb+Pb 2.76 TeV (talk)
  - QM2014 : Jet azimuthal distributions with high pT neutral pion triggers in pp collisions from LHC-ALICE (poster)
  - ATHIC2014 : Jet azimuthal distributions with high pT neutral pion triggers in pp collisions at √s= 7 TeV from LHC-ALICE (talk)
  - TGSW2014 : Jet azimuthal distributions with high pT neutral pion triggers in pp collisions √s = 7 TeV from LHC-ALICE (talk)
  - QM2015 : Jet azimuthal distributions with high pT neutral pion triggers in pp 7 TeV and Pb-Pb 2.76 TeV collisions from ALICE at the LHC (poster)
- Detector work

  - Dcal construction (M1)
  - SRU construction and test (M2)
  - EMCal commisioning (D1, D2)
  - Shift taking (M2, D2, D3)

analysis

A Large Ion Collider Experiment (ALICE)

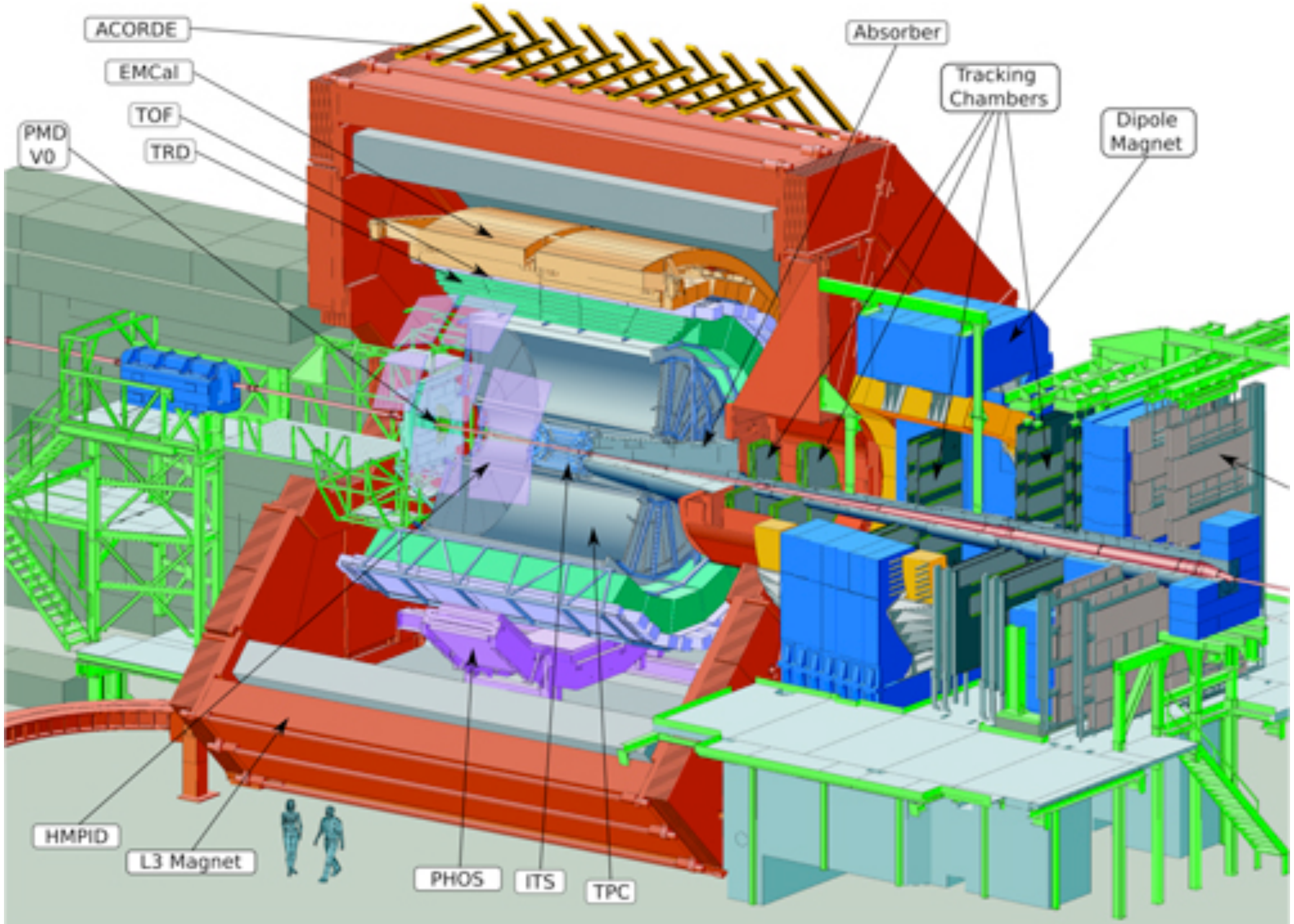

- Data set
  - pp collisions at $\sqrt{s}$ = 7 TeV with EMCal triggered (7 M)
  - Pb-Pb collisions at $\sqrt{s_{NN}}$ = 2.76 TeV with centrality 0- 10 % and EMCal triggered (12M)

Particle reconstruction detectors

EMCal (π^0)

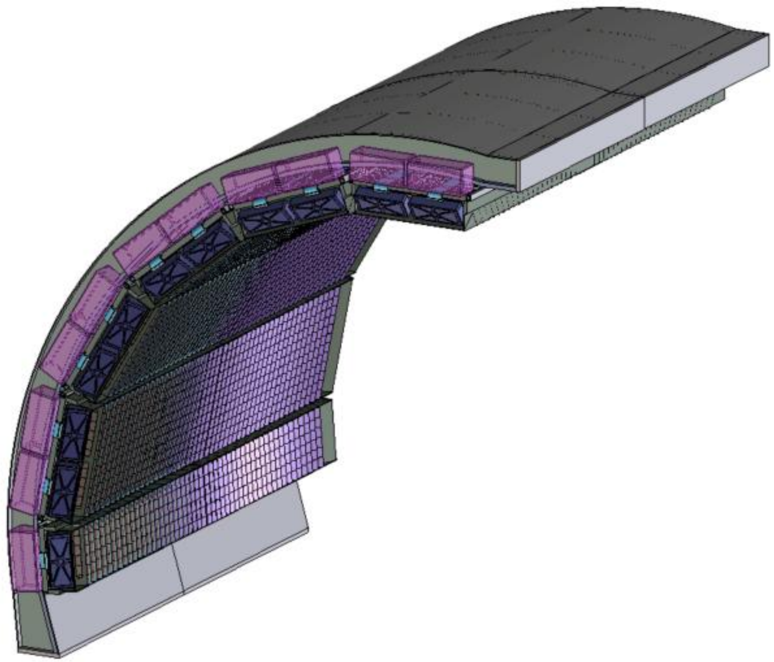

- EMCal : Pb-scintillator calorimenter
- Acceptance : $|\eta| < 0.7$, $\Delta\varphi = 110°$

ITS and TPC (charged particle)

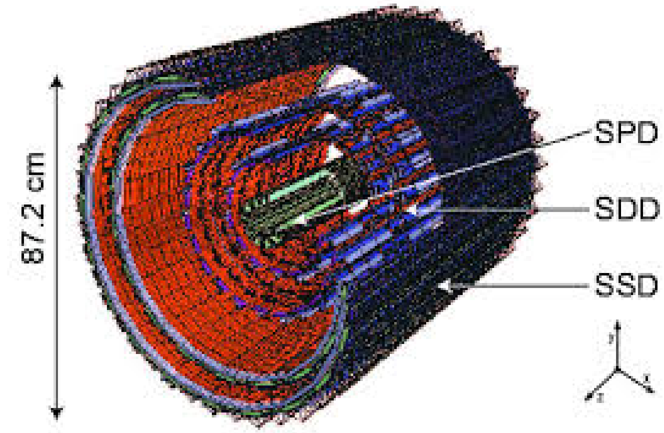

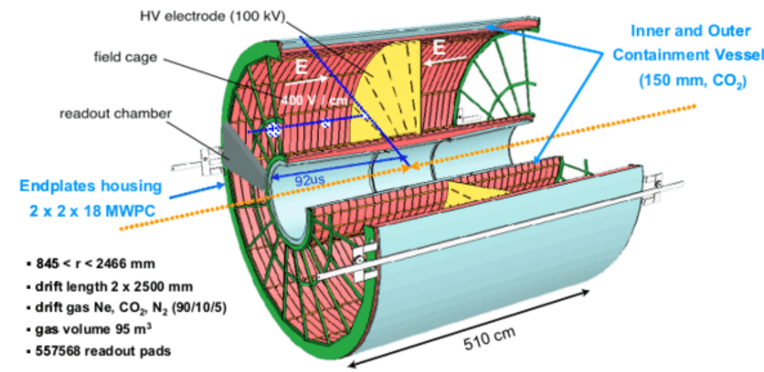

- ITS : Silicon-Pixel, Drift, Strip detector
- TPC : Time Projection Chamber
- Acceptance : $|\eta| < 0.9$, $\Delta\varphi = 360°$

Centrality determination

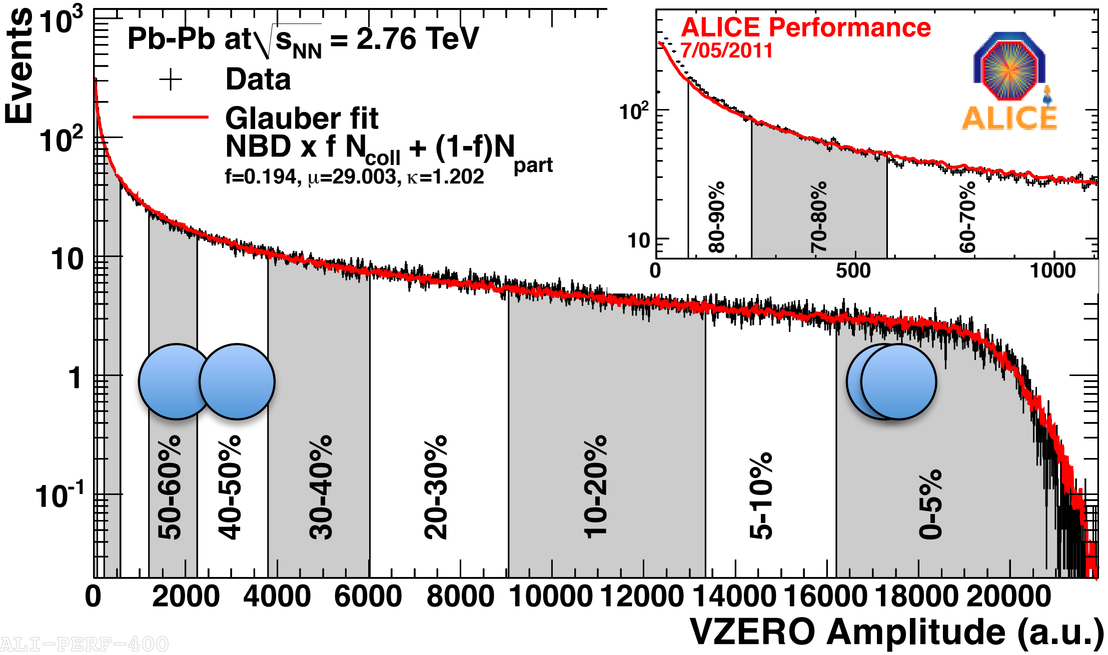

V0 detector

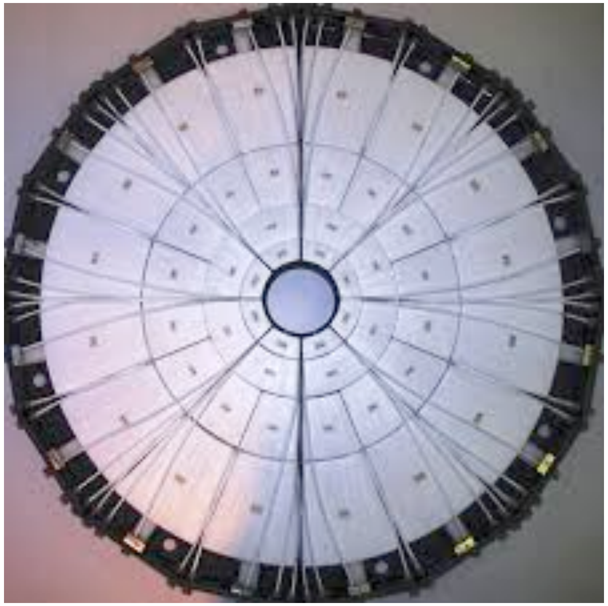

$-3.7 < \eta < -1.7$, $2.8 < \eta < 5.1$

- Centrality
  - used to classify events instead of impact parameter
  - determinated from Glauber fitting to V0 detector amplitude

EMCal trigger determination

- L0 trigger : OR of the 32 L0 calculated by the TRUs   (trigger threshold : 4.5, 5.5 GeV)
- L1- gamma trigger : Same patches as L0, but no boundary effect (trigger threshold : centrality)
- L1-jet trigger : Energy summed over a sliding window of 4 x 4 subregions
  (1 jet patch = 16 x 16 fastOr = 64 x 64 towers)

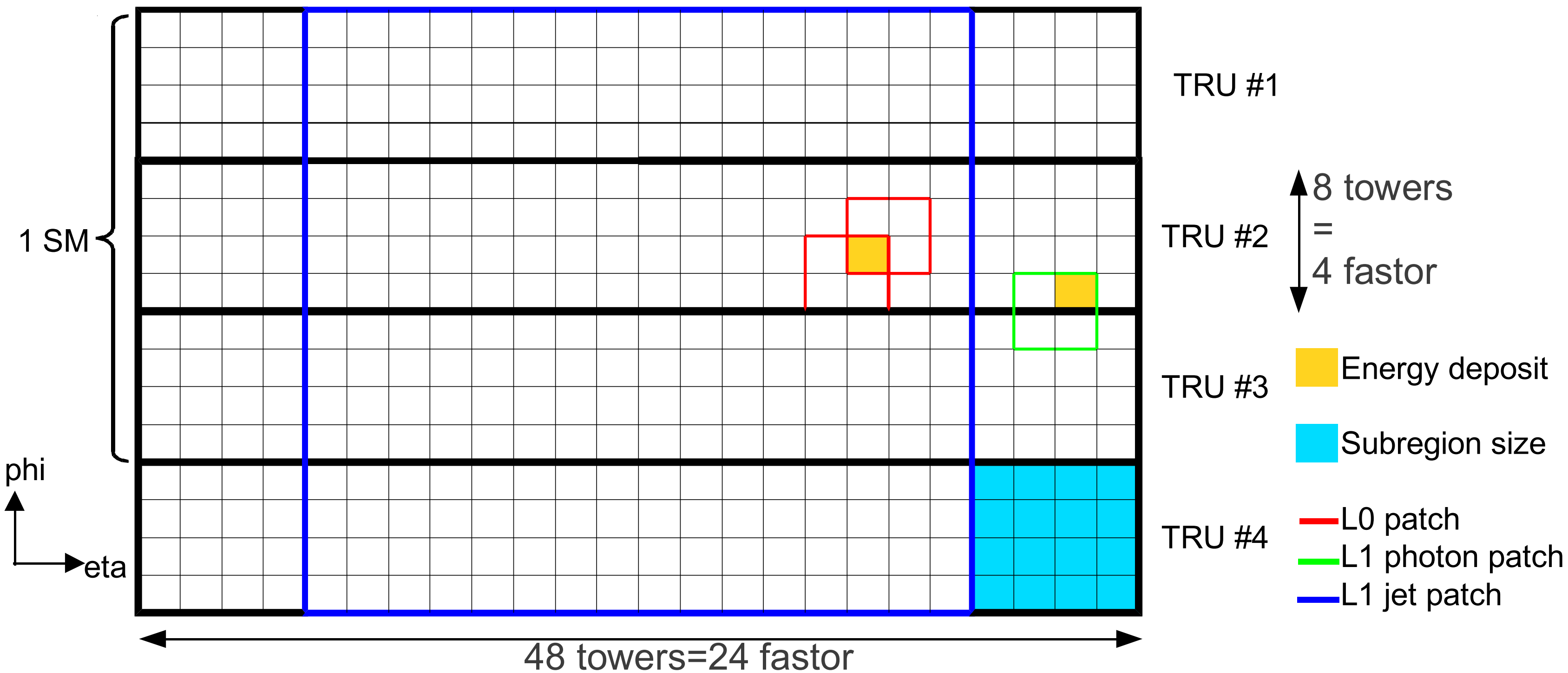

Event plane reconstruction

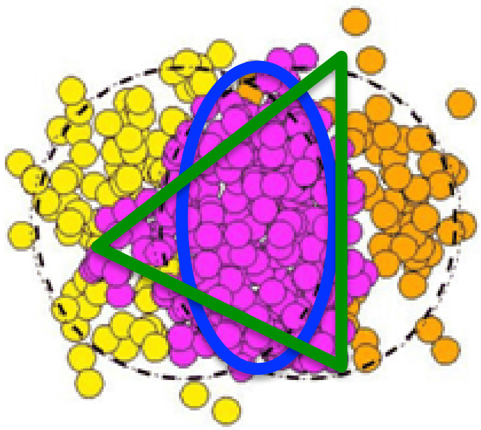

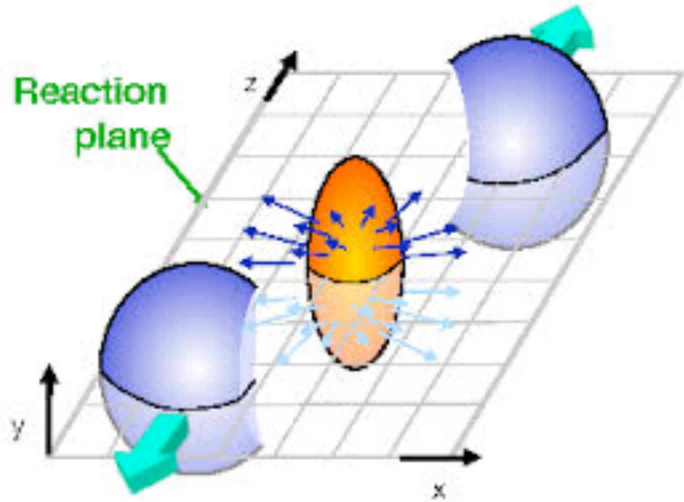

$$Q_y = \sum_{i=0} w_l \sin(n\phi_l) \quad , \quad Q_x = \sum_{i=0} w_l \cos(n\phi_l)$$

Re-centering

$$\Psi^{cor} = \frac{1}{n}\tan^{-1}\left(\frac{Q_y^{cor}}{Q_x^{cor}}\right)$$

$$Q_x^{cor} = \frac{Q_x - \langle Q_x \rangle}{\sigma_x}, \quad Q_y^{cor} = \frac{Q_y - \langle Q_y \rangle}{\sigma_y}$$

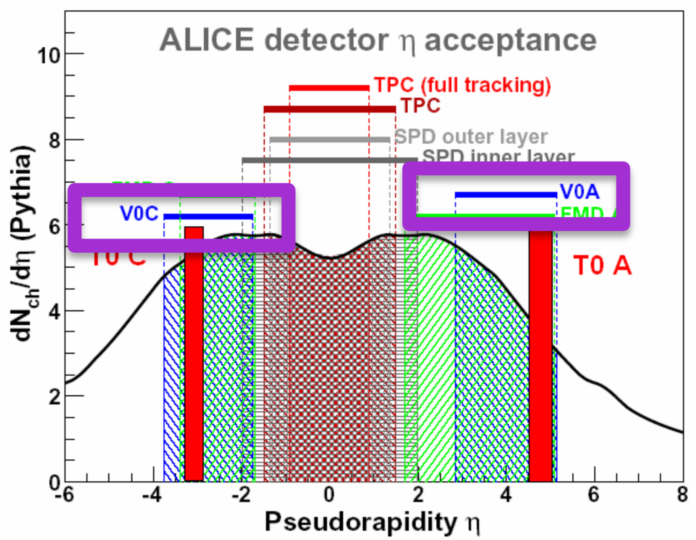

- Large η gaps to reduce non-flow effects
  - V0A side : > 0.9, V0C side : 2.0
- V0 gain and re-centering correction are applied

Energy dependence of shower shape

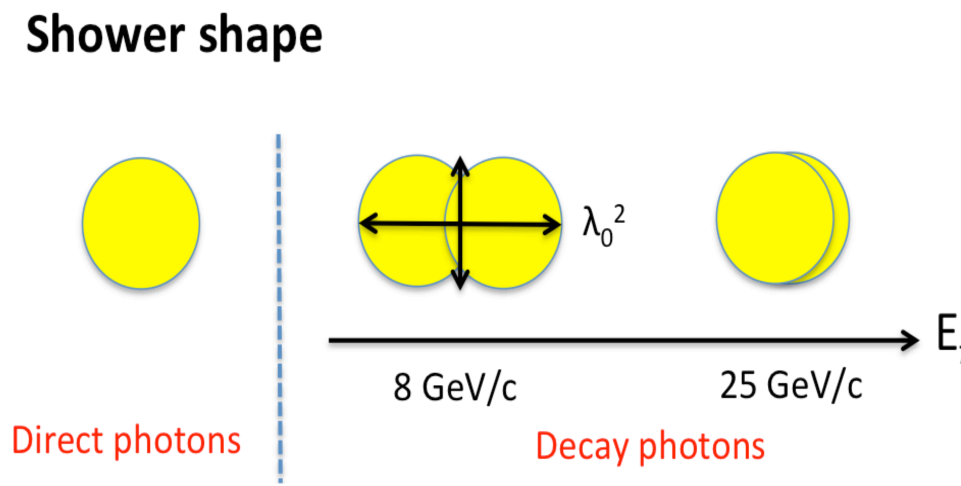

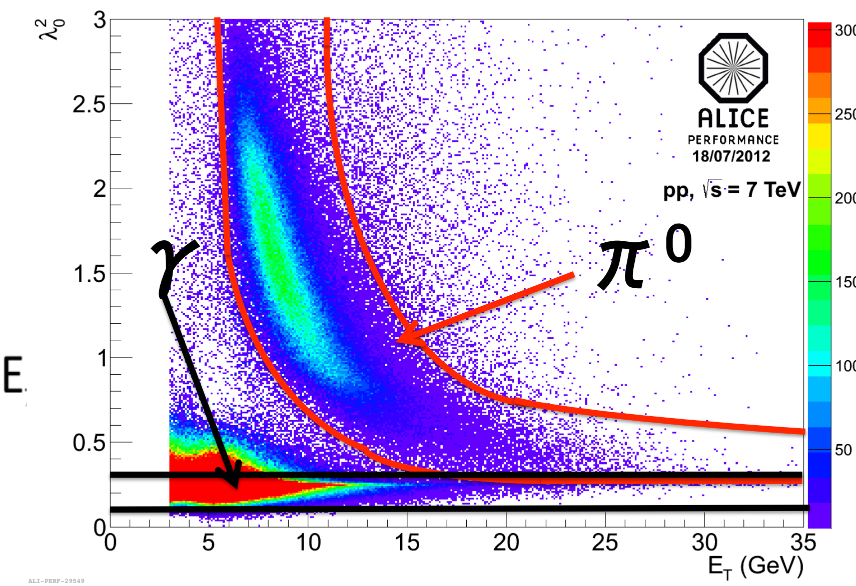

- The opening angle of the neutral mesons decay photon becomes smaller, when increasing the neutral meson energy due to Lorentz boost
- In the EMCAL, when the energy of π^0 is lager than 5 GeV
  - The two clusters of decay photon start to be close
  - The electromagnetic showers start to overlap

The procedure of cluster splitting method ($8 < p_T^{\pi 0}$)

ALICE

1. Select neutral cluster with $\lambda_0^2 > 0.3$, track matching etc.
2. Find local maxima in the cluster.
3. Split the cluster in new two sub-clusters taking the two highest local maxima cells and aggregate all towers around them.(form 3x3 cluster)
4. Get the two new sub-clusters, and calculate energy asymmetry and invariant mass

$$E(Local\,Max\,candidate) - E(ad\,jacent\,cell) > \Delta E_{LM}$$

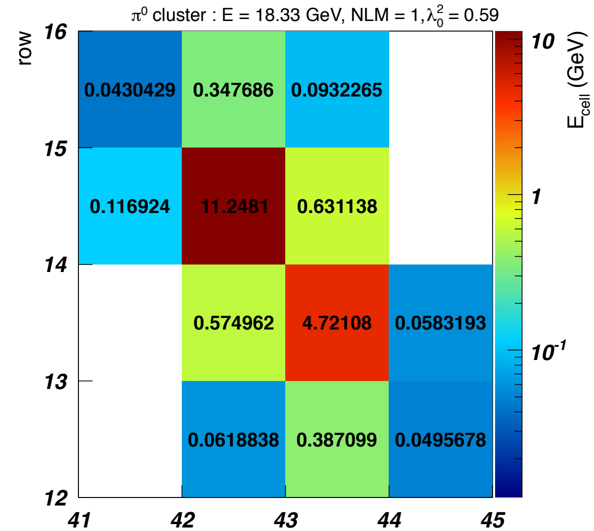

- Overlap cell energy is calculated by using weight of each local maxima cell energy

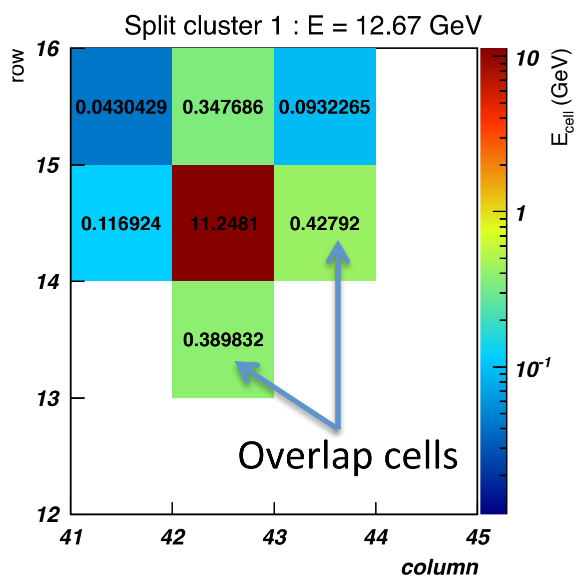

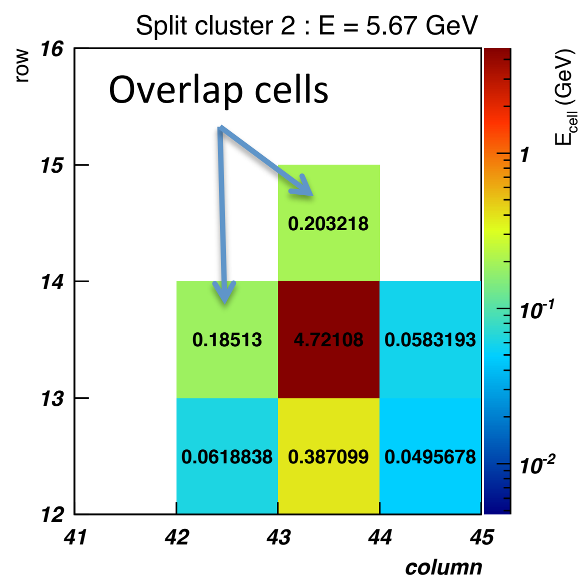

Invariant mass reconstruction (cluster splitting method)

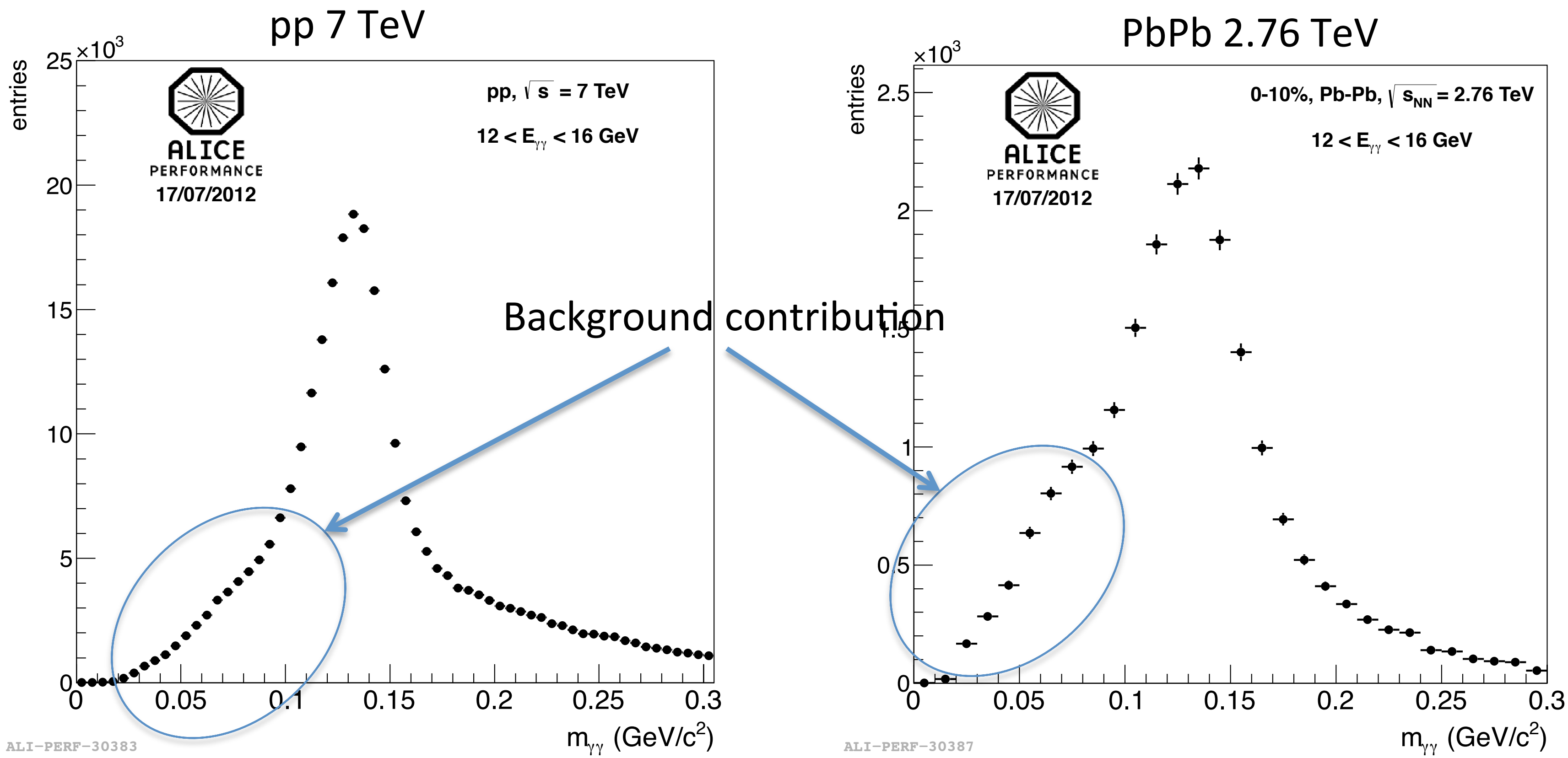

- 3σ invariant mass window from peak mean is selected as π^0
- We can identify π^0 up to 40 GeV/*c*

Charged jet reconstruction (FASTJET)

$$d_{ij} = \min(k_{ti}^{2p}, k_{tj}^{2p}) \frac{\Delta R^2}{R^2} \begin{cases} p = 1 & k_T \text{ algorithm} \\ p = 0 & \text{Cambridge/Aachen algorithm} \\ p = -1 & \text{anti-}k_T \text{ algorithm} \end{cases}$$

Procedure of jet finding

1. Calculate particle distance : d_{ij}
2. Calculate Beam distance : $d_{iB} = k_{ti}^{2p}$
3. Find smallest distance (d_{ij} or d_{ib})
4. If d_{ij} is smallest combine particles
   If d_{ib} is smallest and the cluster momentum larger than threshold call the cluster Jet

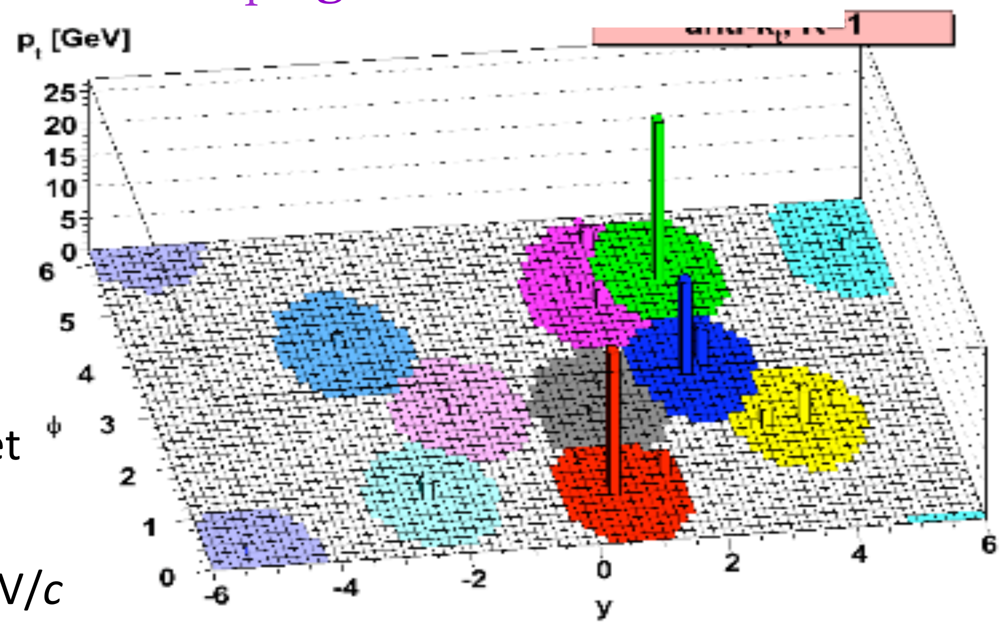

Parameters

- R size ($= \sqrt{\Delta\phi^2 + \Delta\eta^2}$) : 0.4
- p_T cut on a single particle : 0.15 GeV/*c*
- Jet energy threshold : 10 GeV/*c*
- Jet acceptance : $|\eta| < 0.5$, $0 < \phi < 2\pi$

Jet p_T bin:[10-20],[20-40],[40-80] GeV/c
Leading particle p_T cuts : > 7, 9 GeV/c

E-by-E calculation of BKG density in Pb-Pb collisions

ALICE

- In order to estimated the underlying event energy from hydrodynamic flow, fit to each event's $\frac{d\Sigma p_T}{d\varphi}$ distribution (with $0.2 < p_T < 5$ GeV/c)

$$\rho(\varphi) = \rho_0 \times \left(1 + 2\left\{v_2^{\text{obs}}\cos(2[\varphi - \Psi_{2,EP}]) + v_3^{\text{obs}}\cos(3[\varphi - \Psi_{3,EP}])\right\}\right)$$

Jet p_T is corrected on a jet-by-jet basis, where A is the jet area and ρ_{local} is flow modulation UE energy density

$$p_{T,chjet} = p_{T,chjet}^{raw} - \rho_{local}A \qquad \rho_{\text{local}} = \frac{\langle\rho\rangle}{2R\rho_0}\int_{\varphi-R}^{\varphi+R}\rho(\varphi)d\varphi.$$

Procedure of Local BKG density estimation

1. Calculate ρ_0 by using median method
2. Fill a histogram of the ϕ of soft track ($0.2<p_T<5.0$)
3. Exclude area of the leading jet of an event from the sample and all tracks within the same η region of leading jet are rejected from the sample ($|\eta_{track}-\eta_{leading\ jet}| < R$)
4. Calculate the event plane (applied V0 gain correction and re-centering)
5. Fit a histogram
6. Check the fitting quality (Reject fits when PDF(x^2) < 0.01 and any ϕ $\rho(\phi) < 0$)
7. If a fitting is failed, the median method is used to estimate BKG density instead of $\rho(\phi)$

Centrality:0~10%

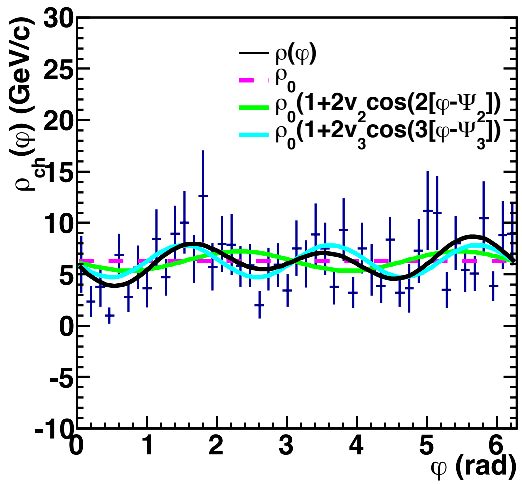

Number of bins in $\frac{d\Sigma p_T}{d\varphi}$ spectrum ≈ $\sqrt{N_{entries}}$

Filled track p_T renge : $0.2 < p_T^{track} < 5$ GeV/c

Jet p_T spectrum with two different event plane regions

Work in progress

Local ρ(ϕ)

Median <ρ>

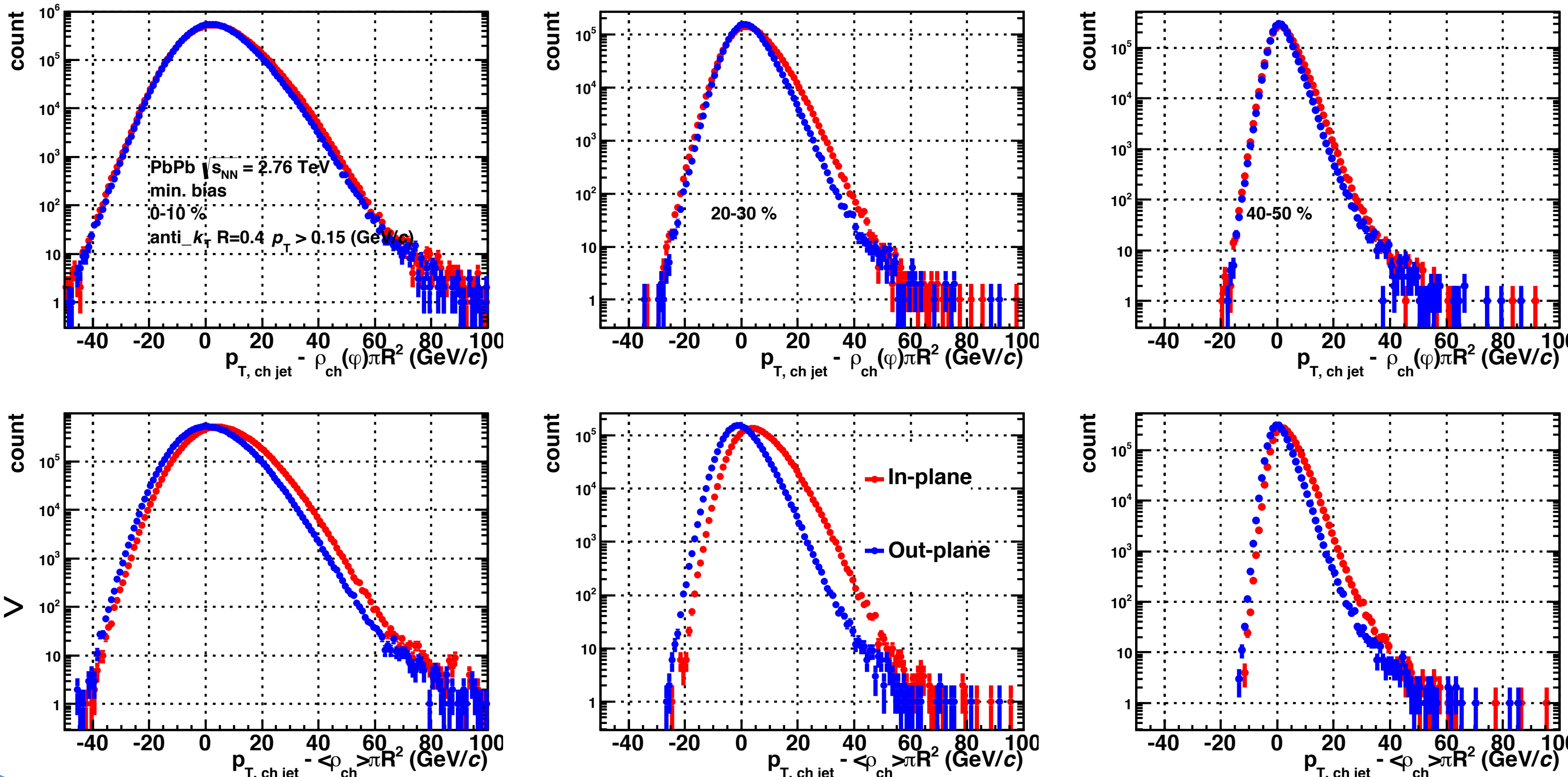

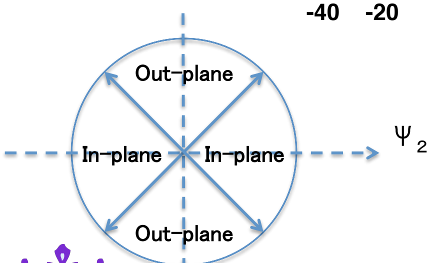

- Distributions of median method have the differences between in and out-of-plane due to flow effect

Flat background subtraction in azimuthal correlation

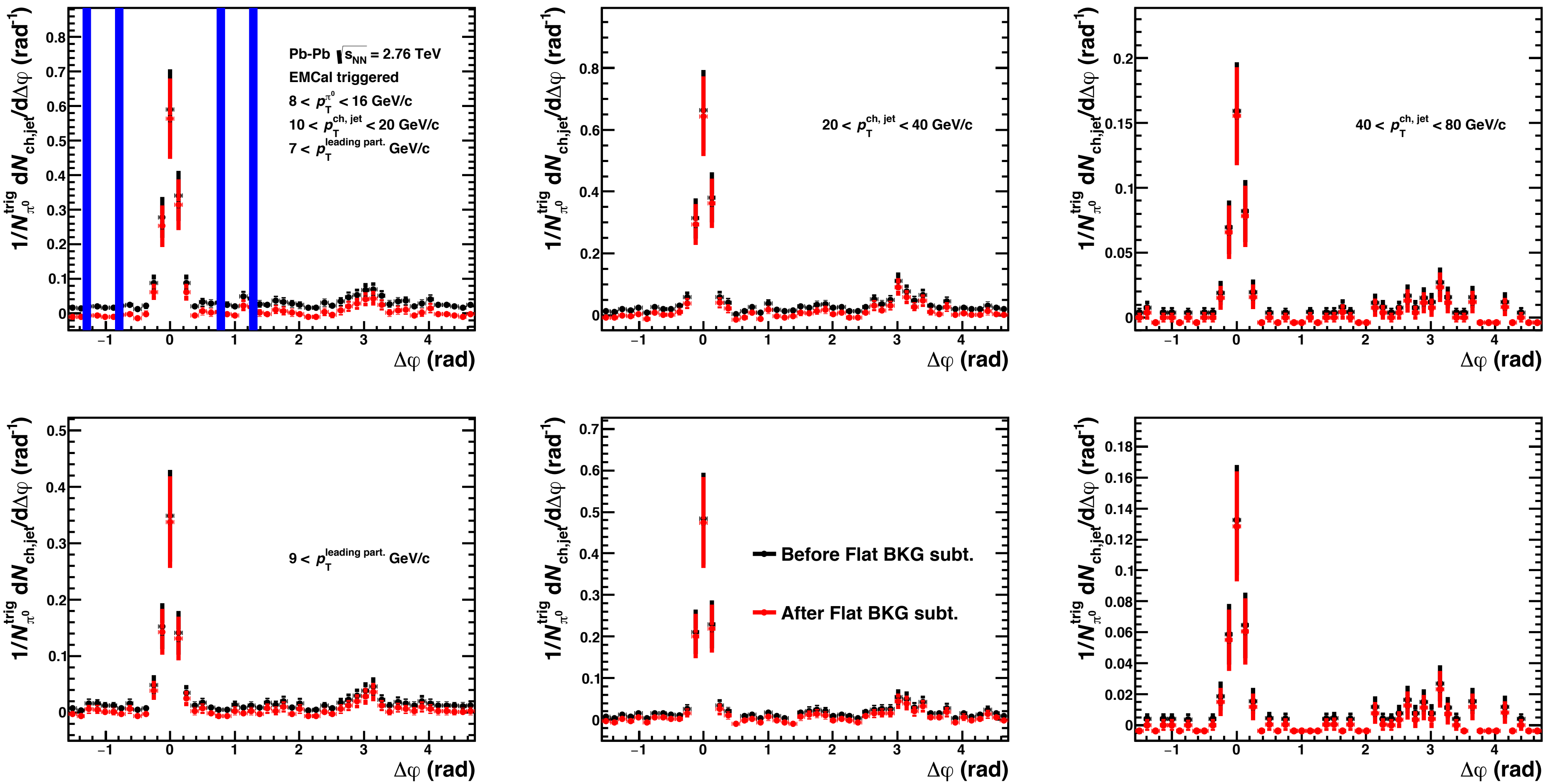

1. Take 4 bins in the valley region on the left and right side from a near side peak region
2. Calculate the average background value from 8 bins in valley regions

Correction

- Detector acceptance correction (event mixing method)
  - 100 events (pp) and 10 events (Pb-Pb) pool
  - Z vertex = (-10, 10) cm, 2 cm wide bins
  - Track multiplicity, 9 bins on multiplicity (pp)
  - Centrality, 10 bins (Pb-Pb)

$$C(\Delta\varphi) = \frac{\int N_{pair}^{mixed}(p_T^{\pi^0}, \Delta\varphi) d\Delta\varphi}{\int N_{pair}^{same}(p_T^{\pi^0}, \Delta\varphi) d\Delta\phi} \cdot \frac{N_{pair}^{same}(p_T^{\pi^0}, \Delta\varphi)}{N_{pair}^{mixed}(p_T^{\pi^0}, \Delta\varphi)}$$

$$\frac{1}{N_{trig}^{\pi^0}} \frac{dN^{jet}}{d\Delta\phi} = \frac{\int N_{pair}^{same}(p_T^{\pi^0}, \Delta\phi) d\Delta\phi}{N_{trig}^{\pi^0}(p_T^{\pi 0})} \cdot C(\Delta\phi)$$

- Jet reconstruction efficiency correction (bin-by-bin correction)
  - Jet finding efficiency : 3 different jet p_T bins

    -> 10-20, 20-30, 30 > GeV/*c*

$$\frac{1}{N_{trig}^{corrected}} \frac{dN_{pair}^{corrected}}{d\Delta\phi} = \frac{1}{\Sigma_{\Delta p_{T,(i)}} \frac{1}{\varepsilon_i^{\pi^0}} \cdot N_{trig(i)}^{\pi^0}(\Delta p_T^{trig})} \sum_{\Delta p_{T,(i)}} \frac{1}{\varepsilon_i^{\pi^0} \varepsilon^{jet}} \frac{dN_{pair(i)}^{Raw}}{d\Delta\phi}(\Delta p_T^{trig})$$

Systematic uncertainty

- Shower shape parameter(λ_0^2) cut
- Invariant mass window
- Flat background (only Pb-Pb)
- π^0 identification purity (pair purity)
- Unfolding method ~ 5 %

Result

π^0 p_T region : $8 < p_T < 16$ GeV/c

Jet p_T bin : [10-20], [20-40], [40-80] GeV/c

Leading particle p_T threshold : > 7, 9 GeV/c

Azimuthal correlation pp 7 TeV

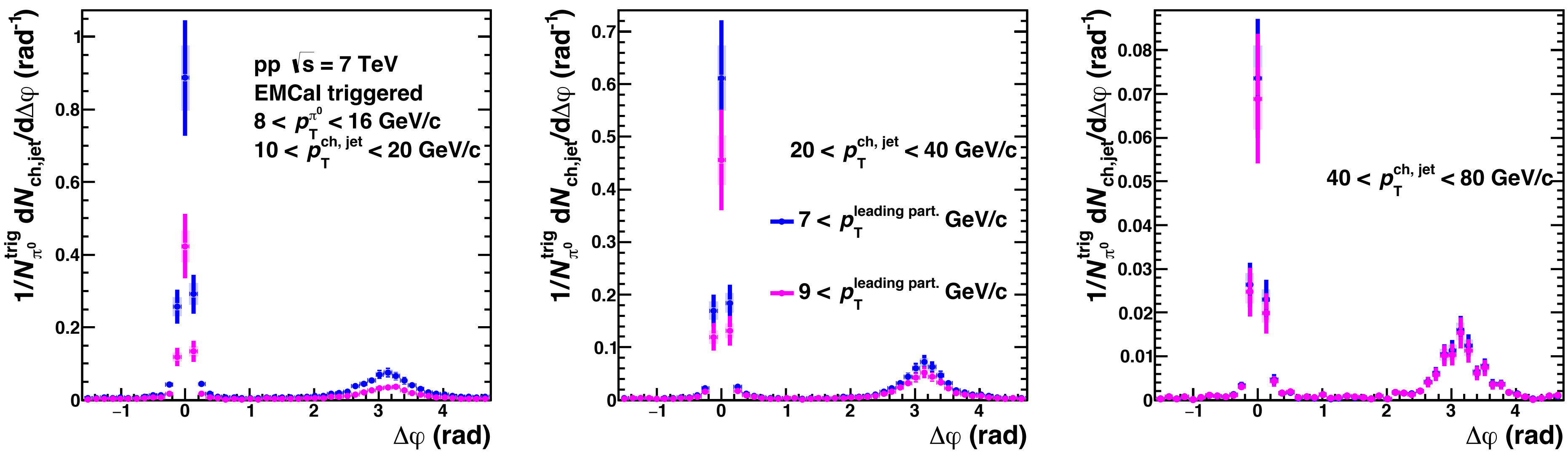

- Two clear jet-like peaks are observed, indicating that high p_T π^0 production is correlated with jet production
- Associated jet yields in the low momentum regions decrease with increasing the leading particle momentum thresholds
- Away side peaks become sharp with increasing the associated jet momentum regions

Azimuthal correlation in Pb-Pb 2.76 TeV

ALICE

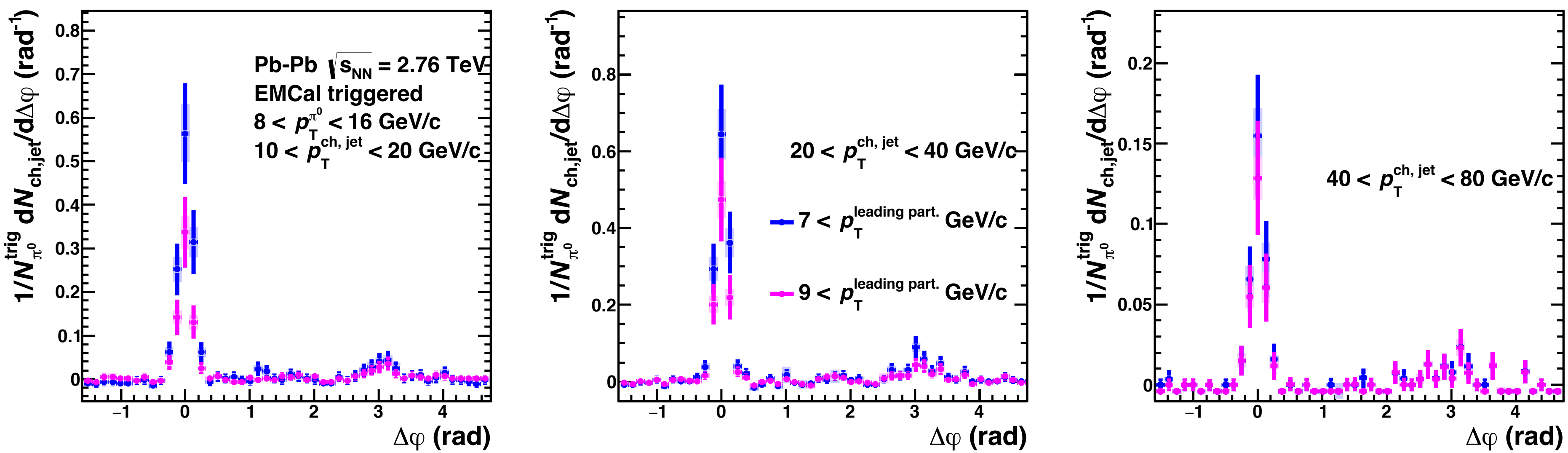

- Clear near side peaks in the all jet momentum regions are observed similar to the pp 7 TeV results
- Small peaks in away sides are observed from Di-jet production
- Evolution of jet momentum range of side shapes are not seen

Comparison of azimuthal correlation of pp 7 TeV and Pb-Pb 2.76 TeV

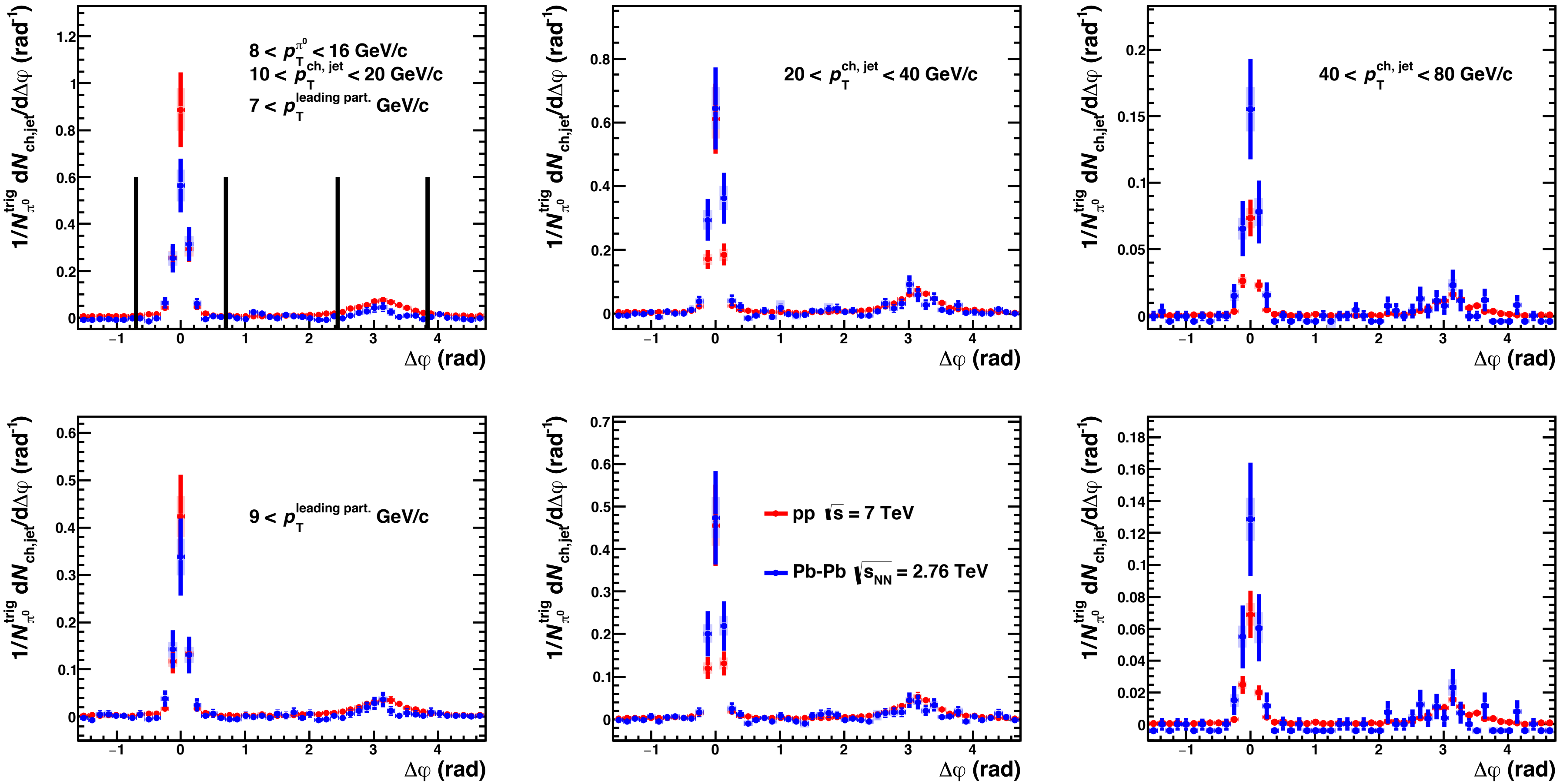

near side : $|\Delta\phi| < 0.7$, away side : $|\Delta\phi - \pi| < 0.7$

- Enhancement of near side jet yields in Pb-Pb collisions increases with increasing the associated jet momentum regions
- Shape differences between pp and Pb-Pb collisions are not seen clearly

Near and away side jet yields with normalized # of trigger

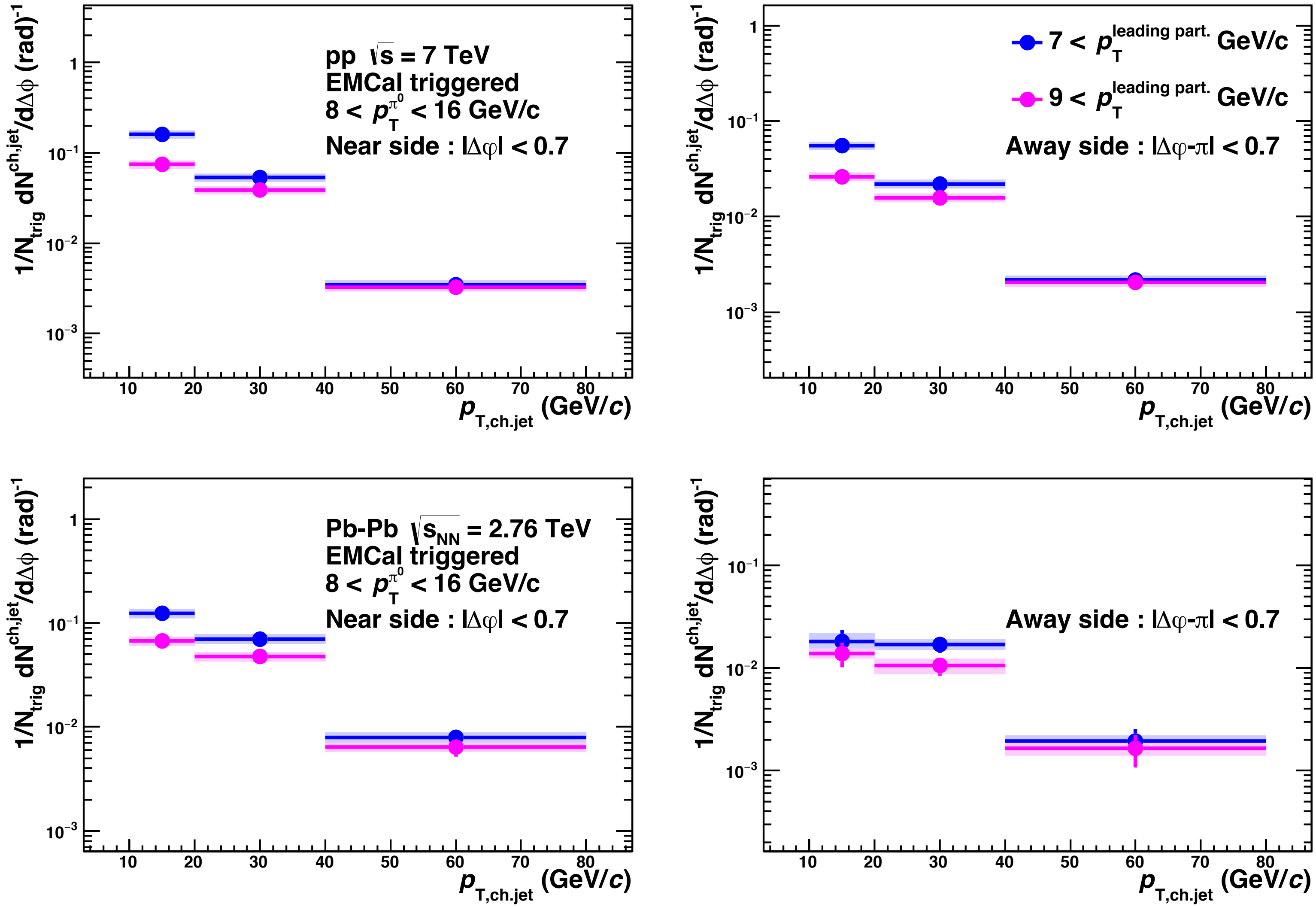

Ratio of per trigger yields I_{AA}

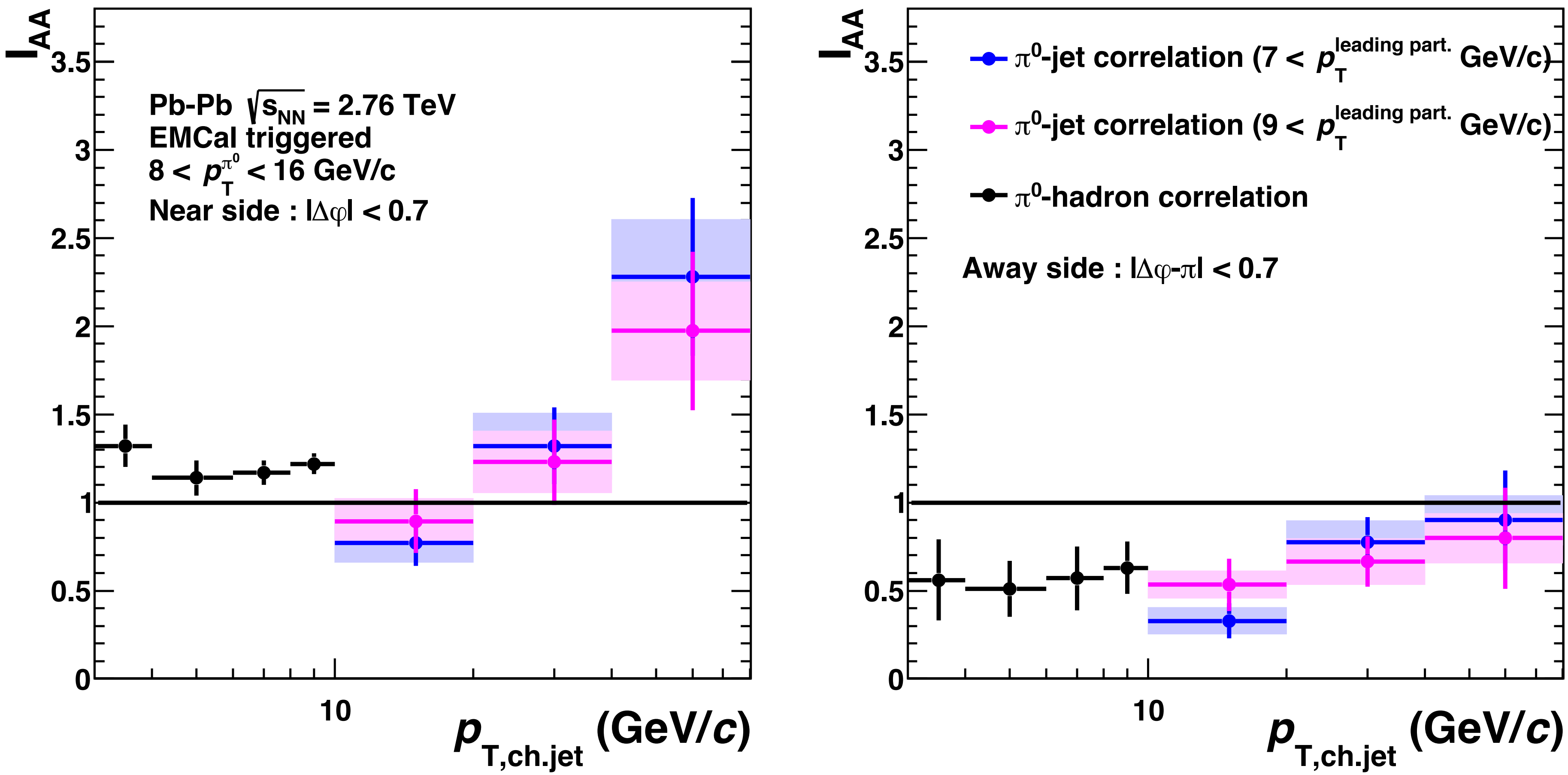

$$I_{AA}(p_T^{\pi^0}, p_{T,ch.jet}) = \frac{Y_{Pb-Pb}(p_T^{\pi^0}, p_{T,ch.jet})}{Y_{pp}(p_T^{\pi^0}, p_{T,ch.jet})}$$

- Enhancement of jet yields on the near side
- Suppression of jet yields on the away side
- Same results with π^0-hadron correlation analysis

筑波大学
University of Tsukuba

Gaussian fit at near and away side in pp 7 TeV

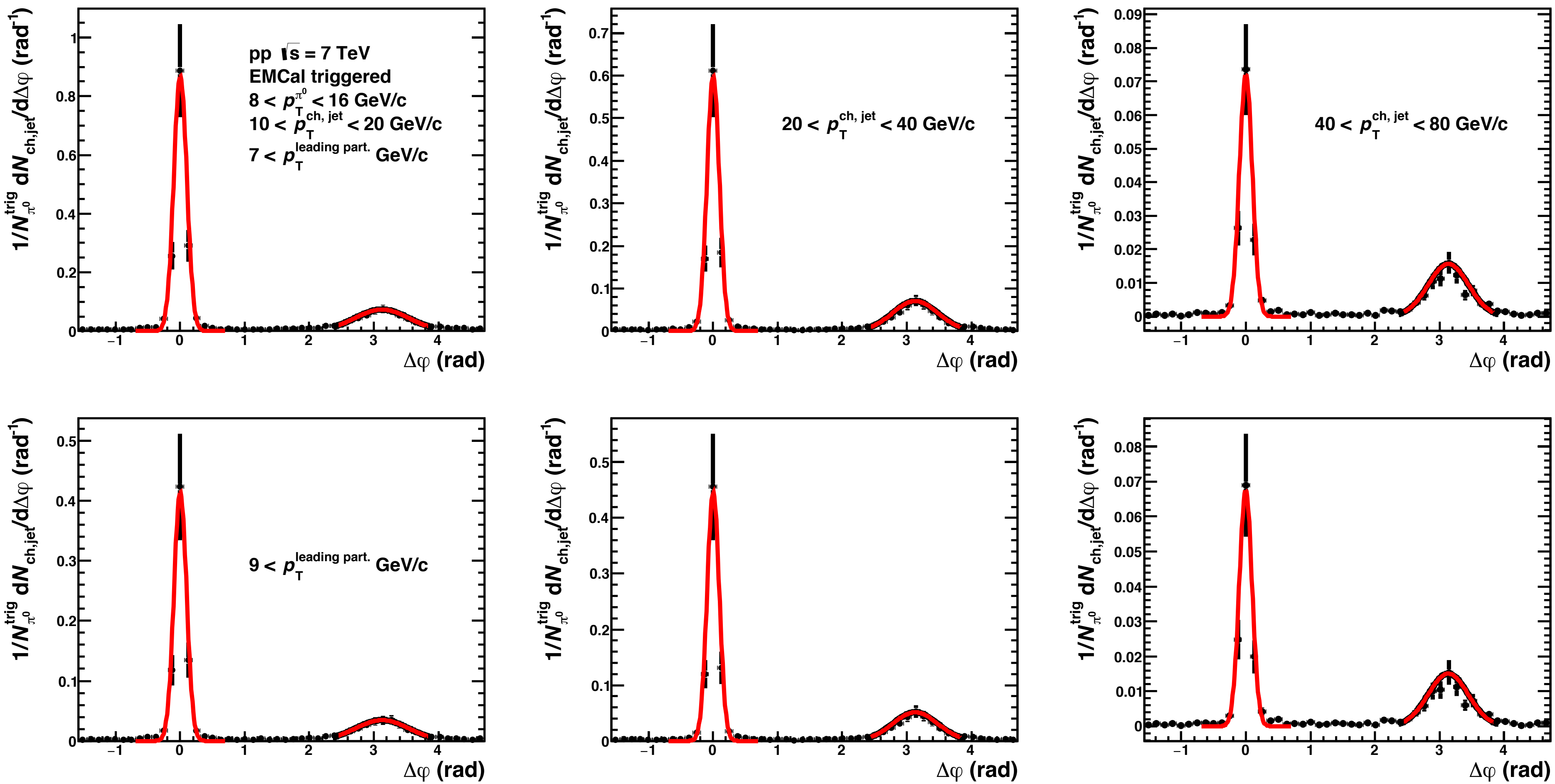

Fit region : near side |Δϕ| < 0.7, away side |Δϕ-π| < 0.7, fit function : Gaus

Gaussian fit at near and away side in Pb-Pb 2.76 TeV

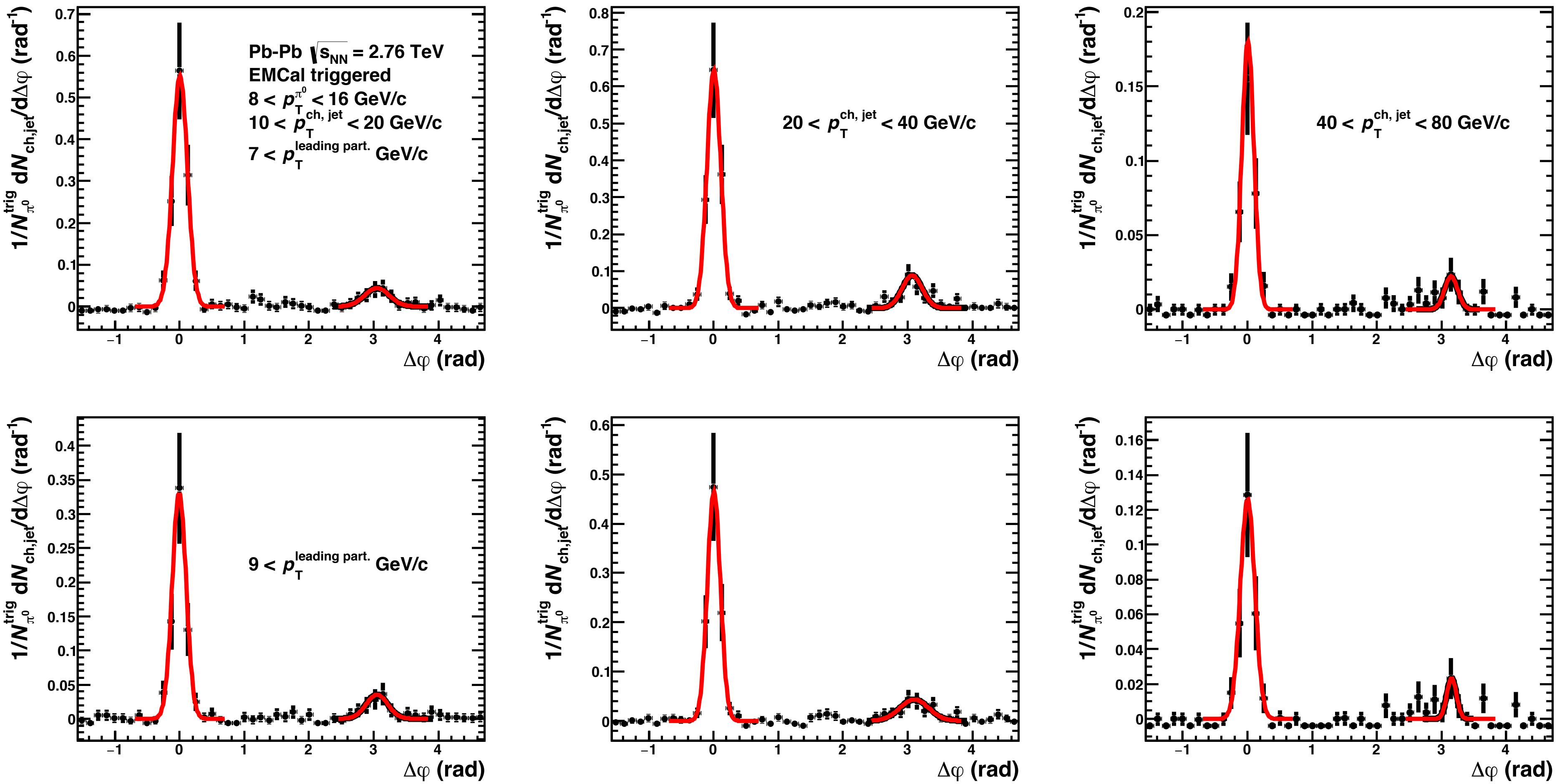

Fit region : near side |Δϕ| < 0.7, away side |Δϕ-π| < 0.7, fit function : Gaus

Near and away side width as a function of jet p_T

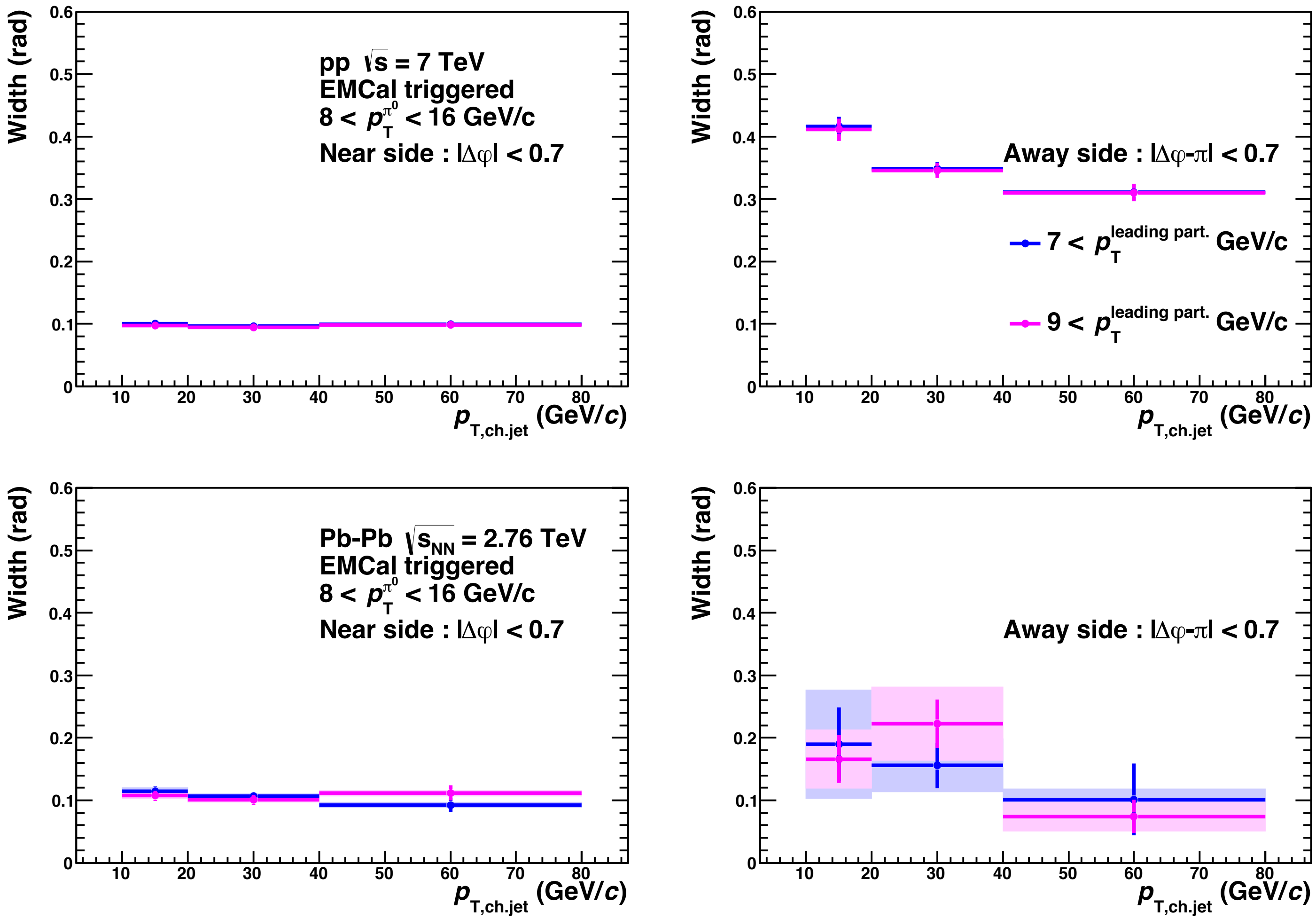

- Away side widths in pp collisions decrease with increasing jet momentum regions
- Differences between pp and Pb-Pb in near side collisions are not seen
- Will measure RMS instead of Widths

Summary

ALICE

- π^0-jet correlations have been measured in pp at $\sqrt{s}$ = 7 TeV and Pb-Pb $\sqrt{s_{NN}}$ = 2.76 TeV
- Two jet peaks are observed in azimuthal correlations in both collision systems
- Enhancement of Near side jet yields in Pb-Pb collisions are observed, while Away side jet yields are suppressed due to energy loss in the medium.
- Away side widths in pp collisions decrease with increasing the associated jet momentum regions
- No significant differences of near and away side widths can be seen between pp collisions and Pb-Pb collisions in statistic and systematic uncertainties.
- To do list

  - correct jet yields by using unfolding method.

  - Comparison of PHYTHIA embedded jets

Back up

π^0 reconstruction

Invariant mass method ($4 < p_T < 8$ GeV/c)

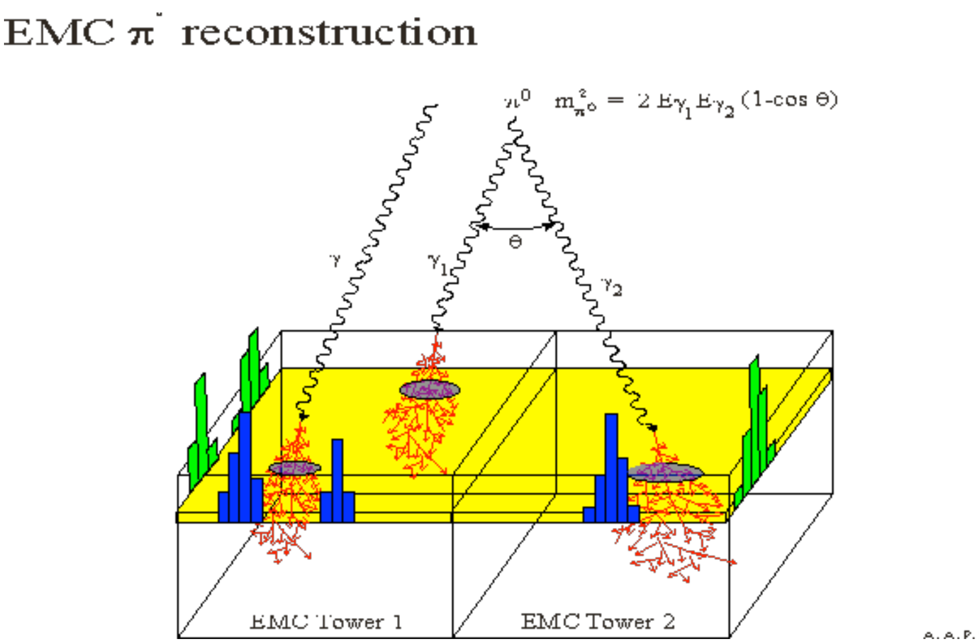

$$M_{\gamma\gamma} = \sqrt{2E_1E_2(1-\cos\Delta\phi)}$$

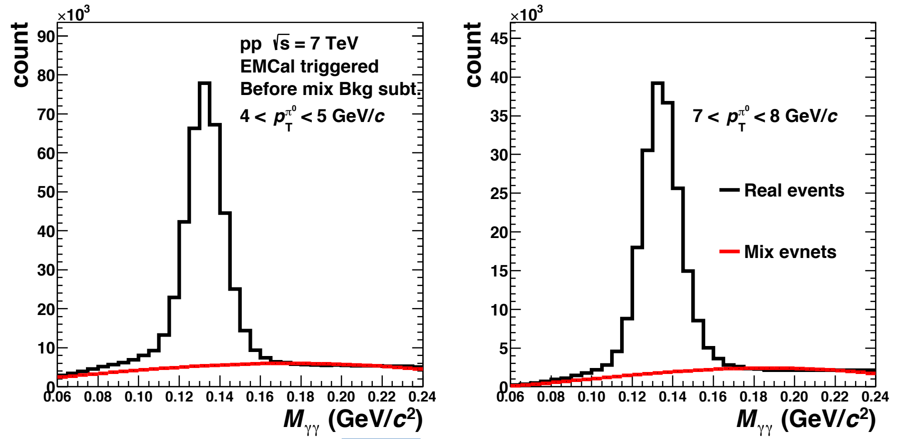

Subtraction of mix bkg

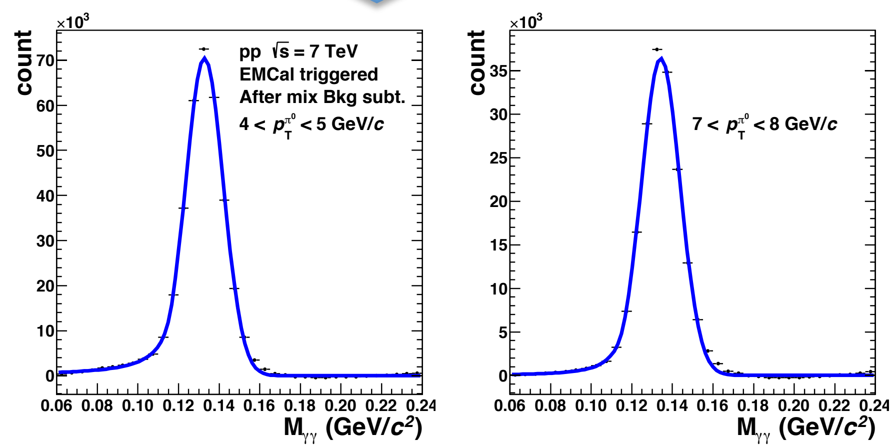

Fit function : Crystall ball function

Shower shape cut

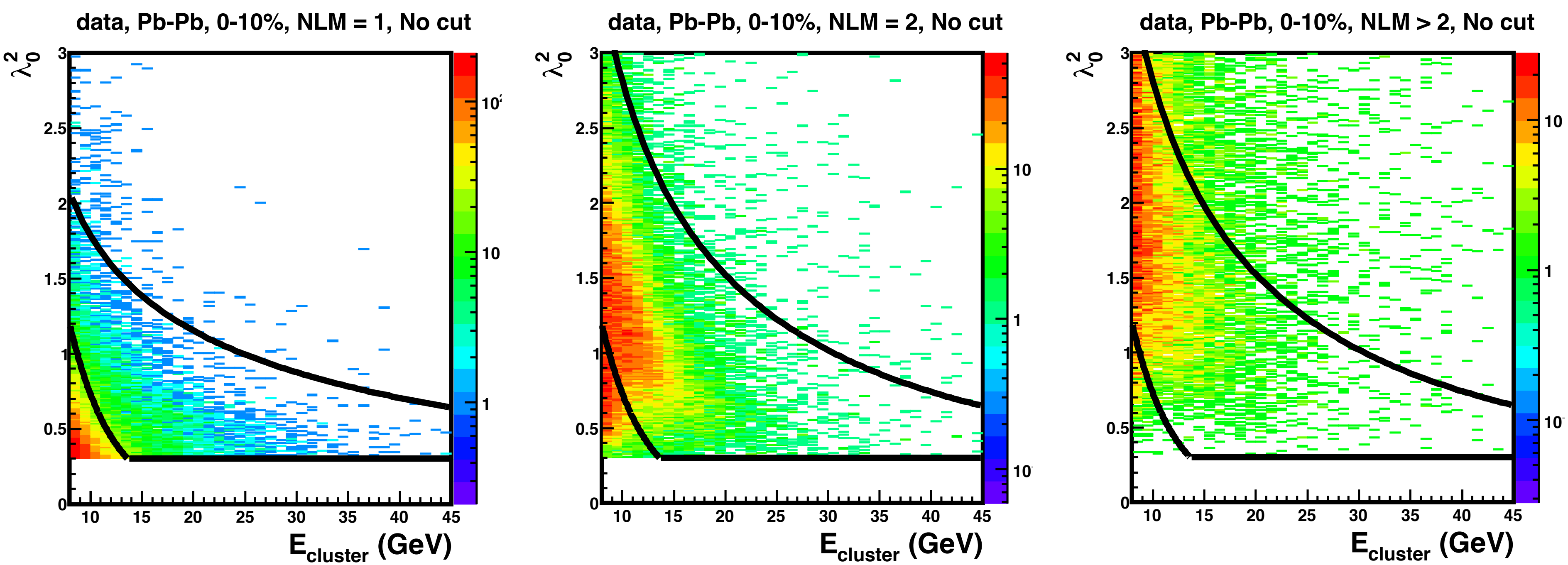

$$\lambda^2_{0,max,min}(E) = e^{a+b*E} + c + d*E + e/E$$

Cluster energy asymmetry

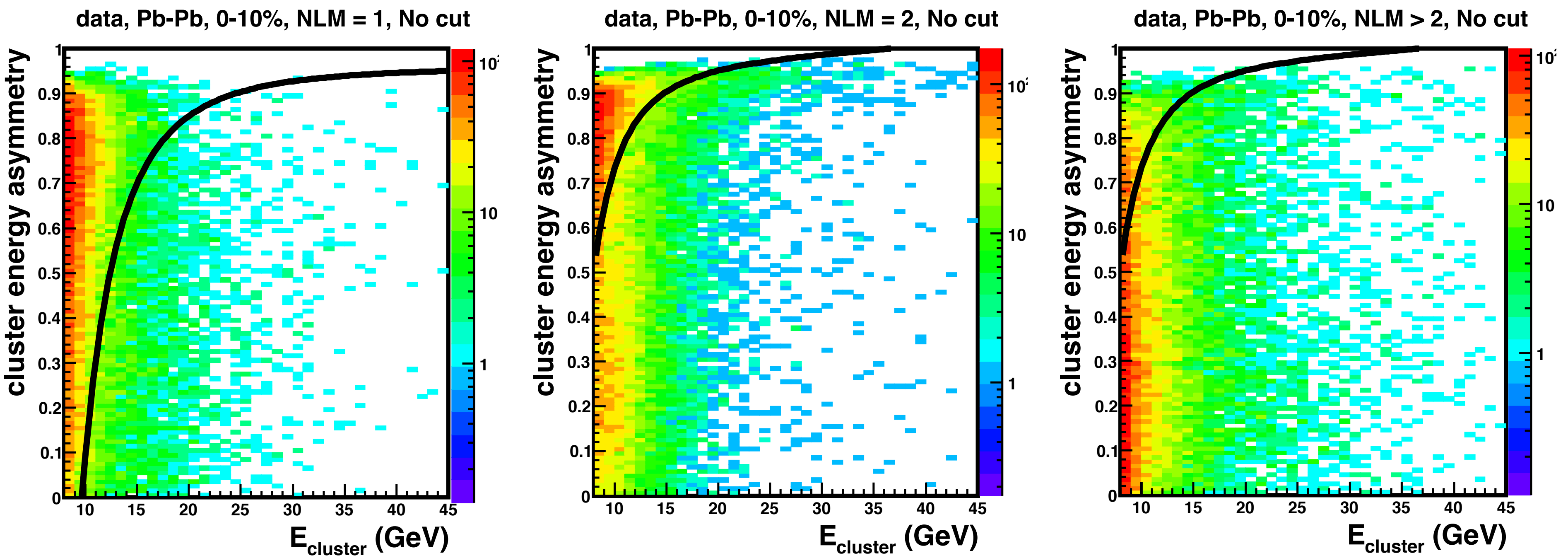

$$A_{min}(E) = a + b * E + c/E^3$$

Mass distribution

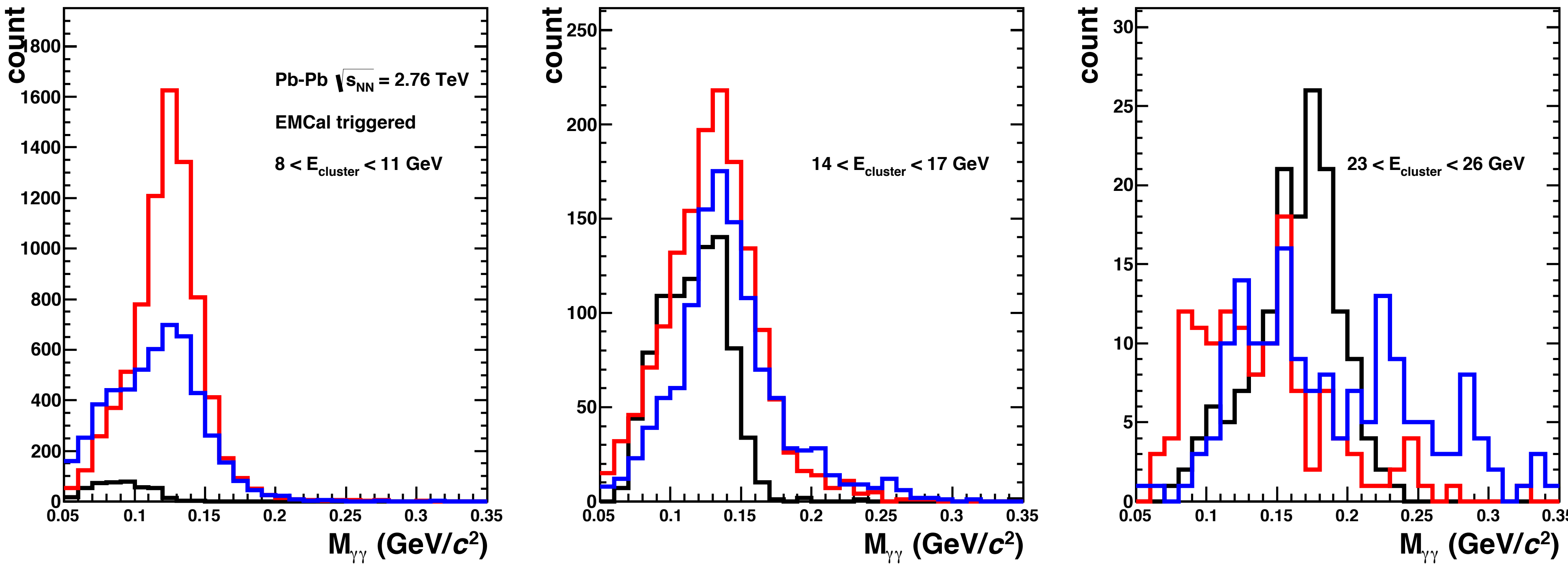

Invariant mass cut and π^0 p_T distribution

From Gustavo's analysis note

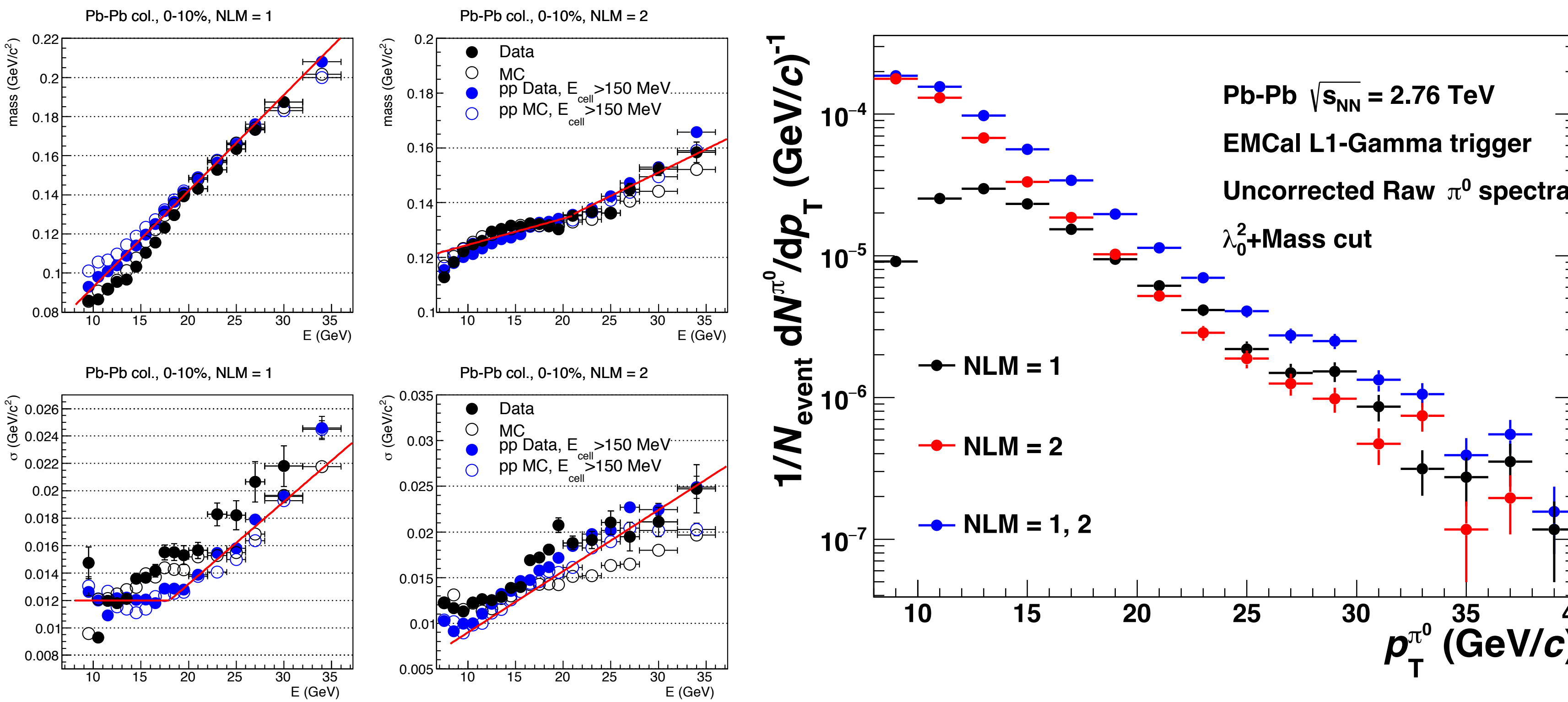

$$M(E), \sigma(E) = a + b * E$$

- Selected clusters as π^0 at 3σ from each mean points.

Jet reconstruction

Information of selected jet in pp 7 TeV

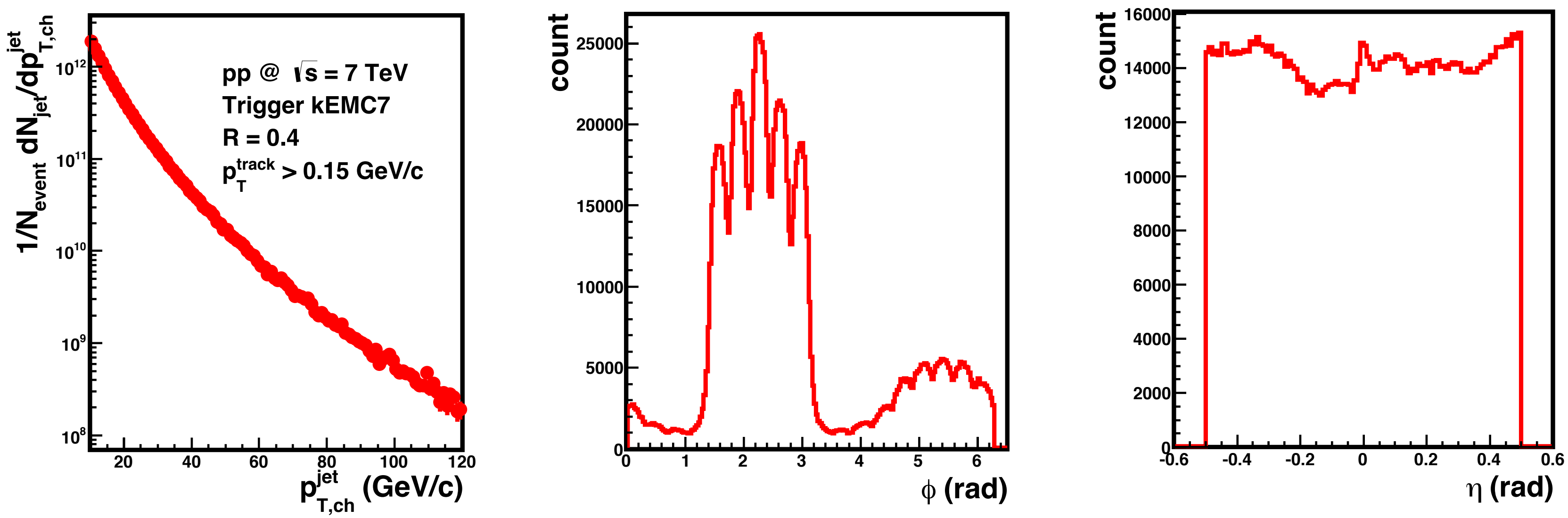

Fitting quality

- Negative values
  - the check on the validity of the ρ(ϕ) approximation is the requirement that ρ(ϕ) has a minimum larger than or equal to 0

- p-values and goodness of fit
  - the fit criterion is a cut on the probability p whick is derived from the x^2 statistic (0.01 < p)

$$\chi^2 = \sum_{n=0}^{i} \left(\frac{x_i - \mu_i}{\sigma_i} \right)^2 \qquad \mathrm{CDF}(k, \chi^2) = \frac{1}{\Gamma\left(\frac{k}{2}\right)} \gamma\left(\frac{k}{2}, \frac{x}{2}\right) \qquad p = 1 - \mathrm{CDF}.$$

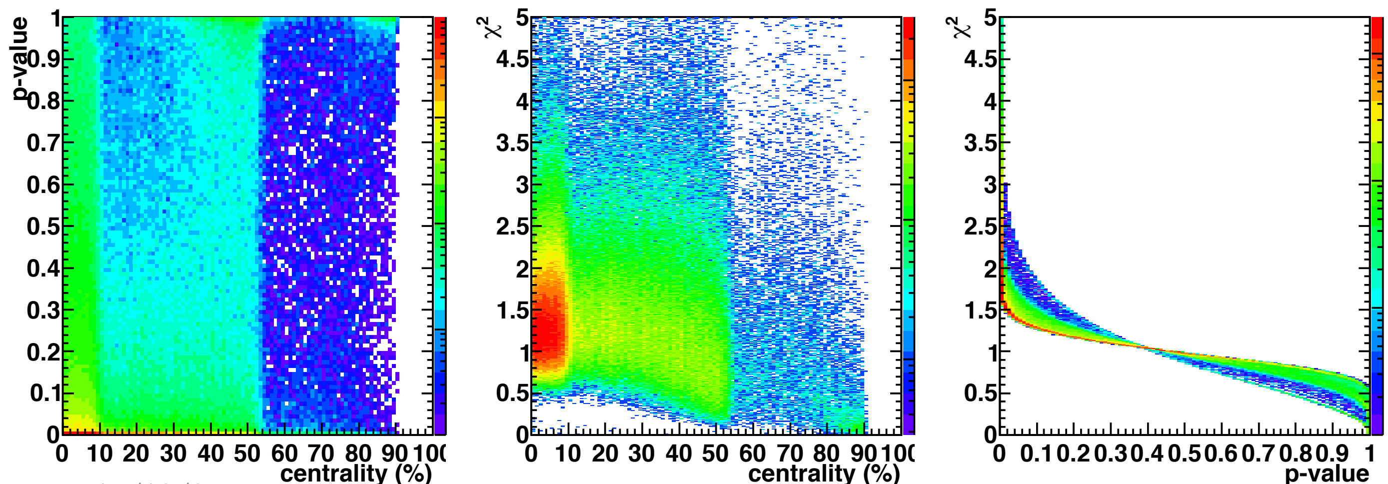

Event plane analysis

Event plane QA

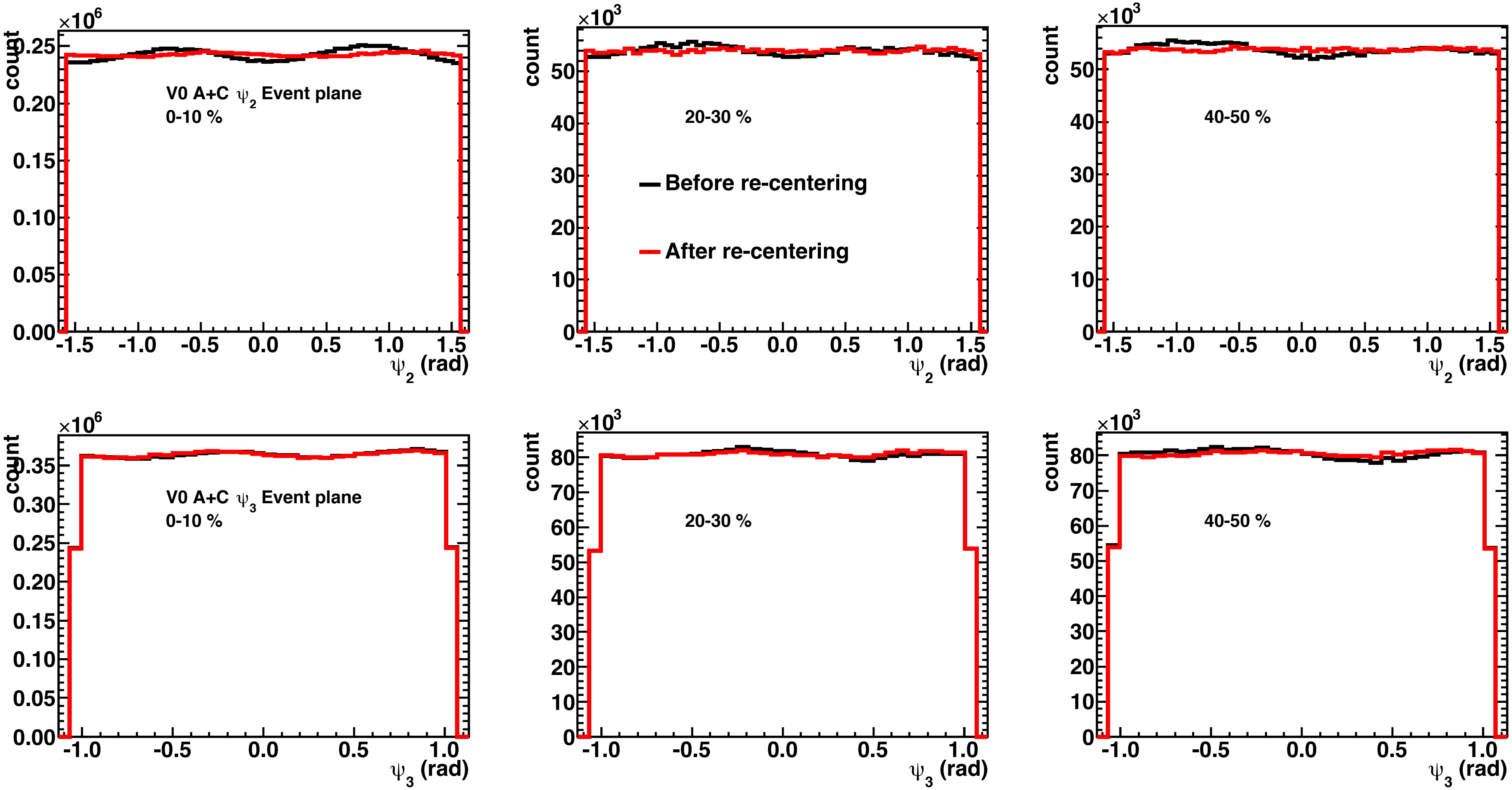

- Applied the V0 gain correction and re-centering correction

Event plane resolution

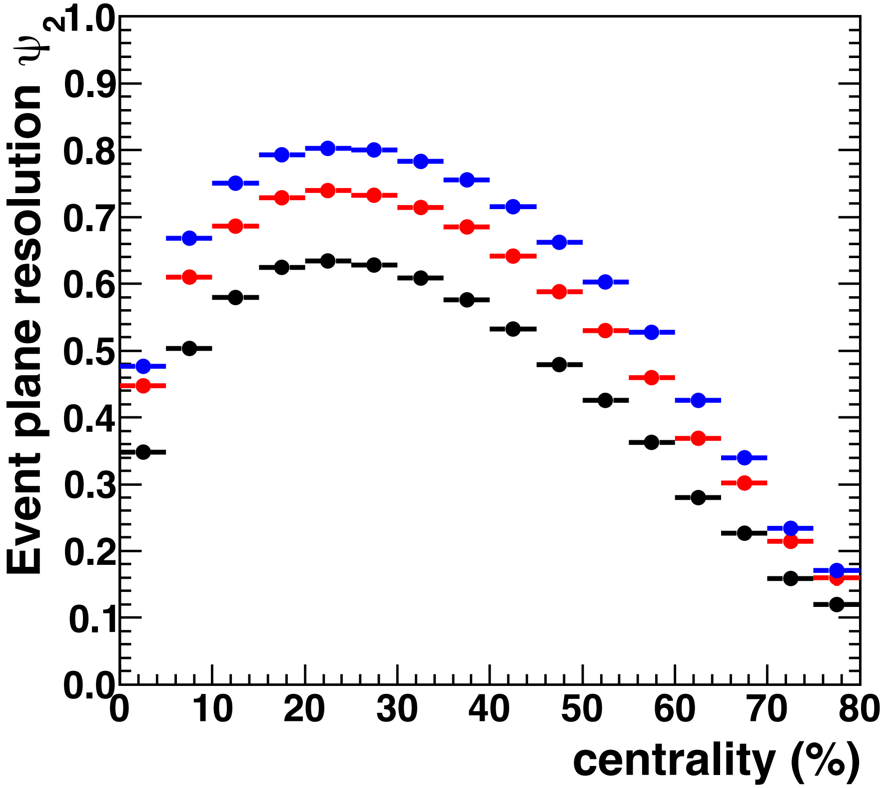

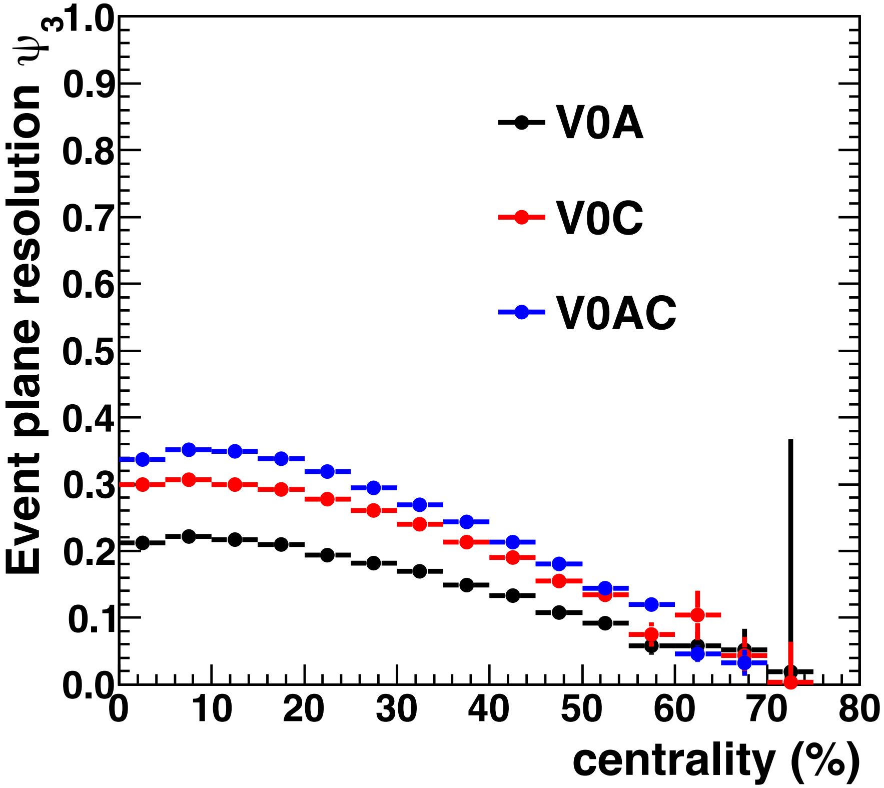

$$\langle \cos(n(\Psi_n^a - \Psi_n)) \rangle = \sqrt{\frac{\langle \cos(n(\Psi_n^a - \Psi_n^b)) \rangle \langle \cos(n(\Psi_n^a - \Psi_n^c)) \rangle}{\langle \cos(n(\Psi_n^b - \Psi_n^c)) \rangle}},$$

v_2 vs p_T (Charged particle)

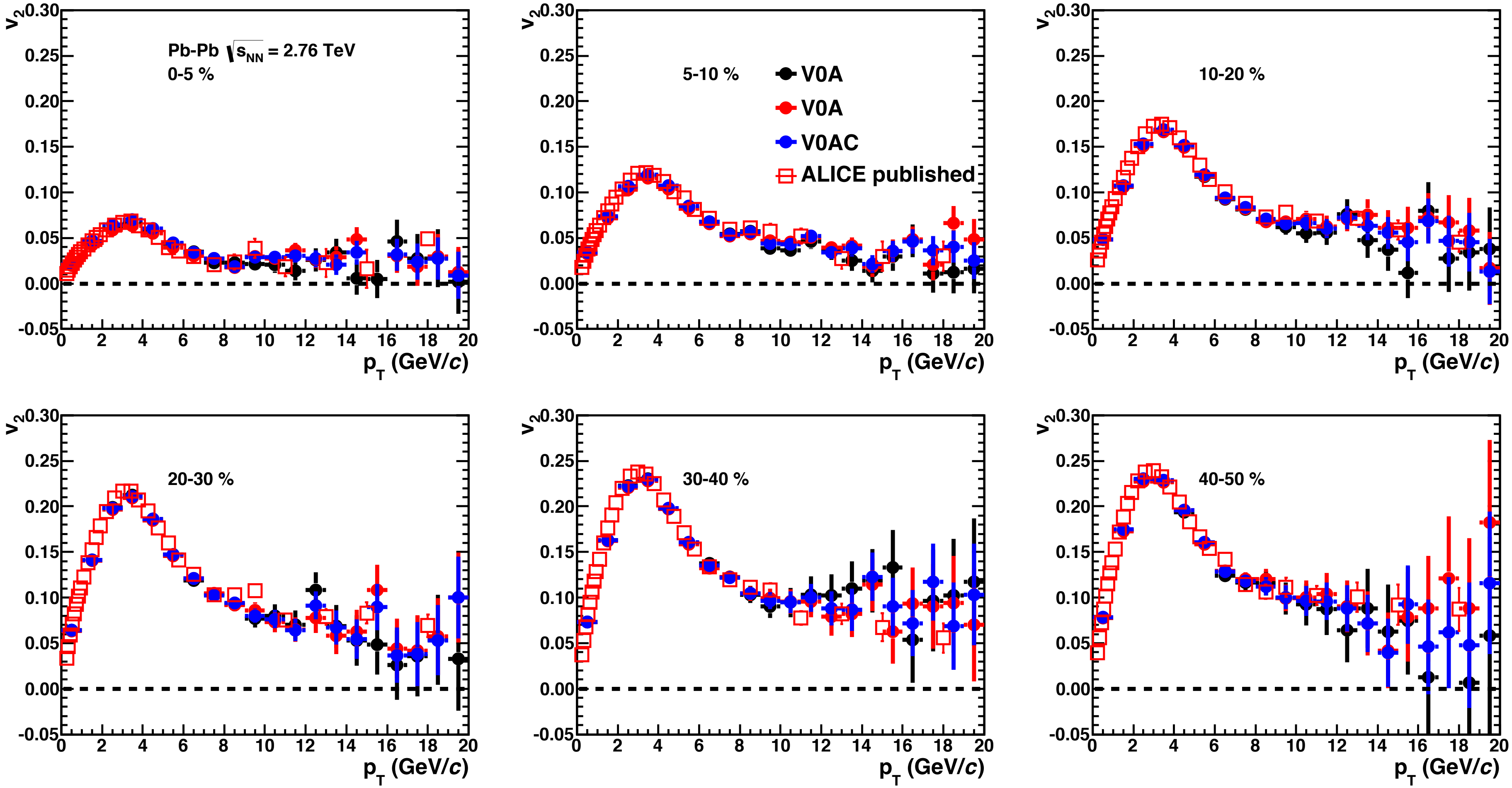

v_3 vs p_T (Charged particle)

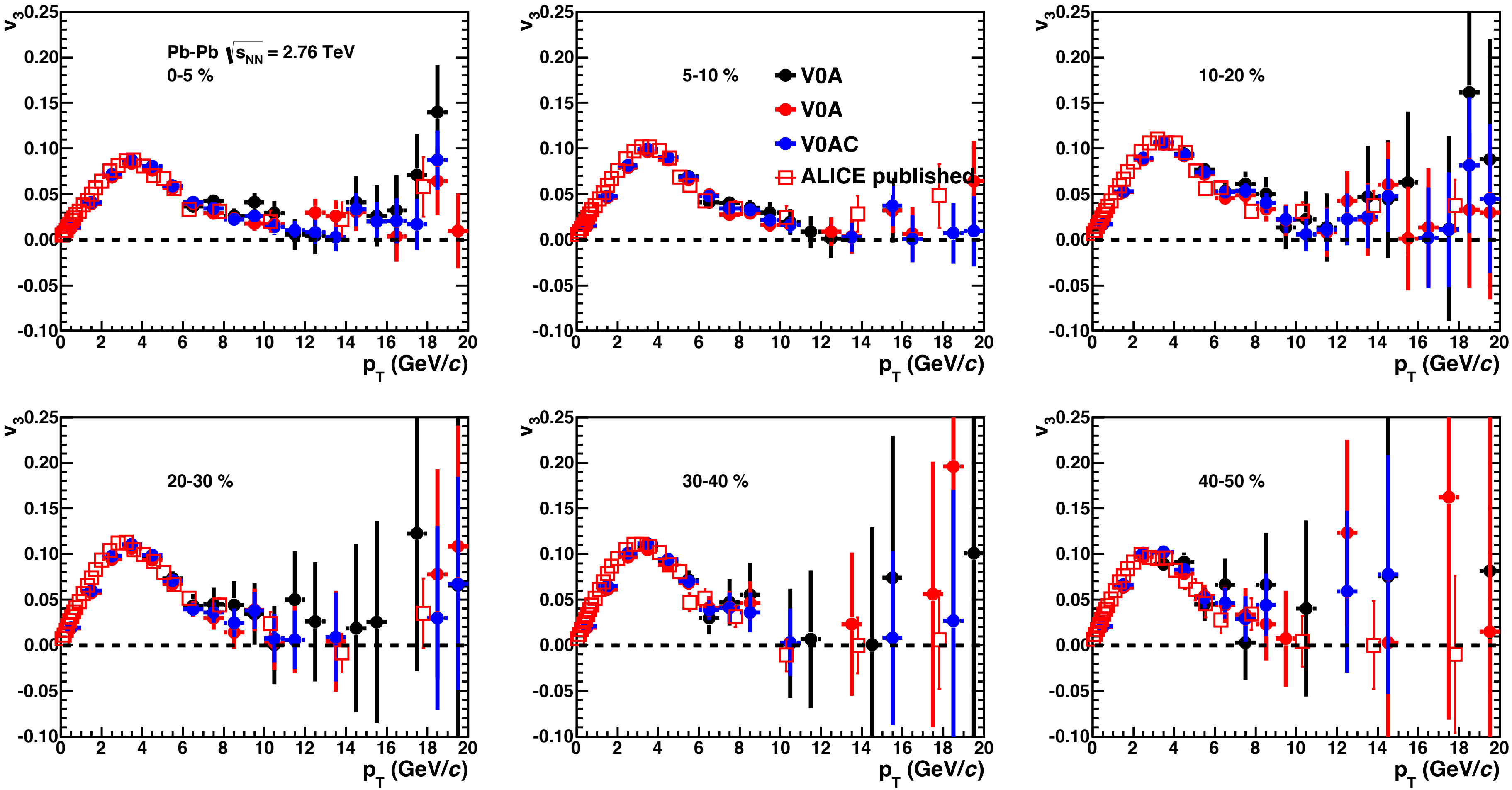

v_2, v_3 vs centrality

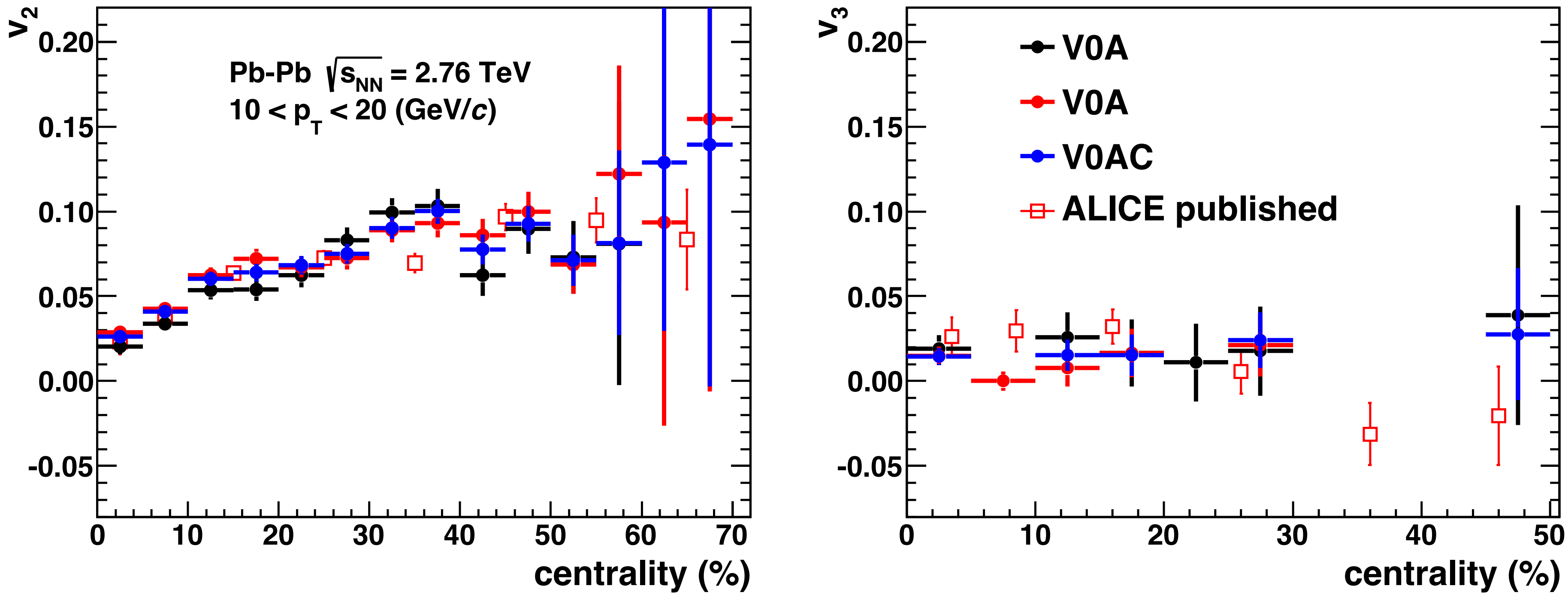

Random cone

- Random cone
  - background fluctuations are characterized by looking at the difference between the summed p_T of all particles in the random cone

$$\delta p_{\mathrm{T}} = \sum_i p_{\mathrm{T,i}} - A \cdot \rho ,$$

- The δp_T distribution has two important role
  - peak and width of δp_T distribution include information of quality of BKG estimation
  - width shows the magnitude of the statistical fluctuations of the background energy density

筑波大学
University of Tsukuba

Event plane ψ_2 correlation

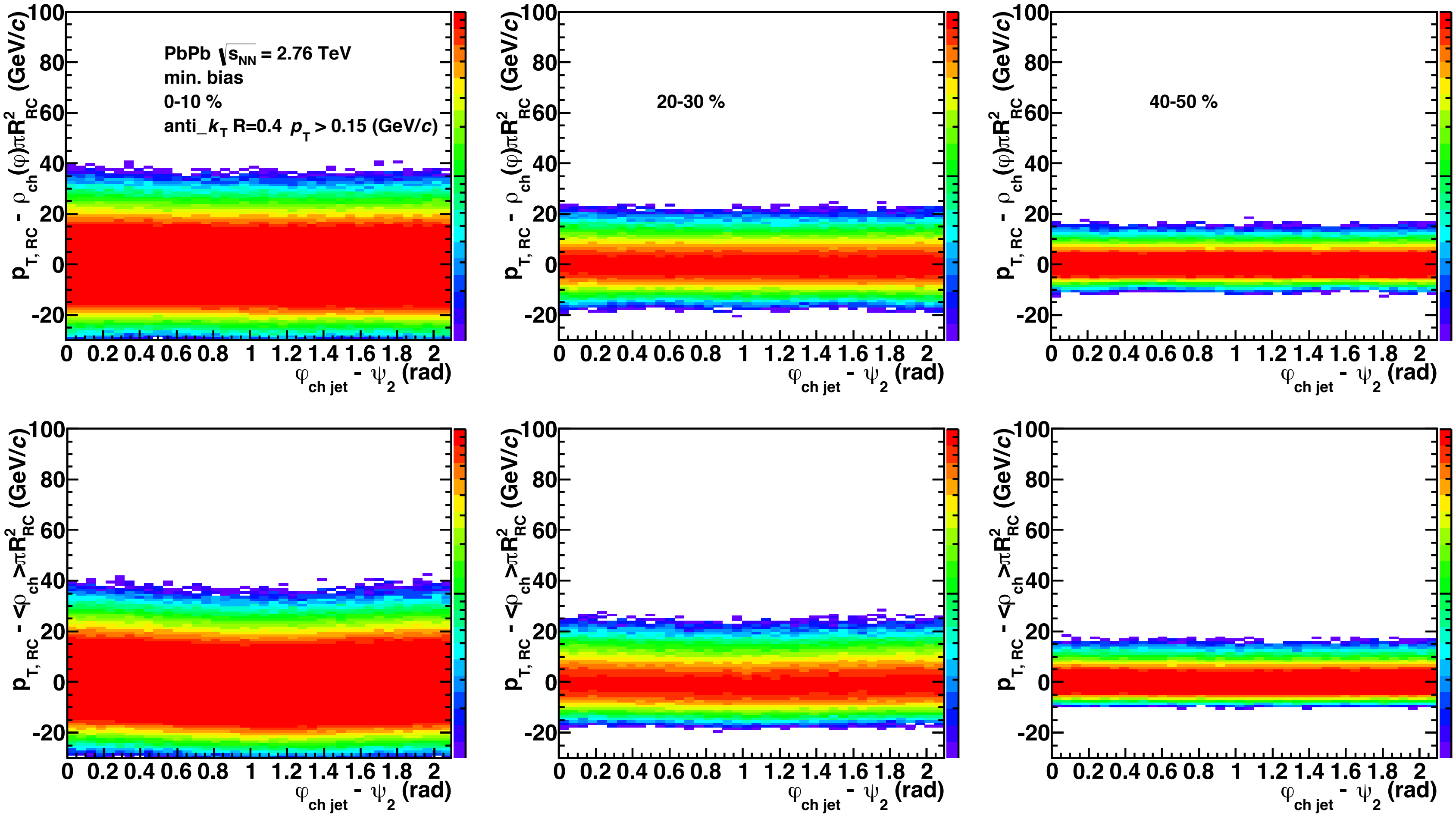

Event plane ψ_3 correlation

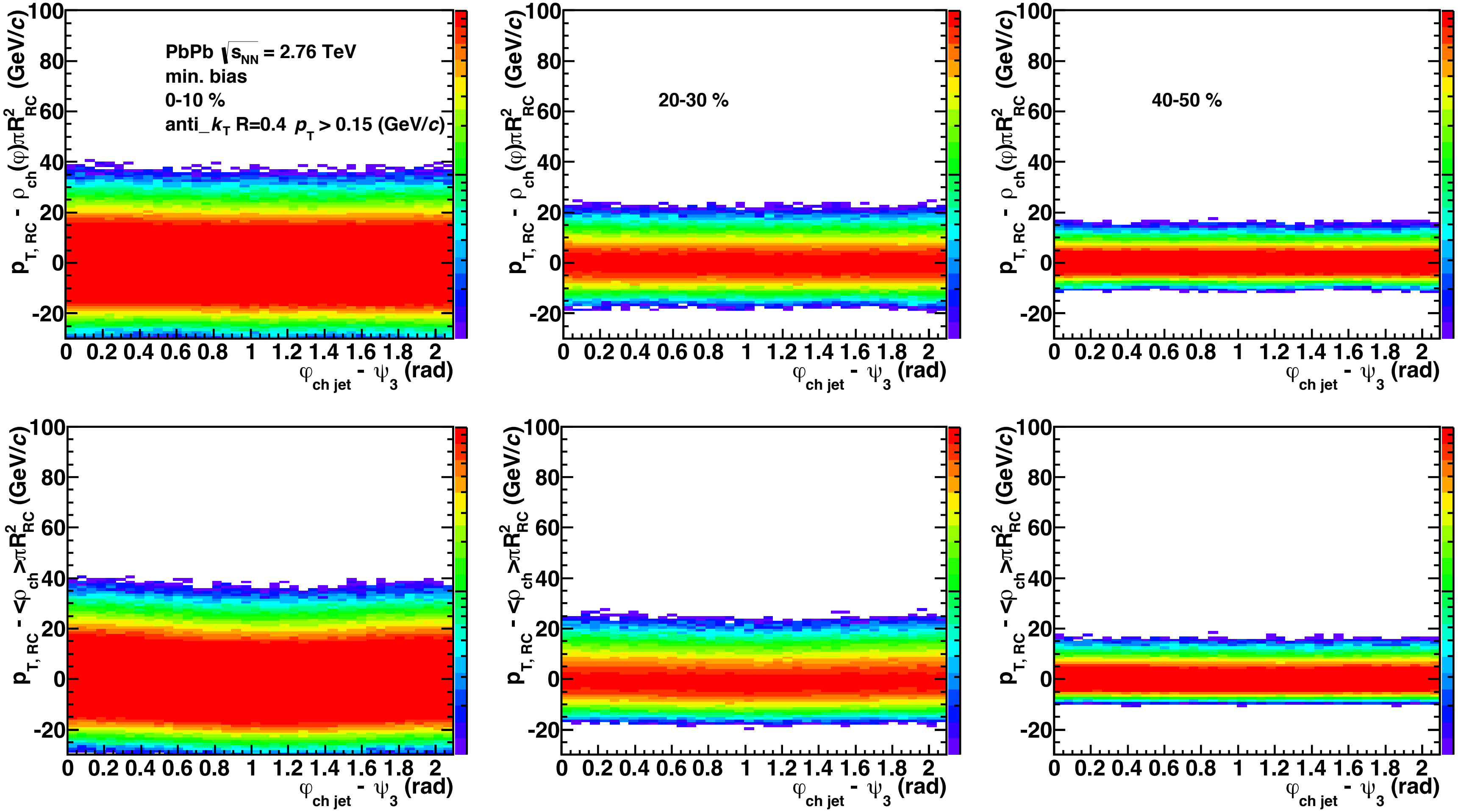

δp_T spectrum with two different event plane regions

ALICE

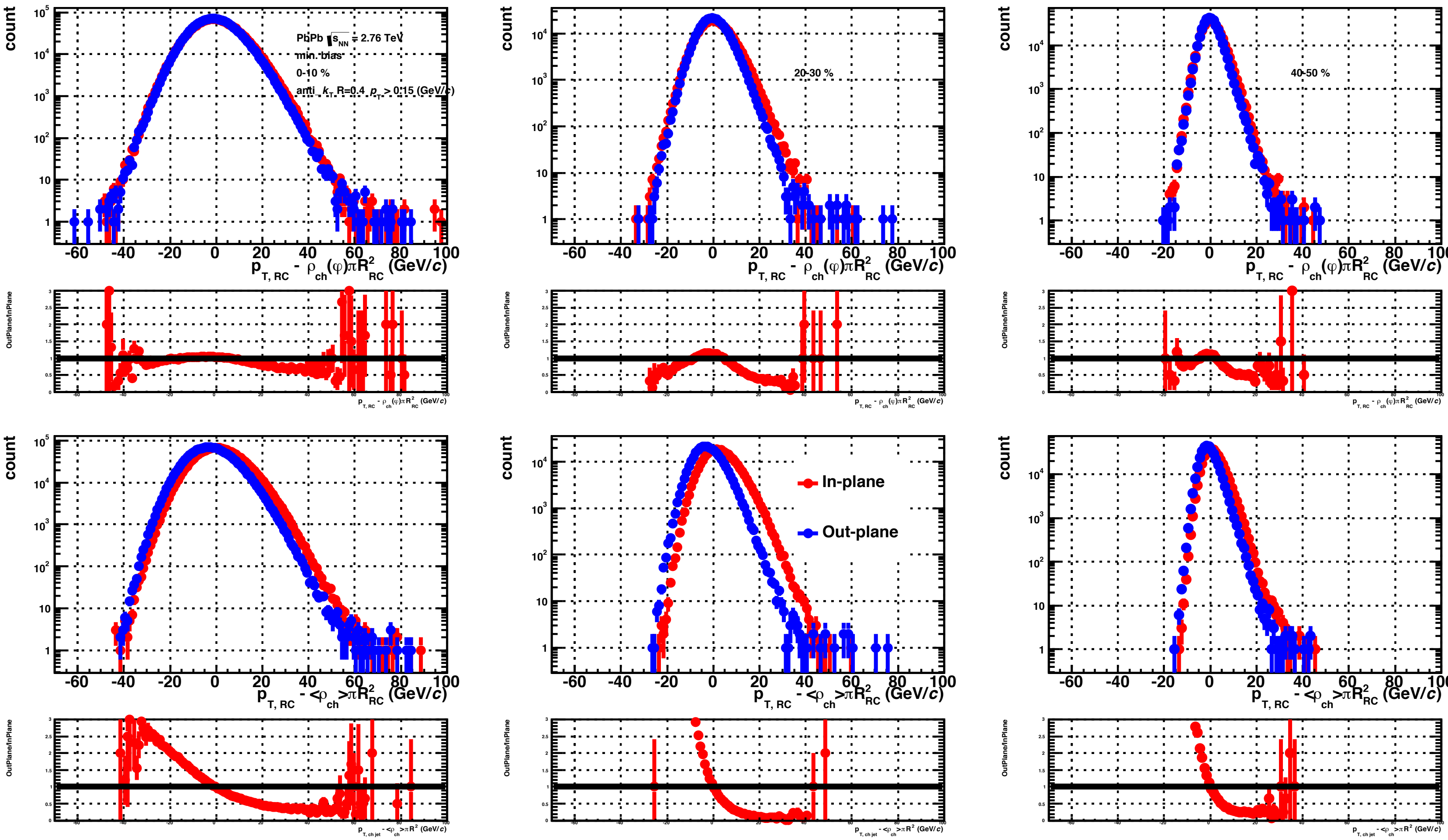

筑波大学
University of Tsukuba

Correction

Azimuthal correlation extraction in low p_T region ($4 < p_T < 8$ GeV/c)

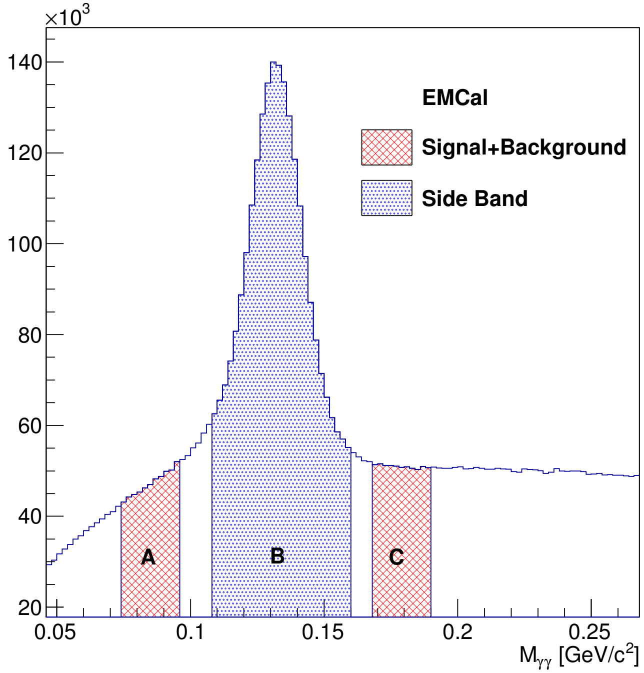

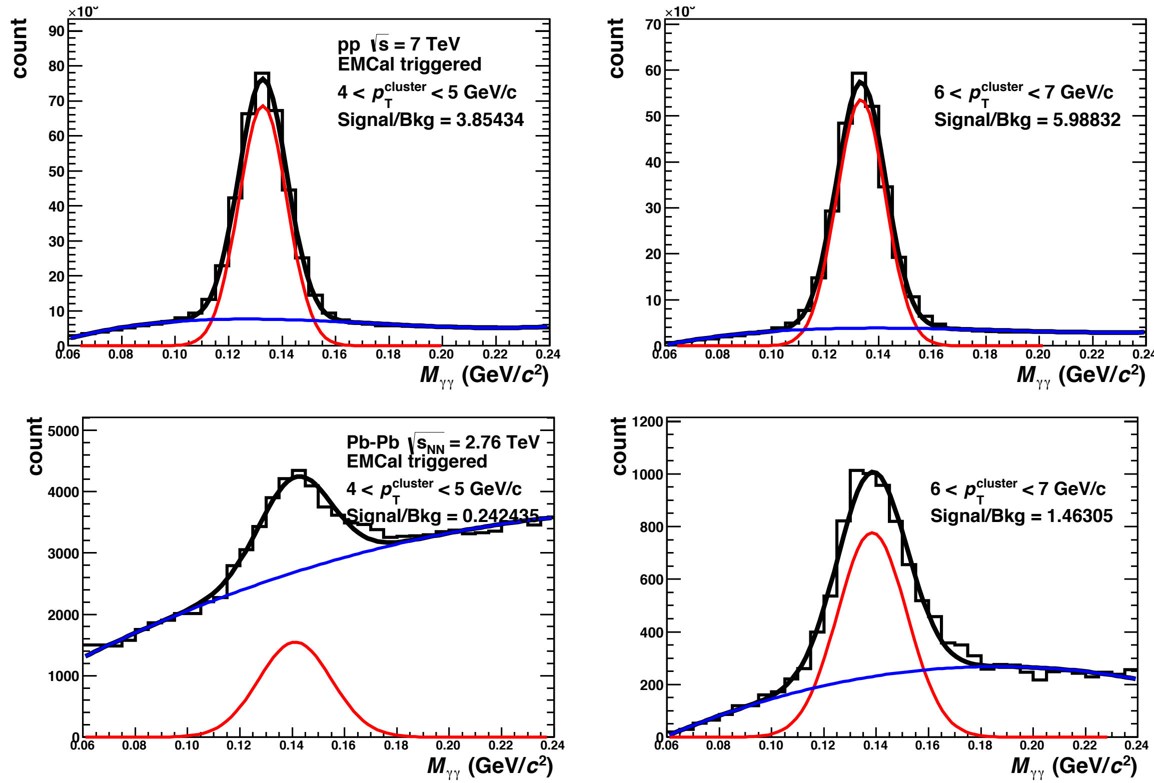

Signal+Bkg : 3σ from peak mean, Bkg (left) : 75 ~ 95 MeV/c^2, Bkg (right) : 170~190 MeV/c^2

Signal fit function : Gaus (red), Background fit function : Pol3 (blue)

Azimuthal correlation with signal+bkg and bkg

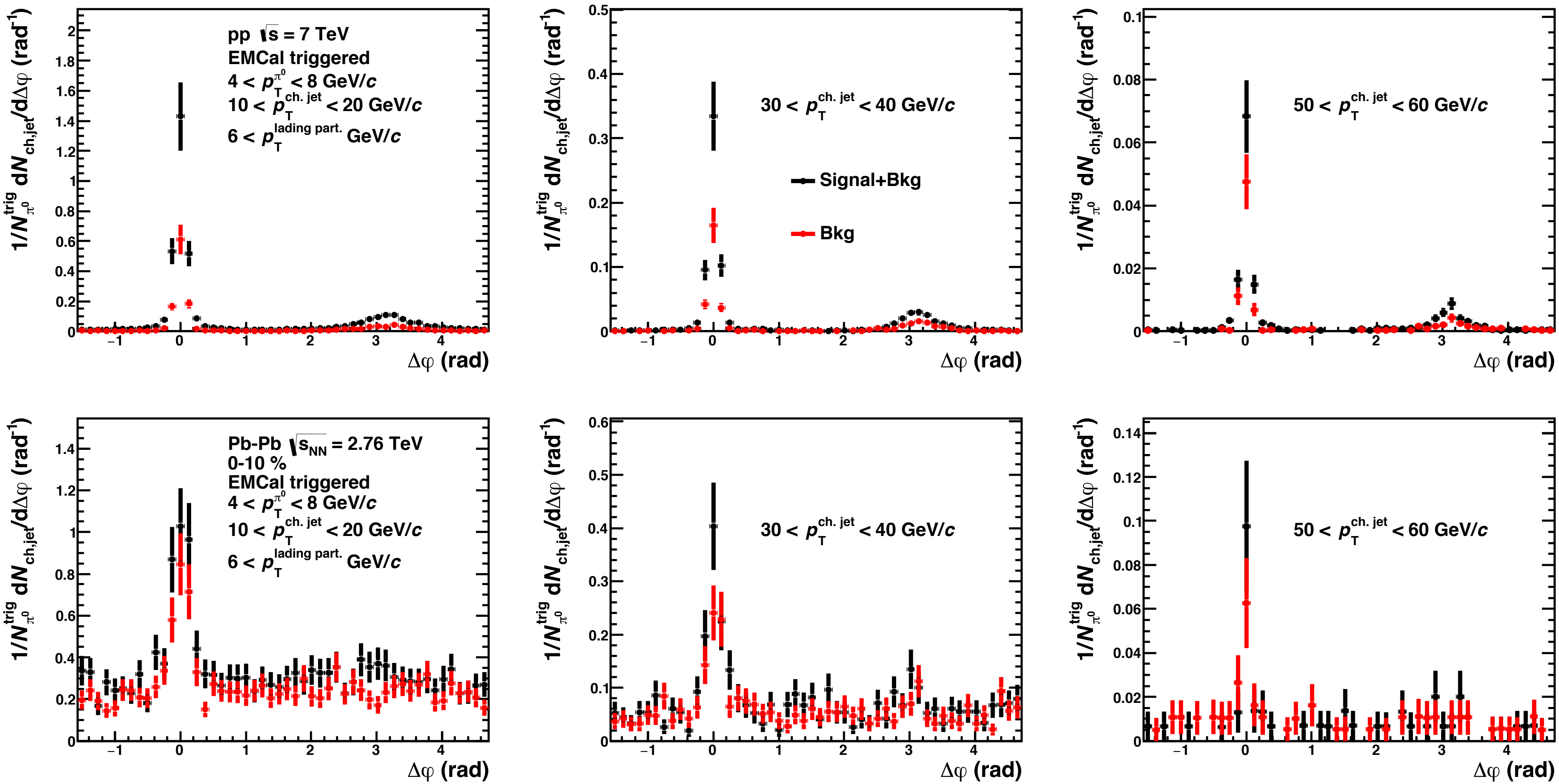

$$Y_S = Y_{S+B}(1+\frac{1}{f_{bkg}}) - Y_B/f_{bkg}$$

Y_{S+B} : per trigger yield of signal and bkg
Y_B : per trigger yield of bkg
f_{bkg} : S/N

Azimuthal correlation after π⁰ bkg subtraction

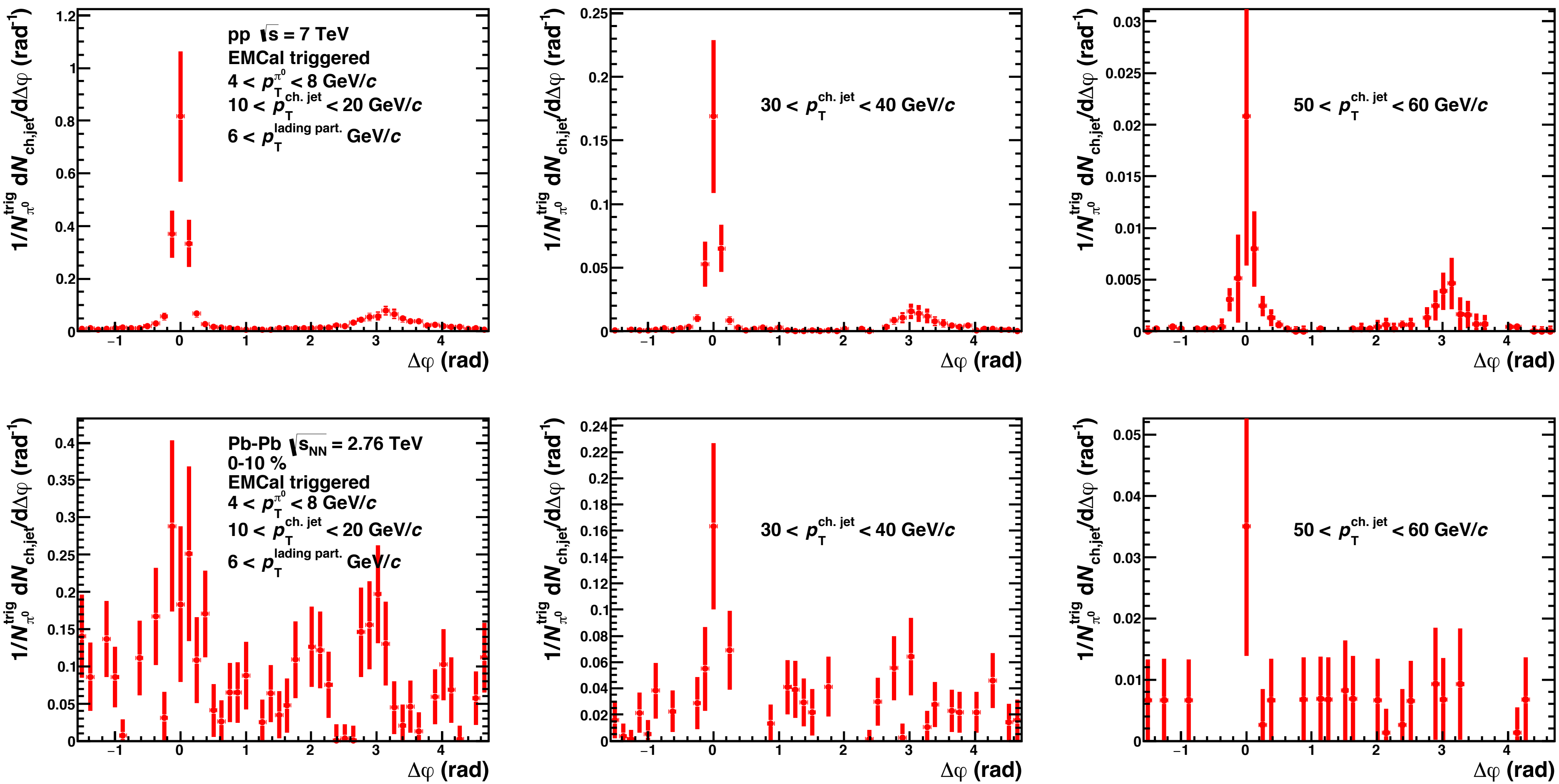

- Azimuthal yields of π^0 background (Y_B) strongly depend on S/N ratio (f_{bkg}) of π^0 reconstruction

Flat BKG subtraction

ALICE

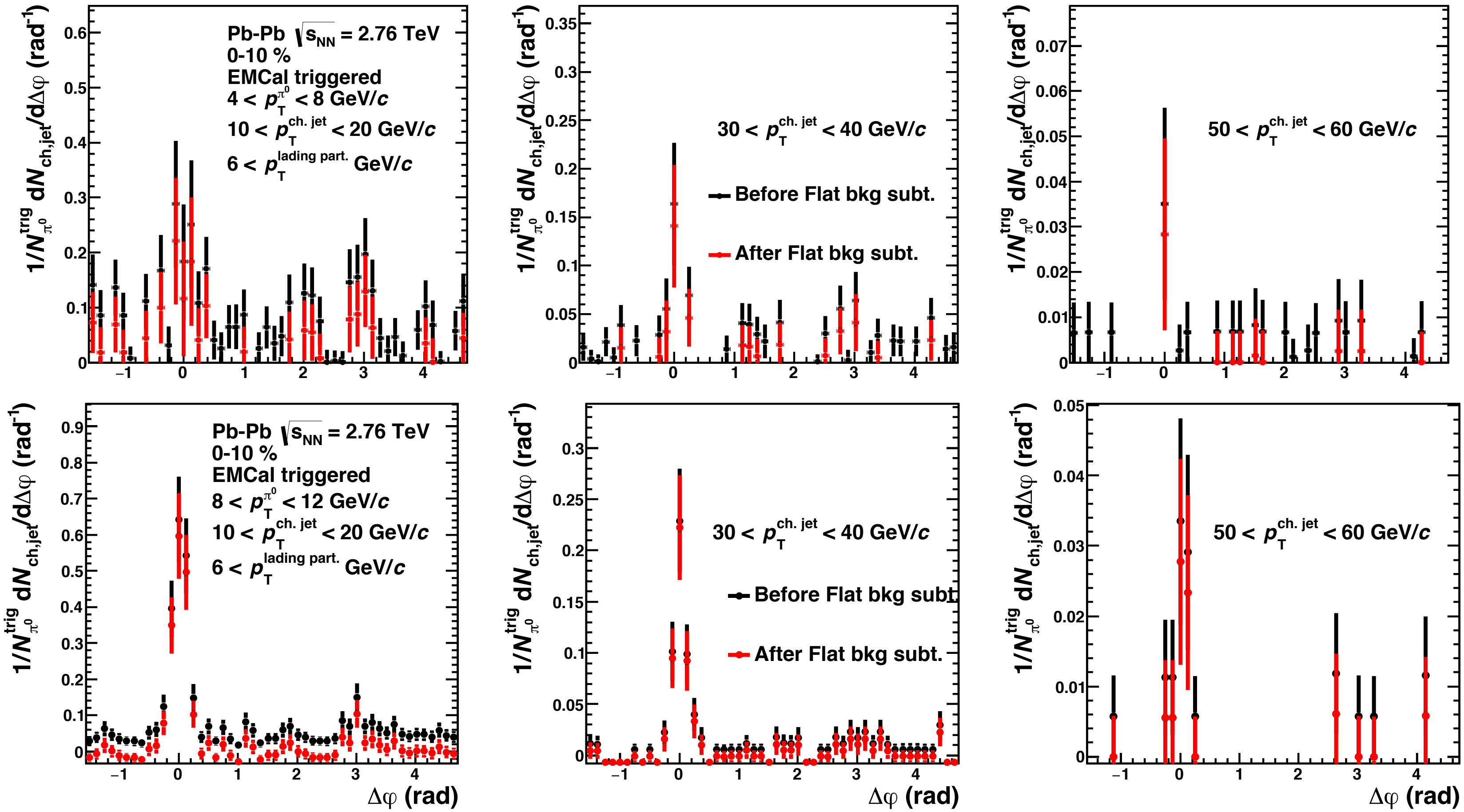

1. Take 4 bins in the valley region on the left and right side from a near side peak region
2. Calculate the average background value from 8 bins in valley regions

π^0 identification efficiency and purity

My analysis

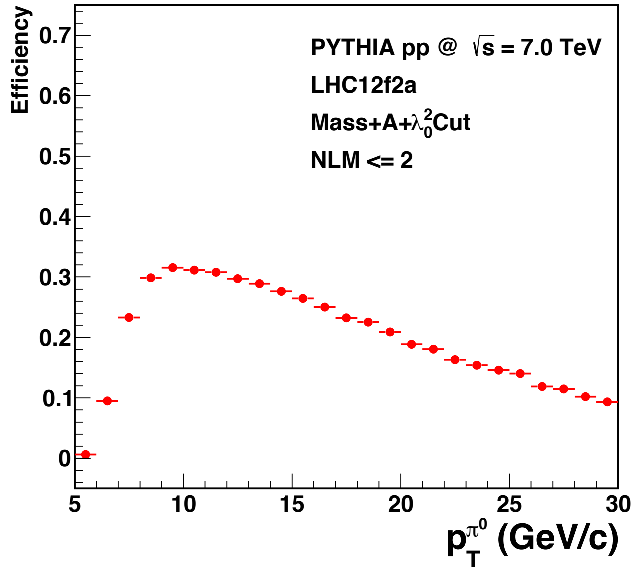

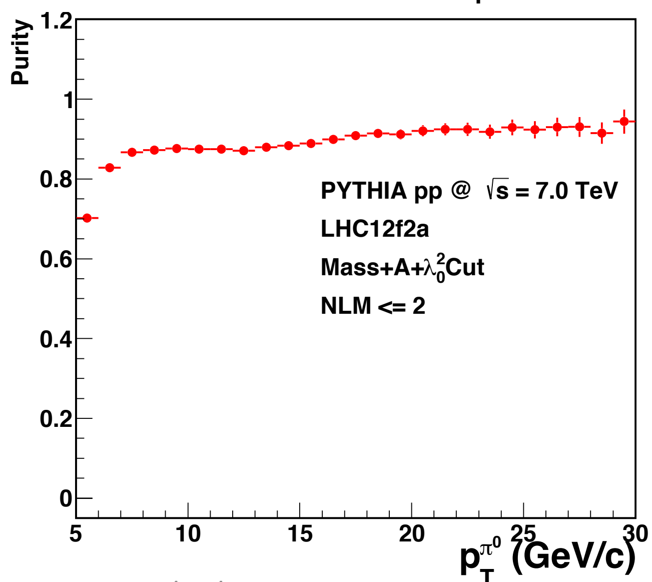

Xiangrong's analysis (π^0-hadron)

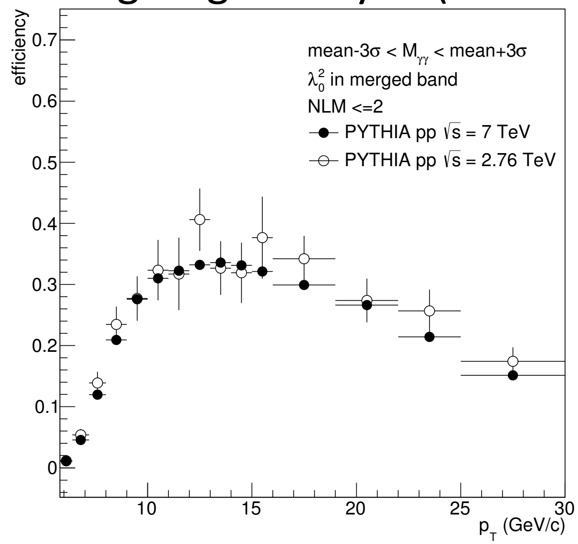

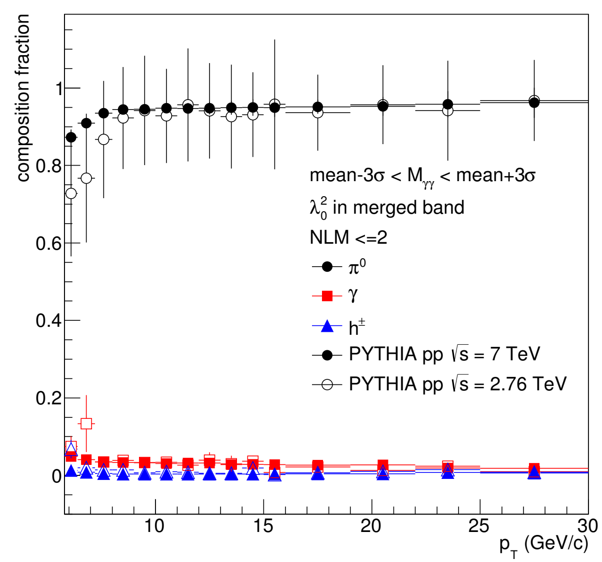

Correction of π⁰ and jet reconstruction efficiency

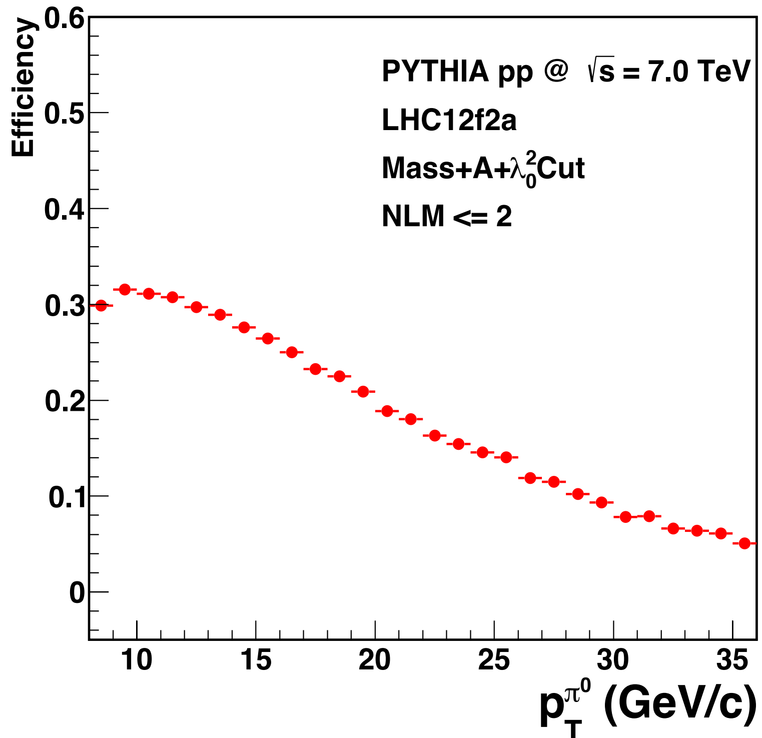

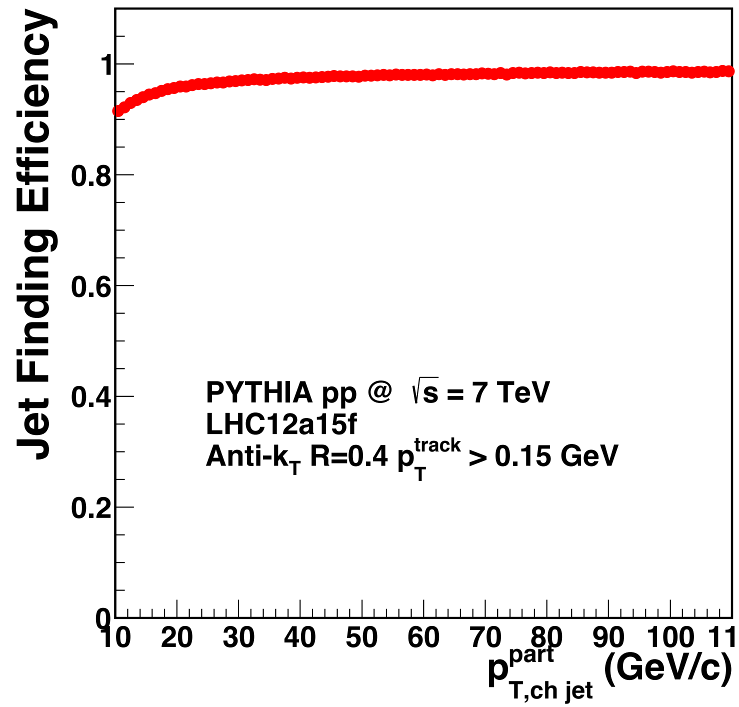

- π^0 reconstruction efficiency
  - Δp_T = 1.0 GeV/c
- Jet finding efficiency
  - 10~20 GeV : 0.93, 20~30 GeV : 0.97, 30~GeV : 0.98

$$\frac{1}{N_{trig}^{corrected}} \frac{dN_{pair}^{corrected}}{d\Delta\phi} = \frac{1}{\Sigma_{\Delta p_{T,(i)}} \frac{1}{\varepsilon_i^{\pi^0}} \cdot N_{trig(i)}^{\pi^0}(\Delta p_T^{trig})} \sum_{\Delta p_{T,(i)}} \frac{1}{\varepsilon_i^{\pi^0} \varepsilon^{jet}} \frac{dN_{pair(i)}^{Raw}}{d\Delta\phi} (\Delta p_T^{trig})$$

Results

Comparison of before and after flat BKG subtraction

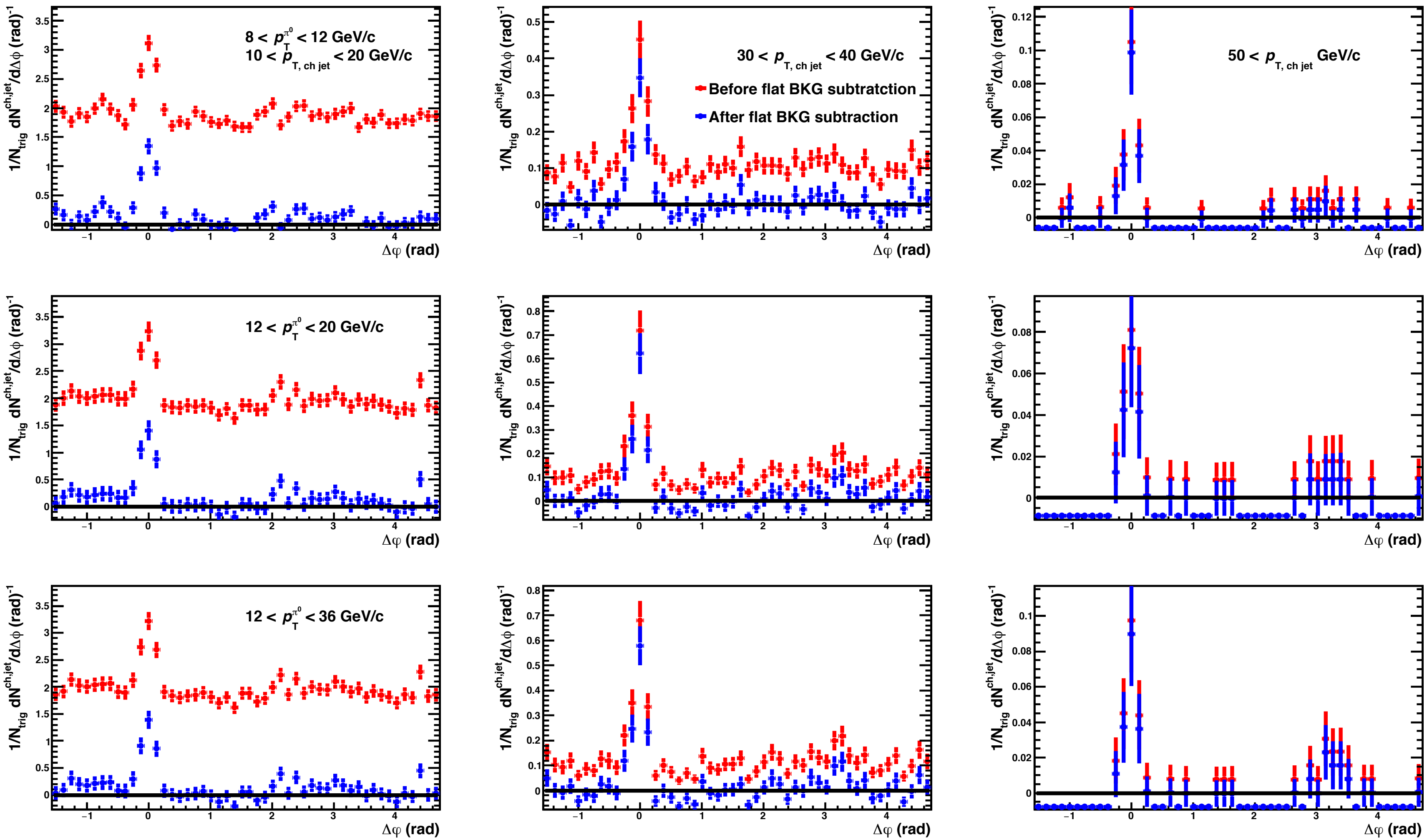

Comparison of near and away side jet yields extracted by the bin counting method and integrated over fitting function in pp 7 TeV

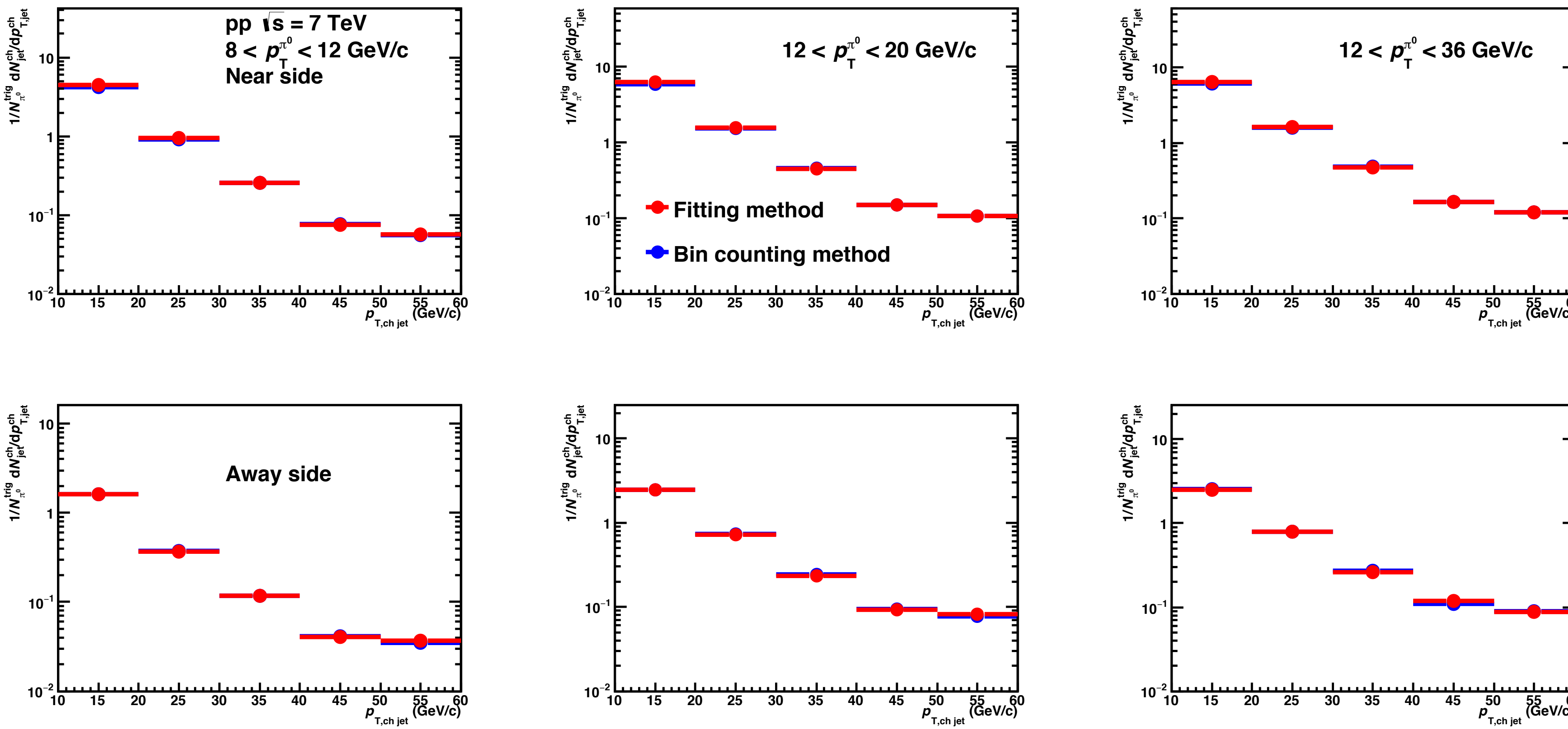

- Two jet yields are good agreement in all trigger π^0 p_T regions and both side

Comparison of near and away side jet yields extracted by the bin counting method and integrated over fitting function (Pb-Pb 2.76 TeV)

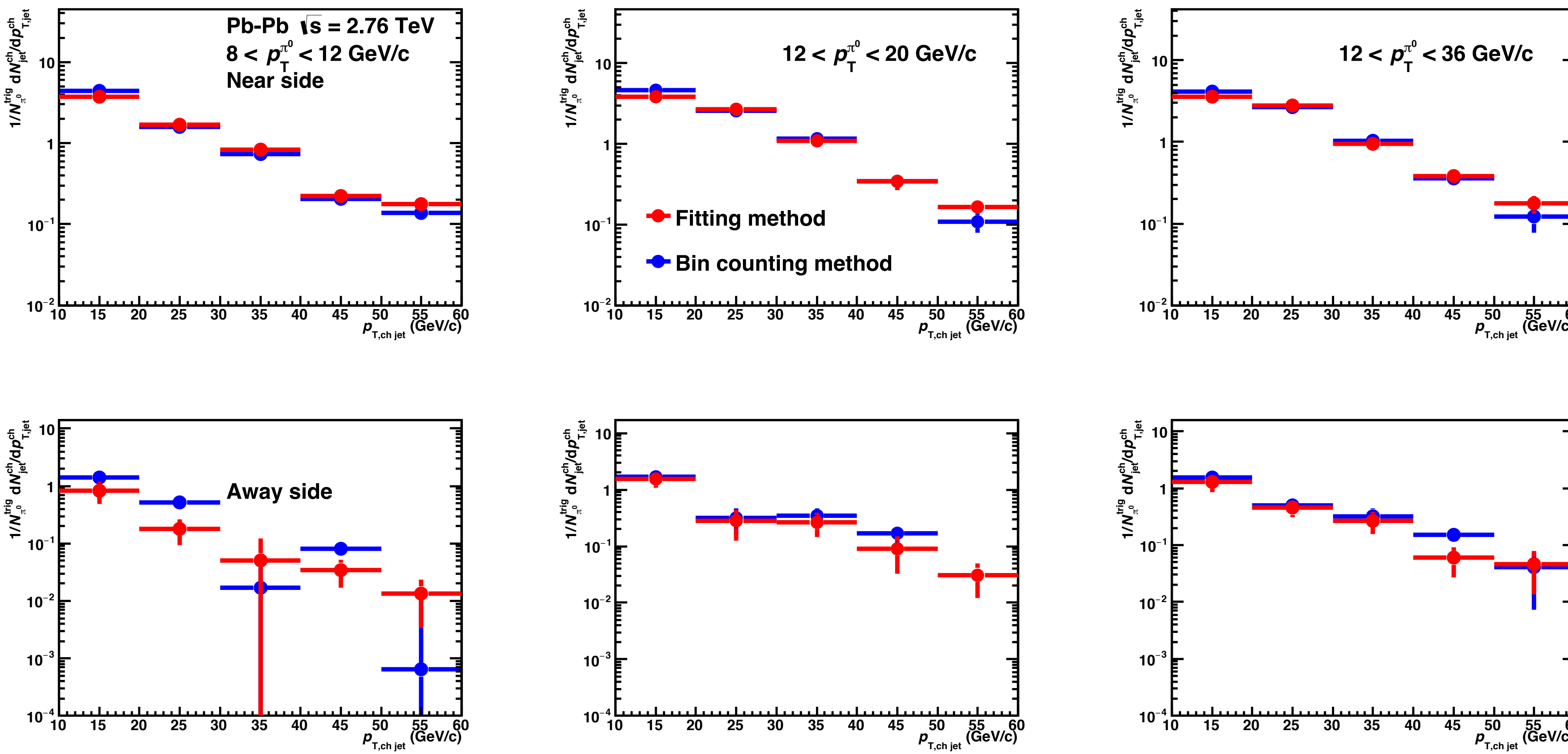

- Near side jet yields are agreement in all trigger π^0 p_T regions
- Away side jet yields of the bin counting method are seen the large fluctuation

PYTHIA pp 2.76 TeV and 7 TeV for scaling factor calculation

- LHC12a15a: PYTHIA pp 2.76 TeV, jet-jet event, LHC11a anchors
- LHC12a15f: PYTHIA pp 7 TeV, jet-jet event, LHC11d anchors

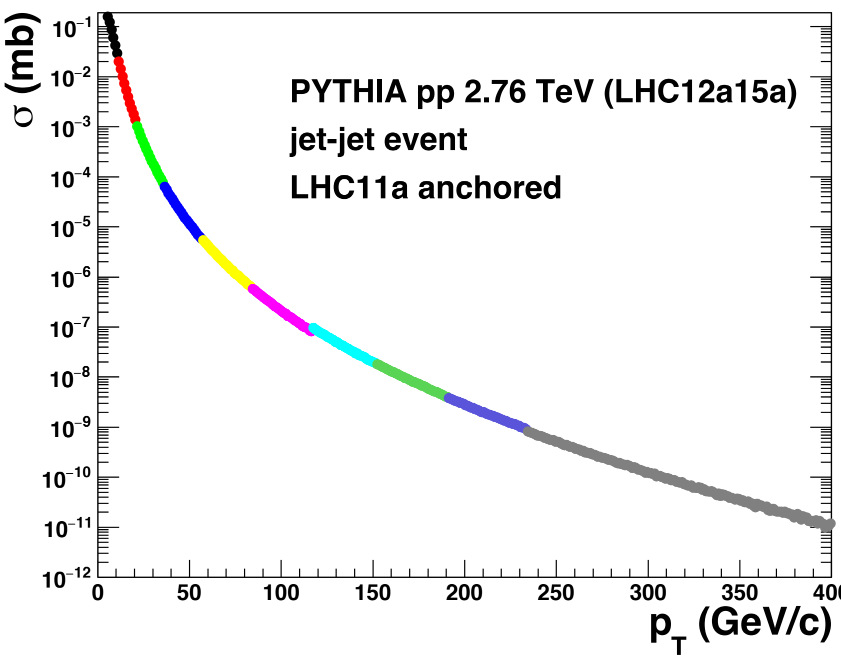

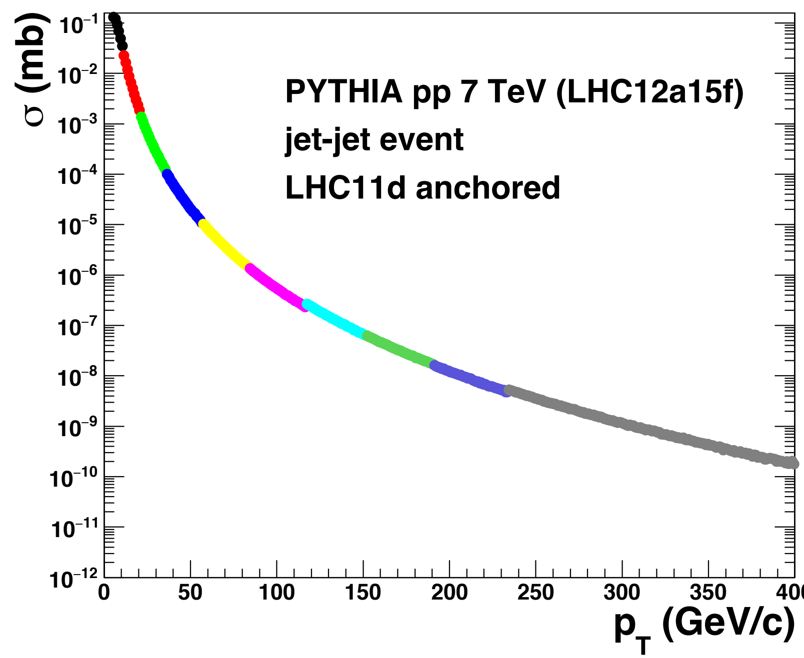

- Analyzed only particle level data with weighted by xsection/ntrials

π^0 : EMCal acceptance, Charged jet : $0 < \Delta\phi < 2\pi$, $|\eta| < 0.5$

Systematic uncertainties

Systematic uncertainty

- Shower shape parameter(λ_0^2) cut : ~ 2.7 %
- Invariant mass window : ~ 3.5 %
- π^0 identification purity (pair purity) : ~ 5.0 %
- π^0 and jet p_T resolution (pair resolution): ~ 12.0%

Total systematic uncertainty

Jet p_T threshold \ $\pi^0 p_T$ region (GeV/c)	[8.0-12.0]	[12.0-16.0]	[16.0-20.0]	[20.0-24.0]	[24.0-36.0]
$10 < p_T^{jet}$ (GeV/c)	2.1 (%)	2.3 (%)	2.6 (%)	3.3 (%)	4.3 (%)
$20 < p_T^{jet}$ (GeV/c)	5.4 (%)	5.1 (%)	6.2 (%)	8.5 (%)	6.9 (%)
$30 < p_T^{jet}$ (GeV/c)	9.3 (%)	9.5 (%)	10.9 (%)	13.9 (%)	11.5 (%)

Recoil jet yields sys. uncertainties

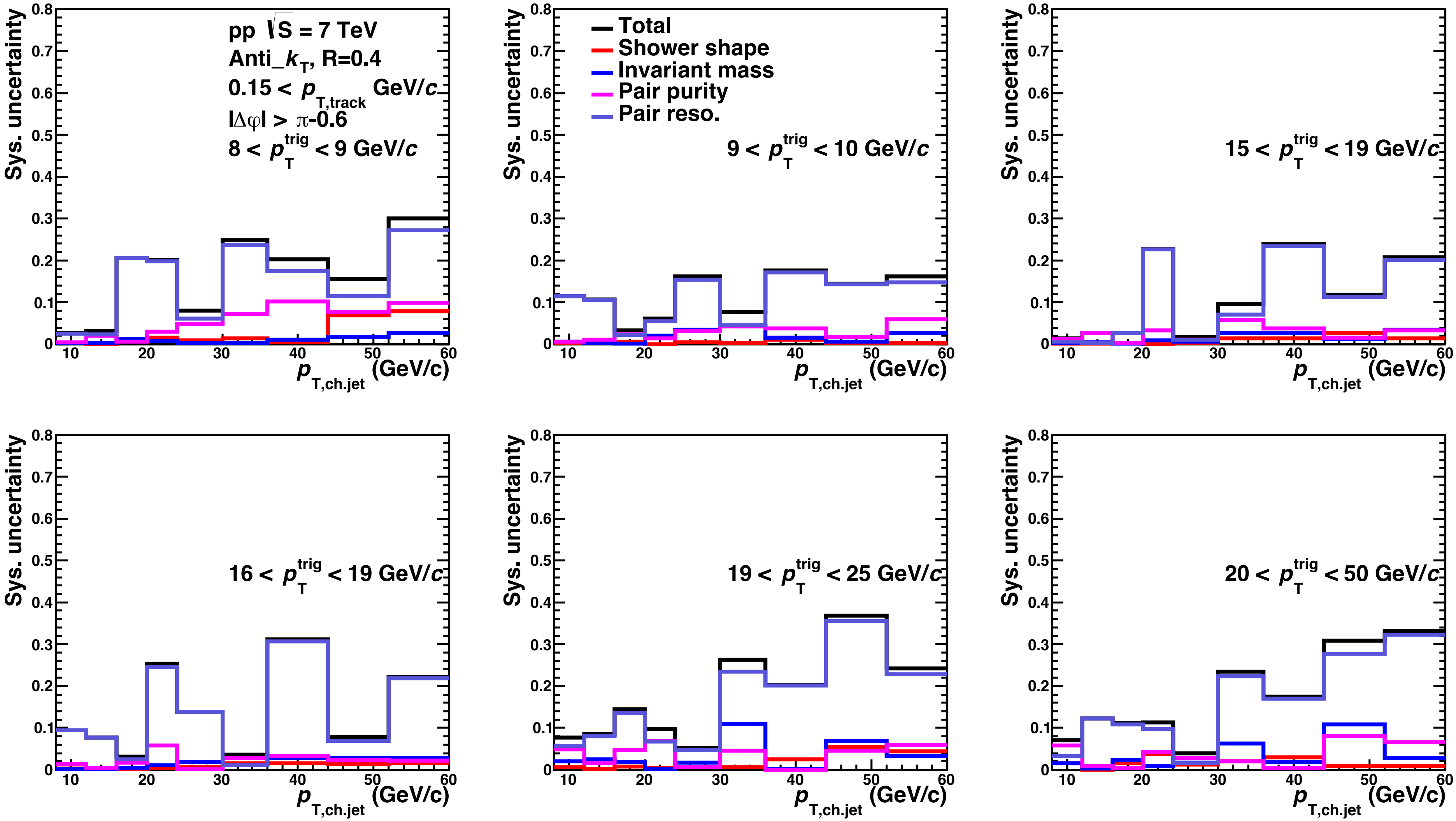

Trigger and leading particle momentum dependence of I_{AA}

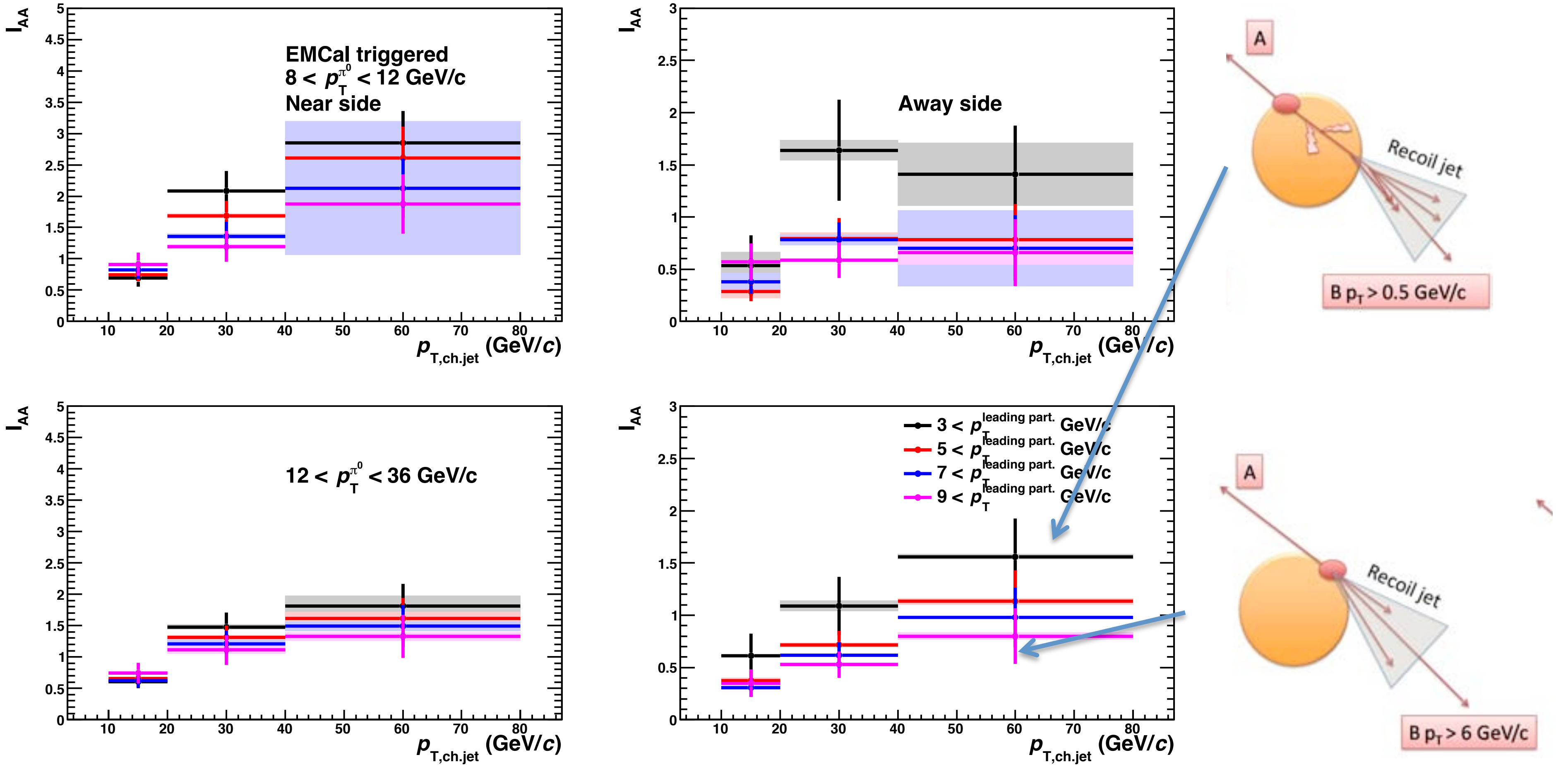

- Can not see the path-length dependence of away side jets by changing trigger and leading particle momentum region

Near and away-side widths as a function of π^0 p_T

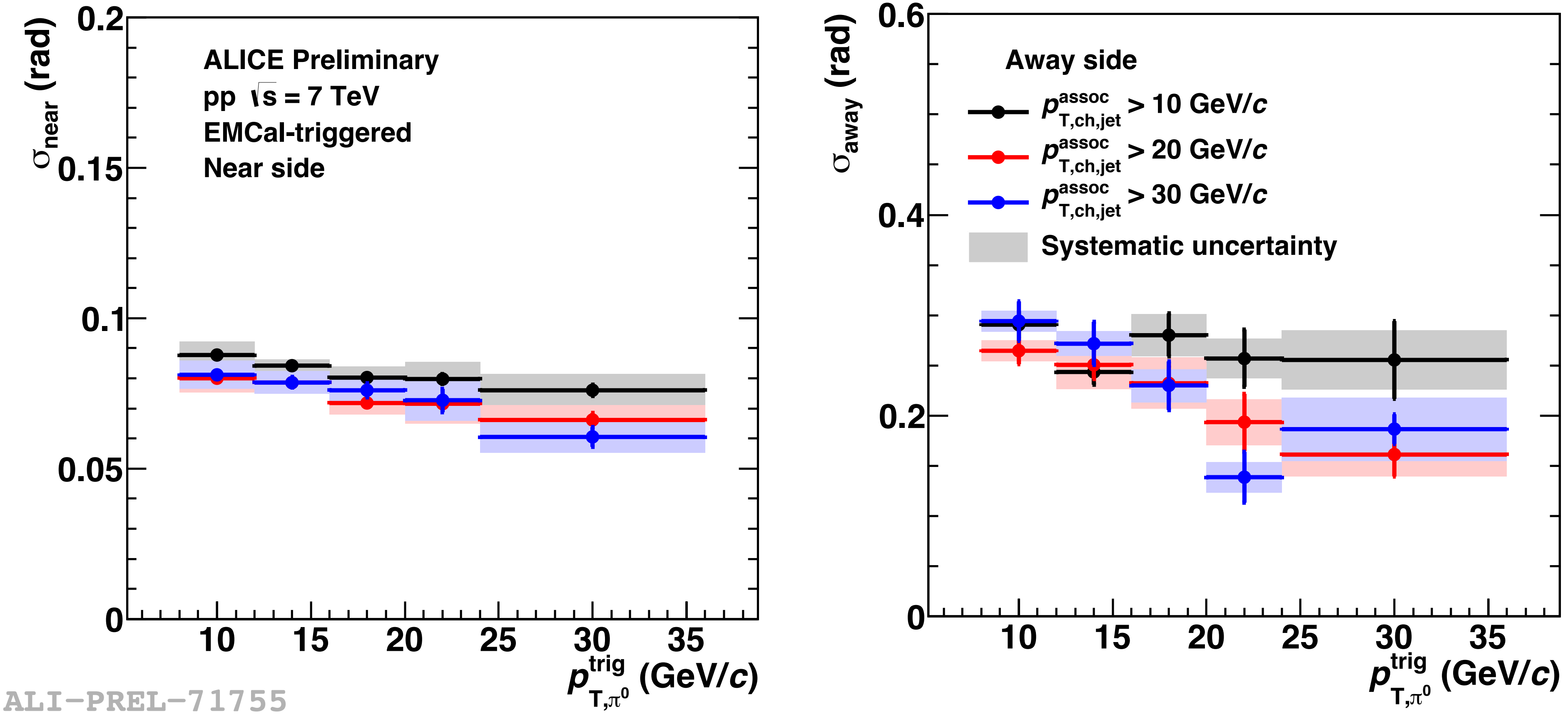

- Near and away-side widths decrease slightly with increasing trigger π^0 p_T
- Neutral particles (π^0 in this analysis) are produced close to a initial parton of hard scatterings

Azimuthal yield comparison to MC (corrected data vs particle level MC)

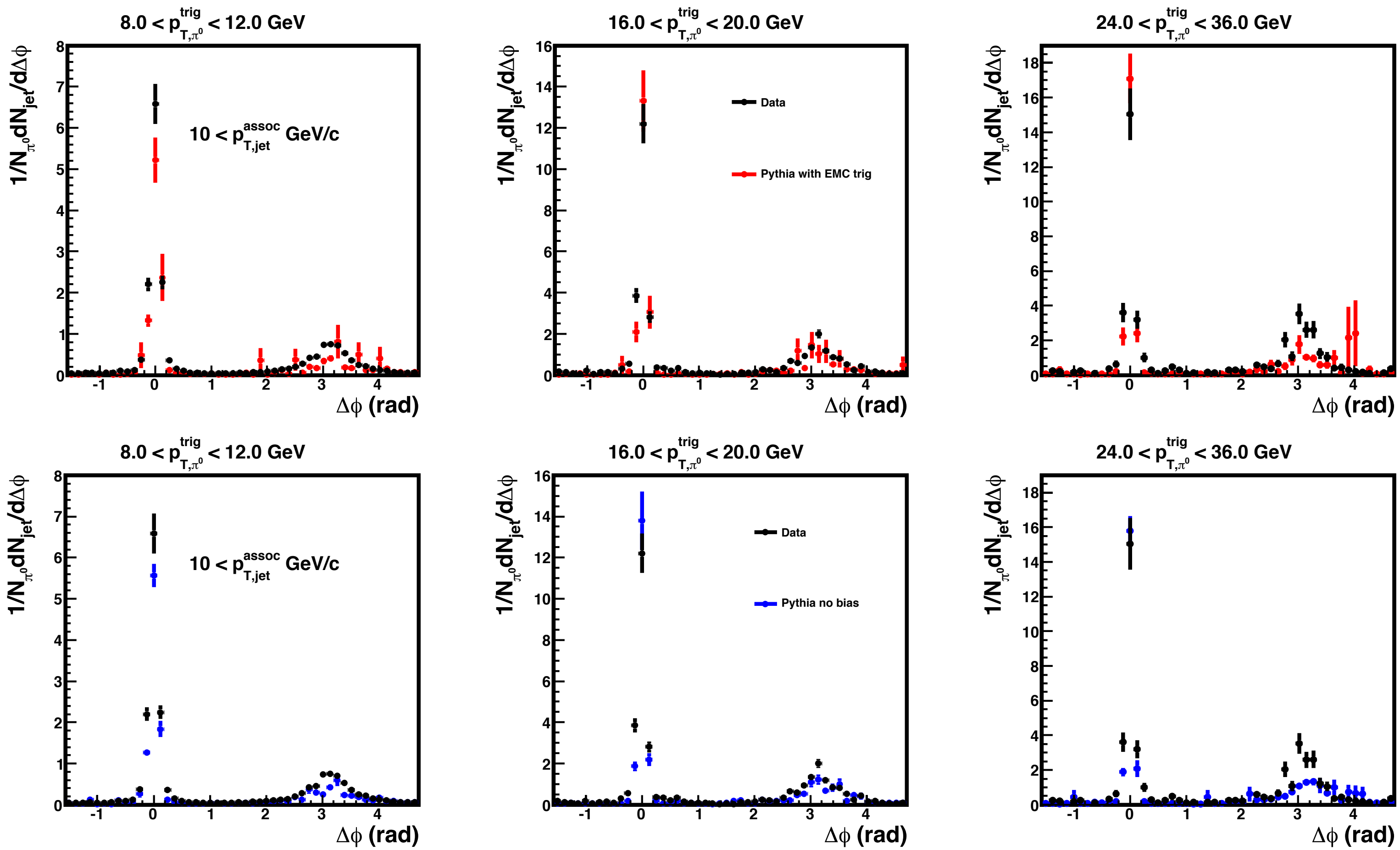

- PYTHIA calculations consistent with pp 7 TeV data

Comparison of away side jet yields to h-jet analysis

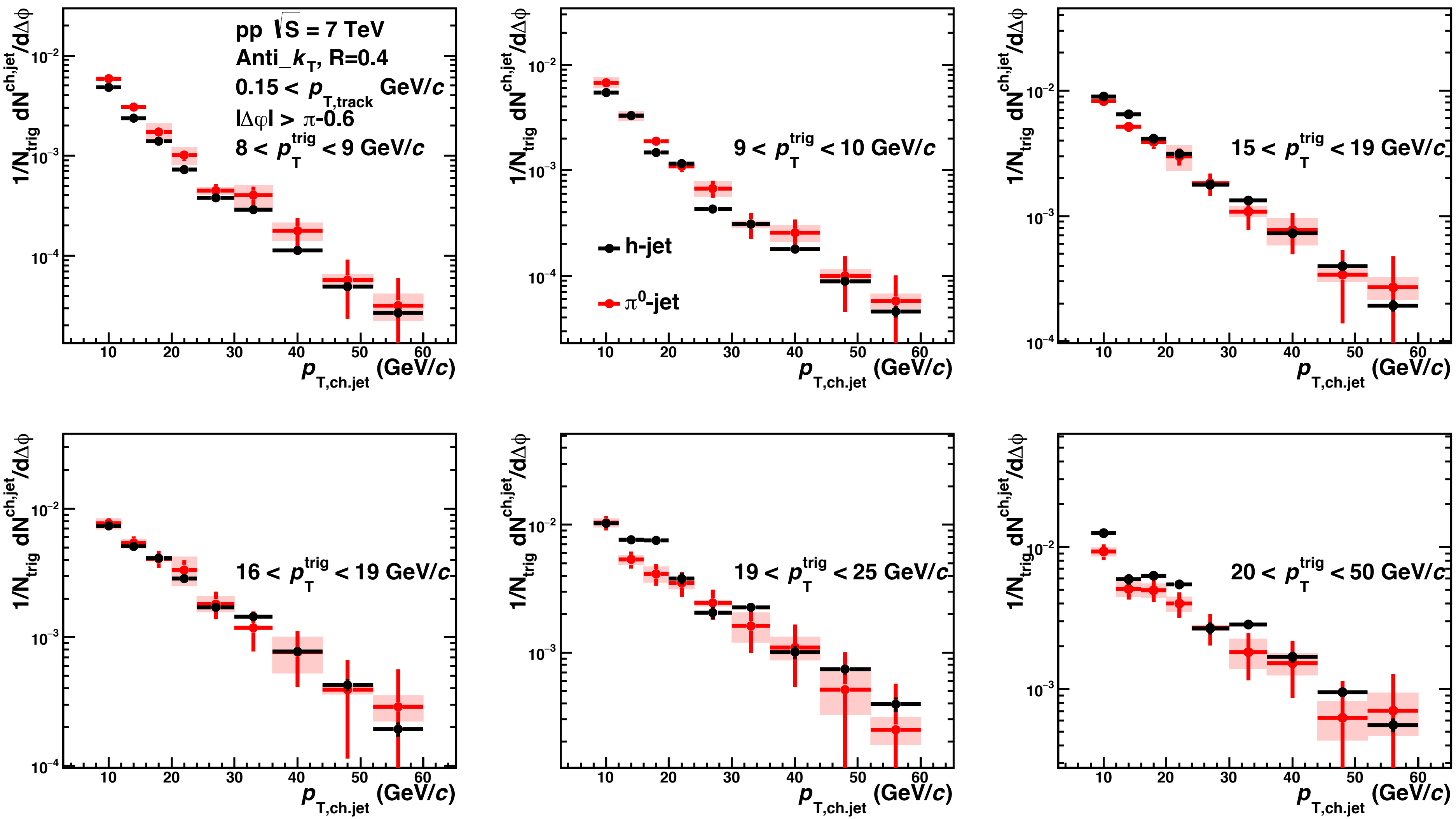

- Consistent with the results of h-jet analysis

Trigger and leading particle momentum dependence of I_{AA}

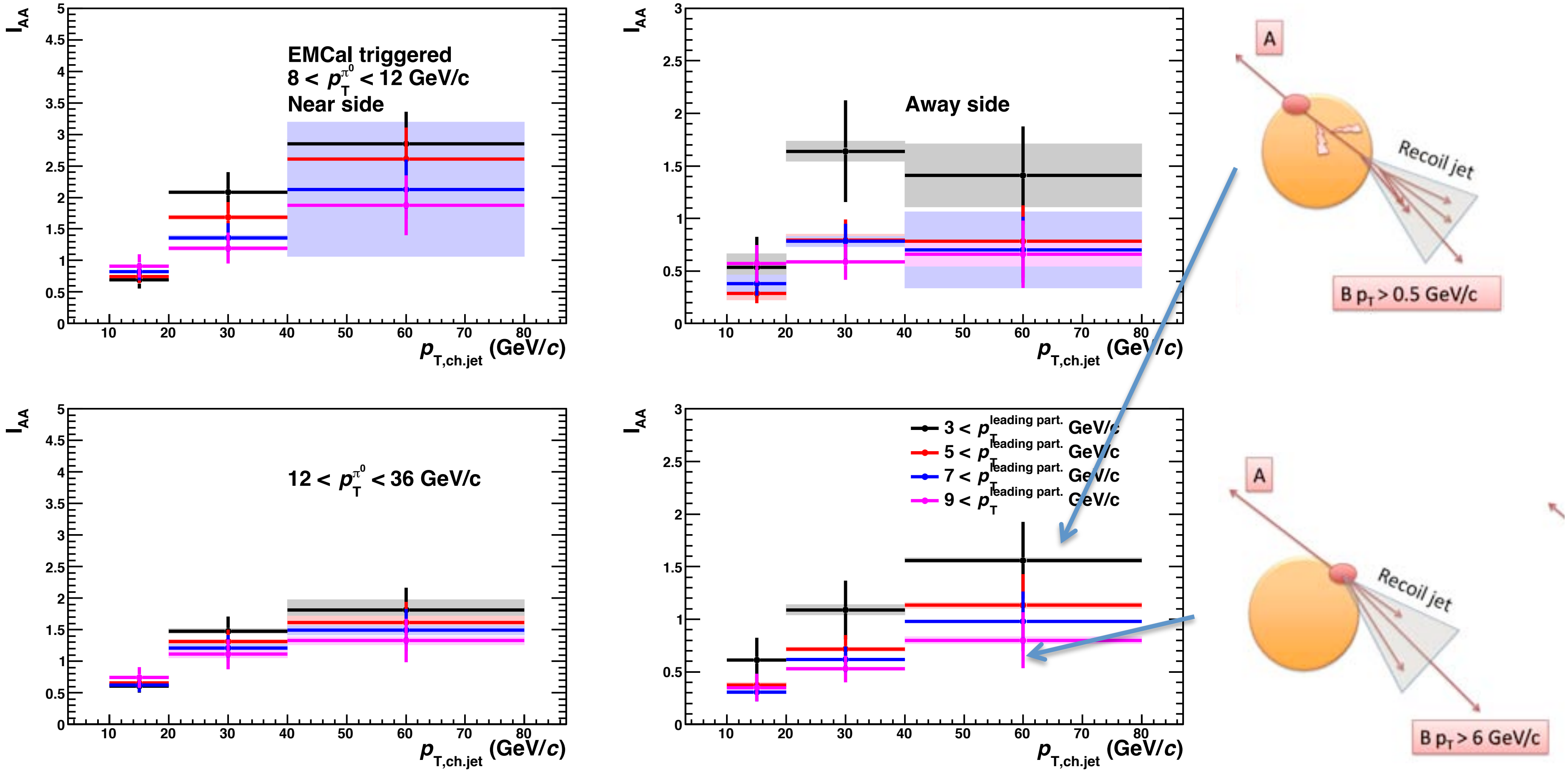

- Can not see the path-length dependence of away side jets by changing trigger and leading particle momentum region